technische universität
dortmund

2018

SCIENTIFIC HIGHLIGHTS

Annual Report

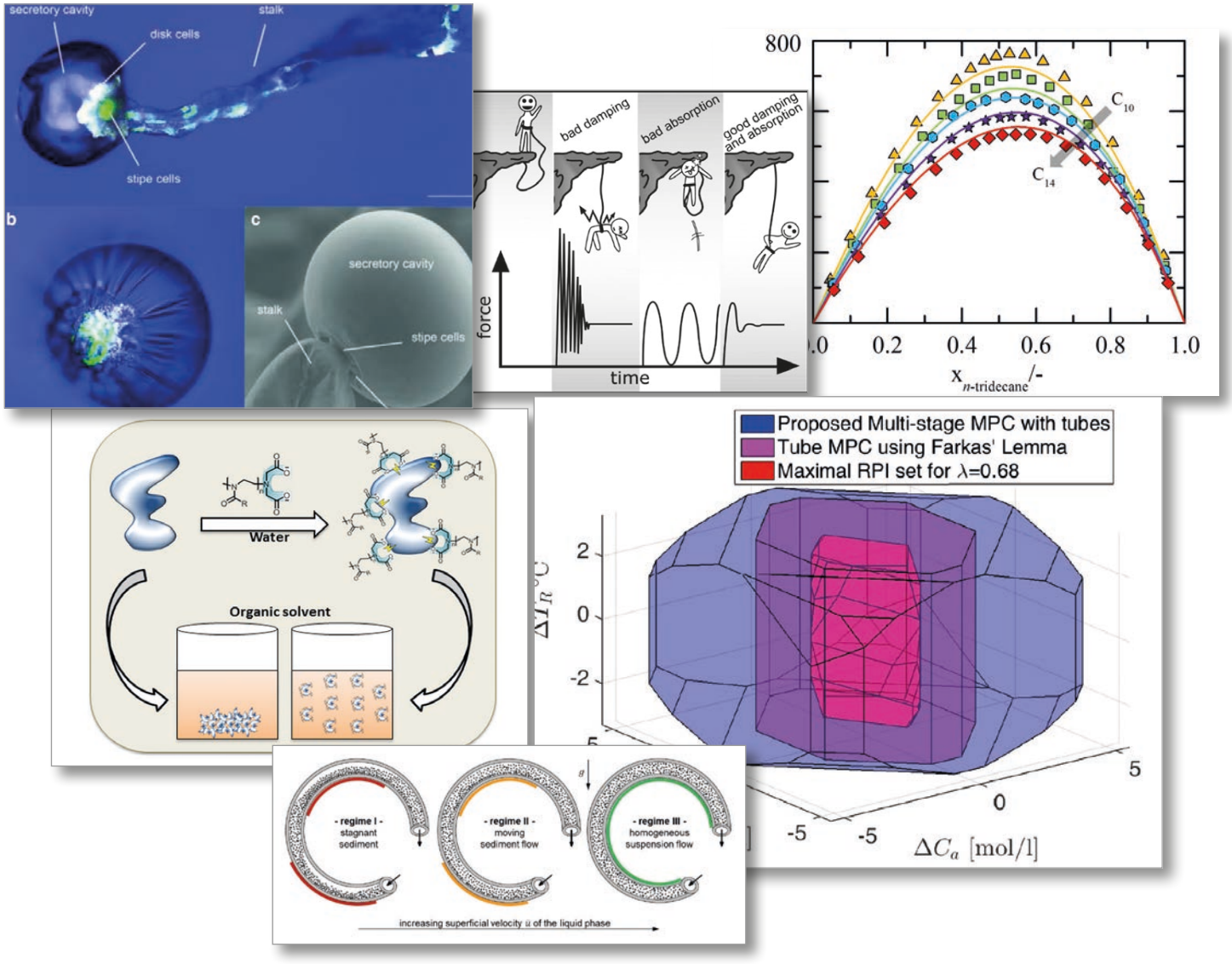

Fakultät Bio- und
Chemieingenieurwesen

Content

Department of BCI **4**
Preface 5

Equipment Design (AD) **6**
Solid-Liquid Suspension Handling in Coiled Tubular Crystallizers for Different Flow Rates 7
Residence Time Distribution and Mass Transfer in Stirred-Pulsed Extraction Columns 8
Publications 2018 - 2016 9

Plant and Process Design (APT) **12**
Size-dependent Particle Classification during the Crystallization Process 13
Enhanced Product Quality Control through Separation of Crystallization Phenomena in a Four-Stage MSMPR Cascade 14
Publications 2018 - 2016 15

Biomaterials and Polymer Science (BMP) **18**
Ciprofloxacin-POx Conjugates delay the Resistance Formation in Bacteria 19
Non-amphiphilic Polymers as Solubilizer for Enzymes in Organic Solvents 20
Critically Cross-Linked Syndiotactic Polypropylene 21
High Strain Storing, High Temperature Shape Memory Polymers with Full Recovery 22
Artificial Metalloenzymes based on Acylated lysozyme and Bovine Serum Albumin 23
Publications 2018 - 2016 24

Bioprocess Engineering (BPT) **26**
Catalytic Promiscuity of cGAS 27
Publications 2018 - 2016 28

Chemical Reaction Engineering (CVT) 30
Slug Velocity in Multiphase Capillary Flows 31
Highly Heat Integrated Adsorber Concepts for use in Direct Air Capture Applications 32
Publications 2018 - 2016 33

Process Dynamics and Operations (DYN) **36**
Tube-enhanced Multi-stage Model Predictive Control 37
Optimization of a Hydroformulation Process in a Thermomorphic Solvent System using a Commercial Steady-state Process Simulator and a Memetic Algorithm 38
Optimal Planning of the Operation of a NH_3 Network 39
Publications 2018 - 2016 40

Solids Process Engineering (FSV) **48**
Development of a Scale-Up Model for the Spheronization of Wet Extrudates 49
Quality by Design for Fused Deposition Modeling 3D Printing: Extrudate Mass Flow Control 50
Modelling the Filtration Performance of Fibrous Depth Filters considering Tomographic Data 51
Using the Phase Field Approach for Simulating Particle Dissolution 52
Correlation of Powder Performance on a Rotary Tablet Press and Standardized Methods for Flowability 53
Publications 2018 - 2016 54

Content

Fluid Separations (FVT) **56**
Efficient Design of Solvent-based Separation Processes 57
Automatic Model Development for Organic Solvent Nanofiltration 58
Developing Rotating Packed Beds for Application in Distillation 59
Publications 2018 - 2016 60

Fluid Mechanics (SM) **64**
Release of a Droplet entering a Shear Flow through a Pore 65
Multiphase Flows in Capillaries 66
Multiphase Flows in Aerated Tanks 67
Publications 2018 - 2016 68

Technical Biochemistry (TB) **70**
Chemical Fingerprinting of Single Glandular Trichomes of *Cannabis sativa* by Coherent Anti-Stokes Raman Scattering (CARS) 71
Radula Marginata; a Prospective Liverwort as an Alternative Source of Cannabinoid-like Compounds 72
Publications 2018 - 2016 73

Technical Biology (TBL) **76**
Engineering Pseudochelin Production in *Myxococcus xanthus* 77
Enhancement of Siderophore Production by Algal-Bacterial Cocultivation 78
Publications 2018 - 2016 79

Industrial Chemistry (TC) **80**
Palladium-catalysed carboxytelomerisation of *ß*-myrcene to highly branched C_{21}-esters 81
One-Step Palladium-Catalysed Synthetic Route to Unsaturated Pelargonic C_9-Amides Directly From 1,3 Butadiene 82
Polyhedral Oligomeric Silsesquioxane Modification of Metathesis Catalysts 83
Amide Versus Amine Ligand Paradigm in the Direct Amination of Alcohols with Ru-PNP Complexes 84
Publications 2018 - 2016 85

Thermodynamics (TH) **90**
Triglycerides as Solvents for Pharmaceuticals 91
Heterosegmental Modeling of Long-Chain Molecules and Related Mixtures using PC-SAFT 92
Influence of High Pressure and of Solvent on a Michael Addition 93
Simultaneous Prediction of Co-Solvent Influences on Michaelis Constants and Reaction Equilibrium of Ketone Reductions 94
Publications 2018 - 2016 95

Department of BCI

Preface

Dear Reader,

it is my great pleasure to present the Scientific Highlights of the Department of Biochemical- and Chemical Engineering of the year 2018. Our department turns 50 this year and the annual presentation of our greatest scientific achievements over the past year has become a tradition. Our faculty consists of a productive mixture of engineers and natural scientists of various disciplines. This variety gives birth to many ground breaking achievements each year, which can be found in numerous publications and patents. In 2018 about 250 Bachelor and Master Theses and over 30 PhD Theses were finalized. The Scientific Highlights do not only give testimony of their scientific productivity and creativity, but are also meant to inspire collaboration with partners from academia and industry. Last year, Prof. Wichmann has been retired. We wish him all the best in Florida.

Enjoy the Reading

Joerg C. Tiller

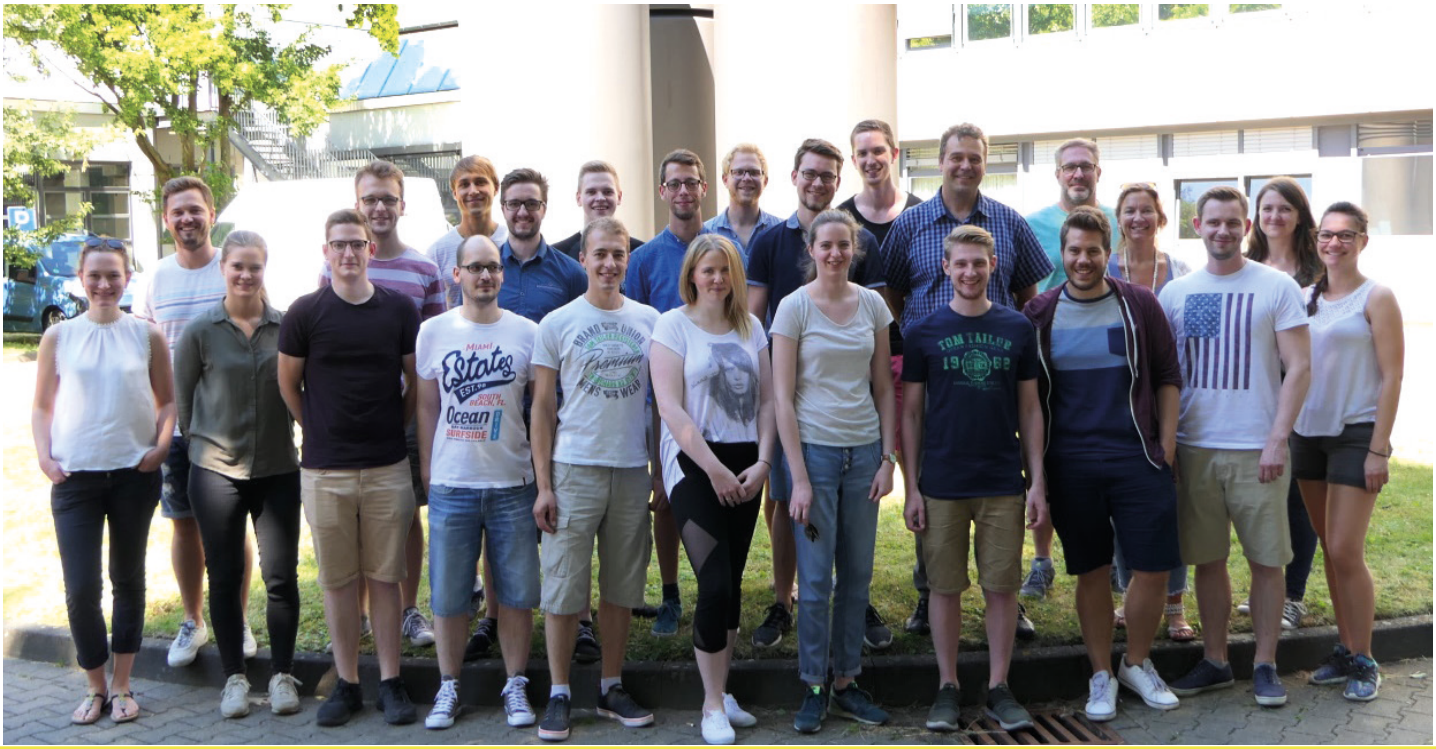

Equipment Design (AD)

Solid-Liquid Suspension Handling in Coiled Tubular Crystallizers for Different Flow Rates

Continuous cooling crystallization investigations for homogeneous suspension flow

Mira Schmalenberg, Lukas Hohmann, Norbert Kockmann

Global competition leads to a need for a fast time to market and increased resource efficiency. Continuous processing, module-based plant design, and multipurpose equipment are recently discussed approaches for the fine-chemical industry. In addition to the particle flow characteristics required for this, the diverse use of coiled flow inverter (CFI) design for the application of continuous cooling crystallization will be presented.

Production of fine chemicals and pharmaceuticals often includes solid-liquid suspension flow. Continuous manufacturing of such products is promising compared to conventional batch production, even though flow processes in tubular devices usually suffer from particle settling and clogging. Therefore, the isothermal suspension flow characteristics of various solid/liquid systems with up to 10 wt.-% of particles were investigated and successfully operated in horizontal helical coil tubes without blockage. The densimetric Froude number is used to describe the flow behavior in the coiled tubes in which three different flow regimes were observed (Figure 1): homogeneous suspension flow, moving sediment flow, and stagnant sediment. Empirical correlations were developed for the critical densimetric Froude number to define the transition between these regimes. Furthermore, the particle residence time distributions (RTDS) in the different flow regimes were investigated and narrow RTDS close to ideal plug flow was found.

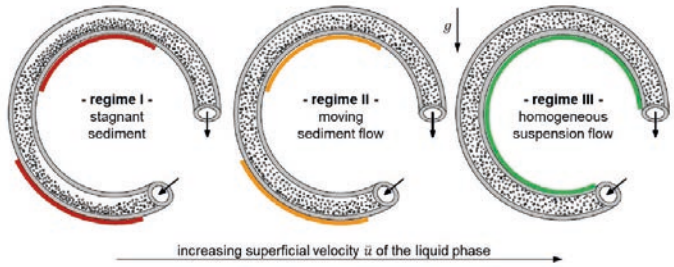

Figure 1: Schematic sketch of particle flow regimes.

Based on this knowledge and correlation a prototype with 4 mm inner diameter for 50 g·min^{-1} process medium was scaled down to a tube-in-tube CFI crystallizer (CFIC) with an inner diameter of 1.6 mm and varying length from 7.8 to 54.6 m for lower total mass flow rates of 15 – 20 g·min^{-1} (Fgure 2). The prototype was characterized and compared with batch experiments. Short-cut calculations were used based on characteristic time scales and the Damköhler number. The base for this comparison was seeded cooling crystallization of the L-alanine system in water under similar conditions. The experimental results reveal crystal growth and growth rate dispersion to be dominating for the product crystal size distribution (CSD).

Furthermore, a crystallizer in CFI design with an inner diameter of 10 mm was implemented in a modular miniplant to represent and test the apparatus in a continuous downstream process for a suspension flow rate of approximately 32 kg·h^{-1}. Upstream of the crystallization unit a wiped-film evaporator concentrated the L-alanine/water solution, while downstream a solid/liquid separation was performed on a vacuum belt filter. In summary, it can be said that the investigations concerning the CFI design for crystallization have been investigated for different stages of process development (d_i = 1.6 mm, 4.0 mm and 10.0 mm).

Acknowledgements: The work was funded by the Federal Ministry of Economics under the grants 03ET1254D and 03ET1528A.

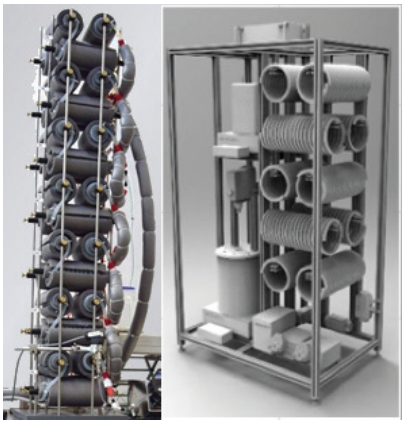

Figure 2: Tube-in-tube CFIC with seven crystallization units and d_i = 1.6 mm (left) and CFIC with five crystallization units and d_i = 10 mm (right).

Contact:
mira.schmalenberg@tu-dortmund.de
norbert.kockmann@tu-dortmund.de

Publications:

L. Hohmann, M. Schmalenberg, M. Prasanna, M. Matuschek, N. Kockmann, Suspension flow behavior and particle residence time distribution in helical tube devices, Chemical Engineering Journal 2018 (Article in press) DOI: 10.1016/j.cej.2018.10.166.

M. Schmalenberg, L. Hohmann, N. Kockmann, Miniaturized tubular cooling crystallizer with solid-liquid flow for process development, ASME 2018 16th International Conference on Nanochannels, Microchannels and Minichannels, ICNMM 2018, DOI: 10.1115/ICNMM2018-7660.

L. Hohmann, L. Löbnitz, C. Menke, B. Santhirakumaran, P. Stier, F. Stenger, F. Dufour, G. Wiese, S. Z. zur Horst-Meyer, B. Kusserow, W. Zang, H. Nirschl, N. Kockmann, Continuous Downstream Processing of Amino Acids in a Modular Miniplant, Chemical Engineering and Technology, Volume 41, Issue 6, June 2018, Pages 1152-1164.

L. Hohmann, T. Greinert, O. Mierka, S. Turek, G. Schembecker, E. Bayraktar, K. Wohlgemuth, N. Kockmann, Analysis of Crystal Size Dispersion Effects in a Continuous Coiled Tubular Crystallizer: Experiments and Modeling, Crystal Growth and Design, Volume 18, Issue 3, 7 March 2018, Pages 1459-1473.

Residence Time Distribution and Mass Transfer in Stirred-Pulsed Extraction Columns

Characterization of counter-current extraction in columns with two energy inputs – stirring and pulsation

Sebastian Soboll, I. Hagemann, Lukas Bittorf, Norbert Kockmann

Axial backmixing is an important issue in extraction columns since it heavily affects the mass transfer performance. A miniaturized, stirred-pulsed column was investigated regarding its backmixing characteristics in the continuous phase, using the system water/n-butyl acetate. To perform the conductivity measurement without distortion of the two-phase flow, electrodes with an annular design that precisely line up with the inner column wall were manufactured.

The DN15 and DN32 extraction column behavior was already investigated via hydrodynamic and mass transfer experiments. To better explain and understand the mass transfer in the column, axial backmixing and dispersion are further analyzed. To gain the residence time distribution RTD of the continuous aqueous phase, the concentration of potassium chloride as tracer is measured via electrical conductivity. Integration of commercial conductivity electrodes into the column is not possible due to the small inner diameter of the column. Thus, customized annular electrodes were manufactured by the mechanical workshops of the TU Dortmund University. As can be seen in Figure 1, these consist of a cylindrical body made of PTFE and two opposing brass rods of 12 mm in diameter and with connections for jack plugs on the outside.

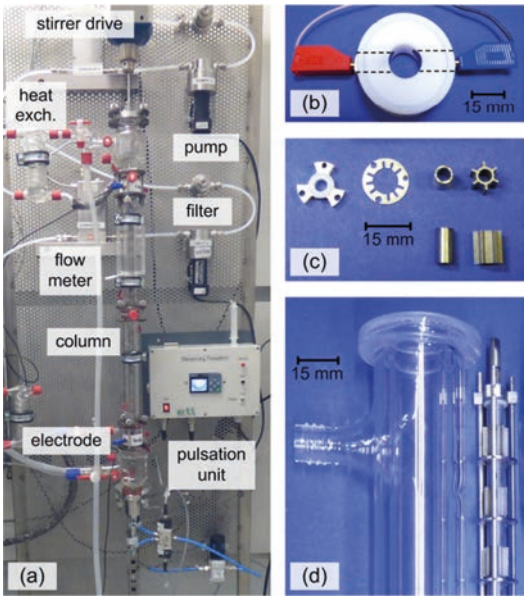

Figure 1: Total DN15 column setup and details: (a) column with periphery, (b) annular electrode, (c) internals, (d) column section with assembled internals.

In order to get a smooth fitting of the outlet concentration curve, the inlet concentration curve of the Dirac signal was measured, too. Based on the input signal $E_{in}(t)$, the output signal $E_{out}(t)$ and a transfer function $g_T(t)$, the calculated output signal can be fitted to the experimental data by varying the axial dispersion coefficient D_{ax} and the phase velocity u, see eqs. (1, 2).

With the information of the axial dispersion coefficient and the

$$E_{out}(t) = \int_0^t E_{in}(\theta) g_T(t-\theta) d\theta \quad (1)$$

$$g_T(t) = \frac{1}{2}\sqrt{\frac{L^2}{\pi D_{ax} t^3}} \exp\left(-\frac{(L-ut)^2}{4 D_{ax} t}\right) \quad (2)$$

phase velocity, Bodenstein numbers Bo can be calculated, too. Furthermore the influence of several operation parameters can be studied very precisely. As an example, D_{ax} and u are plotted in Figure 2. At higher stirrer speeds, the axial dispersion is increasing, while the velocity of the measured phase stays nearly constant. In further studies the theoretical number of stages was correlated with the Bodenstein number to

With this correlation, an estimation of the number of theoretical

$$\frac{u\,L}{D_{ax}} = Bo \approx 2\,N_{tank} = 2\,n_{th} \quad (3)$$

stages can be estimated from the residence time distribution.

Acknowledgements: The work was funded by the German Research Foundation under the grant KO2349-6.

Figure 2: Influence of stirrer speed to D_{ax} and u.

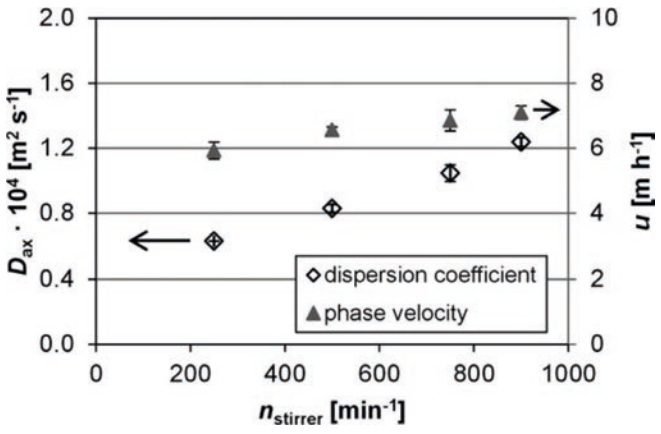

Publications:
S. Soboll, N. Kockmann, Hydrodynamics and Mass Transfer in a Lab-Scale Stirred-Pulsed Extraction Column, Chem. Eng. Technol., 2018, vol. 41, p. 1847-1856.

S. Soboll, L. Bittorf, N. Kockmann, Axial Backmixing and Residence Time Distribution in a Miniaturized, Stirred-Pulsed Extraction Column, Chem. Eng. Technol., 2018, vol.41(1), p. 134-142, 2018.

Contact:
lukas.bittorf@tu-dortmund.de
norbert.kockmann@tu-dortmund.de

Publications 2018 - 2016

2018

Peer Reviewed Journal Papers

- S. Schwolow, B. Mutsch, N. Kockmann, T. Röder
  Model-based scale-up and reactor design for solvent-free synthesis of an ionic liquid in a millistructured flow reactor
  Reac. Chem. & Eng., accepted manuscript October 2018, DOI: 10.1039/C7RE000xxxx

- L. Hohmann, M. Schmalenberg, M. Prasanna, M. Matuschek, N. Kockmann
  Suspension Flow Behavior and Particle Residence Time Distribution in Helical Tube Devices
  Chem. Eng. J., in press, October 2018, doi.org/10.1016/j.cej.2018.10.166

- N. Kockmann
  100 % Digital in der Prozessindustrie – Eindrücke und Ergebnisse vom Tutzing-Symposion 2018
  Chem. Ing. Technik, 90 (11), 1621-1627, 2018; DOI: 10.1002/cite.201800135

- N. Kockmann, L. Bittorf, W. Krieger, F. Reichmann, M. Schmalenberg, S. Soboll
  Smart Equipment – A Perspective Paper
  Chem. Ing. Technik, 90 (11), 1806-1822, 2018; DOI: 10.1002/cite.201800020

- S. Soboll, N. Kockmann
  Hydrodynamics and mass transfer in a lab-scale, stirred-pulsed extraction column
  Chem. Eng. & Technol., 41(9), 1847-1856, 2018; DOI: 10.1002/ceat.201800283

- L. Hohmann, L. Löbnitz, C. Menke, B. Santhirakumaran, P. Stier, F. Stenger, F. Dufour, G. Wiese, S. zur Horst-Meyer, B. Kusserow, W. Zang, H. Nirschl, N. Kockmann
  Continuous Downstream Processing of Amino Acids in a Modular Miniplant
  Chem. Eng. & Technol., 41(6), 1152-1164, 2018; DOI: 10.1002/ceat.201700657

- L. Hohmann, T. Greinert, O. Mierka, S. Turek, G. Schembecker, E. Bayraktar, K. Wohlgemuth, N. Kockmann
  Analysis of Crystal Size Dispersion Effects in a Continuous Coiled Tubular Crystallizer: Experiments and Modelling
  Cryst. Growth & Design., 18 (3), 1459–1473, 2018; DOI: 10.1021/acs.cgd.7b01383

- S. Soboll, L. Bittorf, N. Kockmann
  Axial backmixing and residence time distributions in a stirred-pulsed, miniaturized extraction column
  Chem. Eng. & Technol., 41(1) 134-142, 2018; DOI: 10.1002/ceat.201700152

Peer Reviewed Conference Papers

- F. Reichmann, Y. Jirmann, N. Kockmann
  Mixing Time Scale Measurement with Fast Exothermic Reactions Using Microchannel Reaction Calorimetry
  Proc. ASME-ICNMM2018-7627, Dubrovnik, June 11-13, 2018

- F. Reichmann, N. Kockmann
  Mass Transfer Studies During Bubble Breakup Behind Micronozzles in Laminar and Turbulent Breakup Regime
  Proc. ASME-ICNMM2018-7630, Dubrovnik, June 11-13, 2018

- W. Krieger, R. Dinter, G. Wiese, S. zur Horst-Meyer, N. Kockmann
  Active sensors for gas-liquid mass transfer studies in capillaries
  Proc. ASME-ICNMM2018-7659, Dubrovnik, June 11-13, 2018

- M. Schmalenberg, N. Kockmann
  Miniaturized Tubular Cooling Crystallizer with Solid-Liquid Flow for Process Development
  Proc. ASME-ICNMM2018-7660, Dubrovnik, June 11-13, 2018

Book Chapters

- N. Kockmann
  Historischer Abriss zur Entstehung und Entwicklung der Chemischen Reaktionstechnik
  in W. Reschetilowski, (Ed), Handbuch chemische Reaktoren, Springer Reference, November 2018

Publications 2018 - 2016

2017

Peer Reviewed Journal Papers

- S. K. Kurt, M. Akhtar, K.D.P. Nigam, N. Kockmann
  Gas - Liquid - Solid Flow Profile and Reactive Particle Precipitation in a Modular Coiled Flow Inverter
  Industrial & Engineering Chemistry Research 56 (39) 11320–11335 (2017)

- W. Krieger, J. Lamsfuß, W. Zhang, N. Kockmann
  Local Mass Transfer Phenomena and Chemical Selectivity of Gas-Liquid Reactions in Capillaries
  Chemical Engineering & Technology 40 (11) 2134-2143 (2017)

- F. Reichmann, S. Millhoff, Y. Jirmann, N. Kockmann
  Reaction Calorimetry for Exothermic Reactions in Plate-Type Microreactors Using Seebeck Elements
  Chemical Engineering & Technology 40 (11) 2144-2155 (2017)

- E. Mielke, P. Plouffe, N. Koushik, M. Eyholzer, M. Gottsponer, N. Kockmann, A. Macchi, D. M. Roberge
  Investigation of Overall and Localized Heat Transfer in Curved Micro-Channel Reactor Systems
  Reaction Chemistry & Engineering 2, 763-775 (2017)

- S. Soboll, I. Hagemann, N. Kockmann
  Performance of Laboratory-Scale Stirred-Pulsed Extraction Columns with Different Diameters
  Chemie Ingenieur Technik 89 (12), 1611-1618 (2017)

- C. Heckmann, S. K. Kurt, N. Kockmann, P. Ehrhard
  Simulation und Validierung der Pfropfenströmung im Kanal mit Stofftransport
  Chemie Ingenieur Technik 89 (12), 1642-1649 (2017)

- F. Reichmann, F. Varel, N. Kockmann
  Energy Optimization of Gas-Liquid Dispersion in Micronozzles Assisted by Design of Experiment
  Processes, 2017, paper 229828; DOI:10.3390/pr5040057

- N. Kockmann
  Modular equipment and continuous process development for small-scale production plants
  Chemistry Today 35 (4), 33-35 (2017)

- N. Kockmann, P. Thenée, C. Fleischer, G. Laudadio, T. Noel
  Safety Assessment in Development and Operation of Modular Continuous-Flow Processes
  Reaction Chemistry & Engineering 2, 258-280 (2017)

- I. Vural-Gürsel, N. Kockmann, V. Hessel
  Multiphase Flow in Microstructured Devices - Flow Separation Concepts and Their Integration into Process Flow Networks
  Chemical Engineering Science 169, 3-17 (2017)

- C. Fleischer, N. Krasberg, C. Bramsiepe, N. Kockmann
  Modulbasierter Planungsansatz für kontinuierlich betriebene Kleinanlagen
  Chemie Ingenieur Technik 89 (6), 785-799 (2017)

- S. K. Kurt, F. Warnebold, K. D. P. Nigam, N. Kockmann
  Gas-Liquid Reaction and Mass Transfer in Microstructured Coiled Flow Inverter
  Chemical Engineering Science 169, 164-178 (2017)

- L. Hohmann, K. Kössl, N. Kockmann, G. Schembecker, C. Bramsiepe
  Modules in Process Industry - A life cycle definition
  Chemical Engineering & Processing: Process Intensification 111, 115-126 (2017)

- F. Reichmann, A. Tollkötter, S. Körner, N. Kockmann
  Gas-Liquid Dispersion in Micronozzles and Microreactor Design for High Interfacial Area
  Chemical Engineering Science 169, 151-163 (2017)

- N. Kockmann
  Transport phenomena and chemical reactions in modular microstructured devices
  Heat Transfer Engineering 38 (14-15), 1316-1330 (2017)

Peer Reviewed Conference Papers

- F. Reichmann, M. Koch, S. Körner, N. Kockmann
  Internal Jet Formation During Bubble Generation in Microchannels
  Proc. ASME 2017 15th Intl. Conf. Nanochannels, Microchannels, and Minichannels, ASME-ICNMM2017-5545, Cambridge, USA, August 27-31 (2017)

- F. Reichmann, M. Koch, N. Kockmann
  Investigation of Bubble Breakup in Laminar, Transient, and Turbulent Regime Behind Micronozzles
  Proc. ASME 2017 15th Intl. Conf. Nanochannels, Microchannels, and Minichannels, ICNMM2017-5540, Cambridge, USA, August 27-31 (2017)

- F. Reichmann, S. Millhoff, N. Kockmann
  Seebeck Calorimeter for the Characterization of Highly Exothermic Reactions in a Microreactor Made of PVDF-Foils
  Proc. ASME 2017 15th Intl. Conf. Nanochannels, Microchannels, and Minichannels, ICNMM2017-5539, Cambridge, USA, August 27-31 (2017)

- W. Krieger, J. Lamsfuß, N. Kockmann
  Method To Visualize Local Mass Transfer And Chemical Selectivity Of Gas-Liquid Reaction In Coiled Capillaries
  Proc. ASME 2017 15th Intl. Conf. Nanochannels, Microchannels, and Minichannels, ICNMM2017-5538, Cambridge, USA, August 27-31 (2017)

Book Chapters

- S. Falß, M. Rieks, N. Kockmann
  Process Intensification in Catalysis
  in P. Kamer, D. Vogt, J. Thybaut, (Eds), Contemporary Catalysis, RSC Publishing, June 2017

2016

Peer Reviewed Journal Papers

- L. Hohmann, K. Kössl, N. Kockmann, G. Schembecker, C. Bramsiepe
  Modules in Process Industry - A life cycle definition
  Chemical Engineering & Processing: PI, DOI: 10.1016/j cep.2016.09.017, (2016)

- F. Reichmann, A. Tollkötter, S. Körner, N. Kockmann
  Gas-Liquid Dispersion in Micronozzles and Microreactor Design for High Interfacial Area
  Chemical Engineering Science, DOI: 10.1016/j.ces.2016.10.028, (2016)

- F. Braun, S. Schwolow, J. Seltenreich, N. Kockmann, T. Röder, N. Gretz, M. Rädle
  Highly sensitive Raman spectroscopy with low laser power for fast in-line reaction and multiphase flow monitoring
  Analytical Chemistry, 88 (19), 9368-9374 (2016)

- L. Hohmann, S. K. Kurt, S. Soboll, N. Kockmann
  Separation Units and Equipment for Lab-Scale Process Development
  J. Flow Chemistry, 6 (3), 181-190 (2016)

- S. Schwolow, A. Neumüller, L. Abahmane, N. Kockmann, T. Röder
  Design and application of a millistructured heat exchanger reactor for an energy-efficient process
  Chemical Engineering & Processing: PI, 108, 109-116 (2016)

- L. Hohmann, R. Gorny, O. Klaas, J. Ahlert, K. Wohlgemuth, N. Kockmann
  Design of a Continuous Tubular Cooling Crystallizer for Process Development on Lab-scale
  Chemical Engineering & Technology, 39 (7), 1268-1280 (2016)

- N. Kockmann
  Modular Equipment for Chemical Process Development and Small-scale Production in Multipurpose Plants
  ChemBioEng Reviews, 3 (1), 5-15 (2016)

- R. Trostorf, N. Kockmann
  Methodik zur einfachen Standardisierung von Probenahmesystemen auf Basis der beteiligten Fluidphasen
  Chemie - Ingenieur - Technik, 88 (1-2), 128-138 (2016)

- A. Tollkötter, F. Reichmann, J. Wesholowski, F. Schirmbeck, N. Kockmann
  Gas-Liquid Flow Dispersion in Micro Offices and Bubble Coalescence with High Flow Rates
  J. Electronics Packaging, 138 (1):011013-011013-8, EP-15-1105 (2016)

- S. Schwolow, J. Y. Ko, N. Kockmann, T. Röder
  Enhanced heat transfer by exothermic reactions in laminar flow capillary reactors
  Chemical Engineering Science141, 356-362 (2016)

- N. Kockmann, P. Lutze, A Górak
  Grand Challenges and Chemical Engineering Curriculum-Developments at TU Dortmund University
  Universal Journal of Educational Research 4 (1), 200-204 (2016)

- E. C. Sindermann, A. Holbach, A. de Haan, N. Kockmann
  Single stage and countercurrent extraction of 5-hydroxymethylfurfural from aqueous phase systems
  Chemical Engineering Journal, 283 (1), 251-259 (2016)

- S. K. Kurt, I. Vural-Gürsel, V. Hessel, K. D. P. Nigam, N. Kockmann
  Liquid-Liquid Extraction System with Microstructured Coiled Flow Inverter and Other Capillary Setups for Single-Stage Extraction Applications
  Chemical Engineering Journal, 283 (1), 764-777 (2016)

- I. Vural-Gürsel, S. K. Kurt, Q. Wang, T. Noël, K.D.P. Nigam, N. Kockmann, V. Hessel
  Utilization of Milli-scale Coiled Flow Inverter in Combination with Phase Separator for Continuous Flow Liquid-Liquid Extraction Processes
  Chemical Engineering Journal, 283 (1), 855-868 (2016)

Peer Reviewed Conference Papers

- L. Hohmann, S. K. Kurt, N. Pouya Far, D. Vieth, N. Kockmann
  Micro-/Milli-Fluidic Heat-Exchanger Characterization by Non-Invasive Temperature Sensors
  Proc. ASME 2016 14th Intl. Conf. Nanochannels, Microchannels and Minichannels ICNMM2016-8008, Washington, DC, July 10-14 (2016)

- F. Reichmann, A. Tollkötter, N. Kockmann
  Investigation of Bubble Break-up in Microchannel Orifices
  Proc. ASME 2016 14th Intl. Conf. Nanochannels, Microchannels and Minichannels, ICNMM2016-8048, Washington, DC, July 10-14 (2016)

- S. K. Kurt, M. Akhtar, K.D.P. Nigam, N. Kockmann
  Modular Concept of a Smart Scale Helically Coiled Tubular Reactor for Continuous Operation of Multiphase Reaction Systems
  Proc. ASME 2016 14th Intl. Conf. Nanochannels, Microchannels and Minichannels ICNMM2016-8004, Washington, DC, July 10-14 (2016)

Plant and Process Design (APT)

Size-dependent Particle Classification during the Crystallization Process

Development of an online measurement setup and improvement of the image analysis algorithm for the discrimination of single crystals and agglomerates during the crystallization process

Stefan Heisel, Mareike Rolfes, Kerstin Wohlgemuth

The properties of the final crystalline product depend not only on the particle size distribution (PSD) but also on the agglomeration degree. For solids with a high tendency to agglomerate during crystallization, here adipic acid/water, the control of the crystallization process itself needs to be regarded intently. For this purpose, we developed a setup for online measurement of crystallization processes, where particle images were taken and artificial neural networks (ANNs) were used to convert the PSD into populations of single crystals and agglomerates. In particular, the training set composition was investigated to generate an ANN that is capable of discriminating all particle sizes equally well. We evaluated the effect of the measurement setup on experiments performed for normal cooling crystallization. We found that the major challenge of measuring crystal agglomerates lies in superimposing aggregates that falsify the online measurement results, as offline measurements demonstrated.

Image analysis can be used to detect and to classify particles into single crystals or agglomerates based on different image descriptors, e.g., circularity, number of concavity points or roundness, using ANNs. For the generation of an ANN, the image descriptors were chosen based on proportional similarity. While the overall size-independent performance measurements show a sufficiently high classification accuracy, a closer examination of Figure 1 demonstrates that the classifier is not capable of discriminating bigger particles (> 400 µm) because it is prone to neglect underrepresented size fractions. By using size-dependent training sets, we could improve the results, since all particle sizes are considered evenly and the characteristics of every particle size fraction are taken into account individually. The image descriptor selection based on proportional similarity is also adapted to the size dependency to generate a highly accurate classifier (see Figure 1).

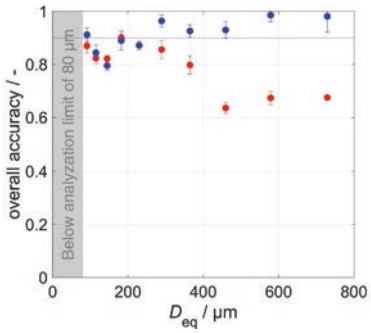

Figure 1: Size-dependent classifier accuracies for different training runs: Size-independent training set (red), Size-dependent training set (blue).

To record images during the crystallization process, we developed an online measurement setup with an external sampling loop. Figure 2 shows, by comparing the crystallization process with and without the periphery, that the external installation alters the concentration profile and the PSD of the crystals. We assumed that the periphery favors nucleation within the tube. Hence, the setup may not be used to investigate the complete process including the stages with high supersaturation but the process stages where supersaturation is low.

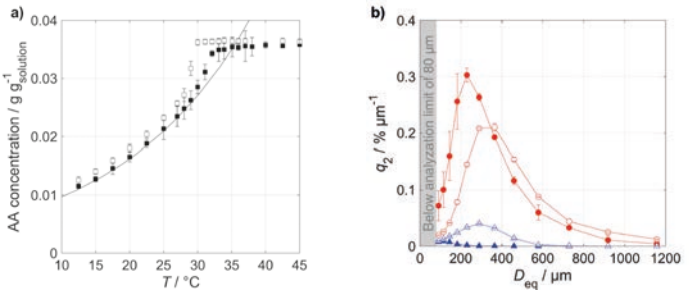

Figure 2: Online measurement comparison of process characteristics with (solid symbols) and without (open symbols) the periphery present during the crystallization run. (a) Concentration profile of adipic acid. (b) Corresponding q_2 distributions for PSD_{sc} (blue triangles) and PSD_{ag} (red circles).

Furthermore, by comparing online with offline measurements (see Figure 3) it is striking that for offline measurements the amount of single crystals increases while the number of particles classified as agglomerates decreases. We found an explanation of this result in the superimposing effect of aggregates during the online measurements.

In summary, to generate a classifier that discriminates particles of all sizes equally well, the training set should be composed of an even number of all relevant particle sizes. Furthermore, the early process stages where supersaturation is high cannot be investigated directly because the setup affects the overall crystallization process in terms of nucleation. Future work will have to focus on the differentiation of aggregates and agglomerates during online measurements to counteract the effect of superimposing of aggregates.

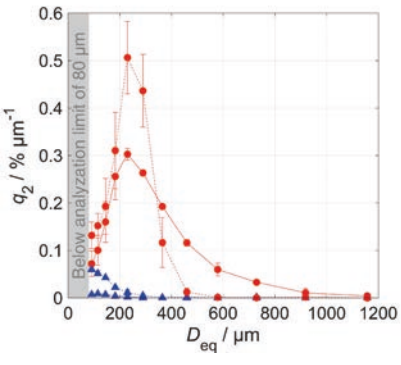

Figure 3: Comparison of online (solid line) and offline (dashed line) measurements at 10 °C by using the periphery.

Contact:
stefan.heisel@tu-dortmund.de
kerstin.wohlgemuth@tu-dortmund.de

Publications:
S. Heisel, M. Rolfes, K.Wohlgemuth, Chem. Eng. Technol.,41, 1218-1225 (2018).

Enhanced Product Quality Control through Separation of Crystallization Phenomena in a Four-Stage MSMPR Cascade

The first step towards tailored crystalline products for the pharmaceutical industry

Marie-Christine Lührmann, Jan Timmermann, Gerhard Schembecker, Kerstin Wohlgemuth

In industrial crystallization processes, a precisely controlled operation mode is decisive to ensure consistent product quality. To meet this challenge, continuously operated crystallizers are promising, because they run at steady state, thus yielding reproducible crystalline product characteristics. Although continuous crystallization is already well established to manufacture large-volume commodity products such as sugar and inorganic salts, batch processing remains the method of choice in the pharmaceutical and fine chemical sector. To satisfy the high demands placed on the products, a four-stage cascade of MSMPR crystallizers has been designed and set up for the production of L-alanine crystals to achieve an enhanced control of product quality in terms of crystal size and size distribution. The cascade is characterized by a local separation of the crystallization phenomena nucleation and crystal growth as well as by the fact that no pumps were used to transfer the suspension from one vessel to the next.

The designed cascade consists of a nucleation vessel (34 mL) and three growth vessels (370 mL each) which are spatially separated and connected by tubes (see Figure 1).

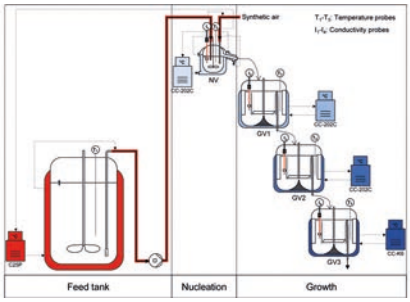

Figure 1: Schematic drawing of the four-stage MSMPR cascade with spatially separated nucleation and growth zone as well as the feed tank zone.

The nucleation vessel is equipped with an overflow tube into the next vessel to circumvent a necessary transport via pumps. The nucleation is induced via gassing with saturated and heated synthetic air in a controlled manner. The resulting nuclei display a narrow crystal size distribution and possible encrustation at the vessel walls is minimized. We measured the temperature with an installed PT100 probe and used a conductivity probe to identify a steady-state inside the nucleation vessel was used. The employed growth vessels are explicitly designed to prevent encrustation and accumulation of crystals inside of them. A cylindrical draft tube is installed in the center of the vessel to direct the flow along the desired path, which is further improved by a cone-shaped bottom of the vessel. Crystals present inside the growth vessels are suspended well and do not accumulate at the bottom of the vessel. The crystals suspended at the surface are now able to exit the growth vessels through a vertical overflow tube. By performing a washout experiment the solid phase residence time of the growth vessels is determined. A defined amount of crystals is placed inside a saturated solution in a growth vessel. While stirred, a clear saturated solution is fed to the vessel and crystals are entrained. The results show an almost ideal exponential decay of the crystal mass inside the growth vessels (see Figure 2).

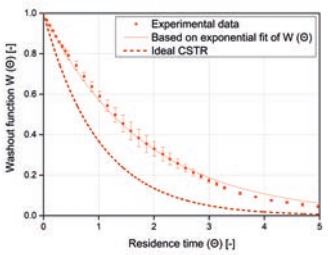

Figure 2: Solid phase residence time distribution showing the washout function against the residence time θ.

During operation of the MSMPR cascade, it is necessary to prevent unwanted primary nucleation. By keeping the temperature steps between each vessel smaller than the experimental determined primary nucleation threshold, it is possible to separate the crystallization phenomena nucleation and growth. During operation of the MSMPR cascade, it was possible to maintain constant nucleation via gassing for more than 9 hours. After a startup of growth vessels 1 and 2 of approximately 6.5 hours, a steady state was reached and microscopic images were acquired after reaching the steady state (see Figure 3).

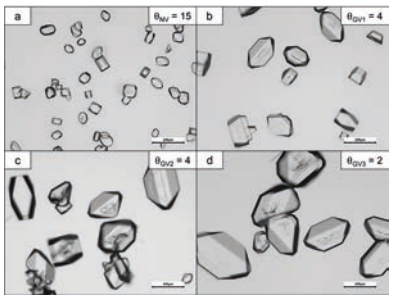

Figure 3: Microscopic images of crystal suspensions at steady state (NV, GV1 and GV2) and shortly after connection of GV3.

The images show that only crystal growth took place and no further unwanted nucleation was induced in the cascade. In summary, the designed MSMPR cascade offers the possibility to decouple the crystallization phenomena nucleation and growth. Thereby, we can facilitate an increased control over crystal quality namely a defined crystal size and narrow crystal size distribution. The gravimetric overflow concept enables minimal attrition of crystals. All of this offers a huge potential for tailored continuous crystallization processes in the pharmaceutical industry.

Publications:
M.-C. Lührmann, J. Timmermann, G. Schembecker, K. Wohlgemuth, Cryst. Growth Des. 18 (2018) 7323-7334.

Contact:
kerstin.wohlgemuth@tu-dortmund.de
marie-christine.luehrmann@tu-dortmund.de

Publications 2018 - 2016

2018

Peer Reviewed Journal Papers

- M.-C. Lührmann, J. Timmermann, G. Schembecker, K. Wohlgemuth
  Enhanced Product Quality Control through Separation of Crystallization Phenomena in a Four-Stage MSMPR Cascade
  Crystal Growth & Design 18 (2018) 7323-7334

- M. Eilermann, A. Tebbe, D. Schwarz, S. Leufke, C. Bramsiepe, G. Schembecker
  Approach for the characterization of industrial process tasks as basis for the generation and application of an equipment module database
  Chemical Engineering Science 191 (2018) 42-55

- M. Eilermann, C. Post, H. Radatz, C. Bramsiepe, G. Schembecker
  A general approach to module-based plant design
  Chemical Engineering Research and Design 137 (2018) 125-140

- I. Kaplanow, J. Stecker, G. Schembecker, J. Merz
  Multistage Processing of Tunable Aqueous Polymer Phase Impregnated Resins (TAPPIR®)
  Chemical Engineering and Technology 41 (2018) 1324-1330

- I. Lukin, J. Merz, G. Schembecker
  Techniques for the recovery of volatile aroma compounds from biochemical broth: A review
  Flavour and Fragrance Journal 33 (2018) 203-216

- D. Wetzel, T. Rolf, M. Suckow, T. Rolf, M. Suckow, A. Kranz, A. Barbian, J-A. Chan, J. Leitsch, M. Weniger, V. Jenzelewski, B. Kouskousis, C. Palmer, J.G. Beeson, J. Merz, M. Piontek
  Establishment of a yeast-based VLP platform for antigen presentation
  Microbial Cell Factories 17 (2018) 17

- M.- C. Lührmann, M. Termühlen, J.Timmermann, G. Schembecker, K. Wohlgemuth
  Induced nucleation by gassing and its monitoring for the design and operation of an MSMPR cascade
  Chemical Engineering Science 192 (2018) 840-849

- T. Kleetz, R. Scheel, G. Schembecker, K. Wohlgemuth
  Cooling Crystallization: Does Gassing Compete with Seeding?
  Crystal Growth & Design 18 (2018) 4906-4910

- S. Heisel, M. Rolfes, K. Wohlgemuth
  Discrimination between Single Crystals and Agglomerates during the Crystallization Process
  Chemical Engineering and Technology 41 (2018) 1218-1225

- M.-C. Ostermann, M. Termühlen, G. Schembecker, K. Wohlgemuth
  Growth Rate Measurements of Organic Crystals in a Cone-Shaped Fluidized-Bed Cell
  Chemical Engineering and Technology 41 (2018) 1165-1172

- L. Hohmann, T. Greinert, O. Mierka, S. Turek, G. Schembecker, E. Bayraktar, K. Wohlgemuth, N. Kockmann
  Analysis of Crystal Size Dispersion Effects in a Continuous Coiled Tubular Crystallizer: Experiments and Modelling
  Crystal Growth & Design 18 (2018) 1459–1473

- I. Kaplanow, M. Schmalenberg, I. Borgmann, G. Schembecker, J. Merz
  Tunable Aqueous Polymer Phase Impregnated Resins (TAPPIR®): Investigation of the impregnation stability
  Separation and Purification Technology 190 (2018) 1-8

2017

Peer Reviewed Journal Papers

- M. Heitmann, G. Schembecker, C. Bramsiepe
  Framework to decide for a volume flexible chemical plant during early phases of plant design
  Chemical Engineering Research and Design 128, 85-95 (2017)

- L.-M. Terdenge, J. A. Kossuch, G. Schembecker, K. Wohlgemuth
  Potential of gassing crystallization to control the agglomeration degree of crystalline products
  Powder Technology 320, 386-396 (2017)

- S. Heisel; T. Kovačević; H. Briesen, G.Schembecker, K. Wohlgemuth
  Variable Selection and Training Set Design for Particle Classification using a Linear and a Non-Linear Classifier
  Chemical Engineering Science 173, 131-144 (2017)

- J. Krause, J. Merz
  Hydrodynamic influences on the reaction performance of a crude yeast lysate in the CPC reactor
  Biochemical Engineering Journal (2017), DOI: 10.1016/j.bej.2017.05.025

- J. Krause, J. Merz
  Comparison of enzymatic hydrolysis in a centrifugal partition chromatograph and stirred tank reactor
  Journal of Chromatography A 1504, 64-70 (2017)

- L.-M. Terdenge, K. Wohlgemuth
  Effect of drying method on agglomeration degree of crystalline products
  Chemical Engineering Science 167, 88-97 (2017)

- C. Schwienheer, J. Krause, G. Schembecker, J. Merz
  Modelling centrifugal partition chromatography separation behavior to characterize influencing hydrodynamic effects on separation efficiency
  Journal of Chromatography A 1492, 27–40 (2017)

- J. Sieberz, E. Cinar, K. Wohlgemuth, G. Schembecker
  Clarification of a monoclonal antibody with cationic polyelectrolytes: analysis of influencing parameters
  Biochemical Engineering Journal 122, 60–70 (2017)

- H. Radatz, J.M. Elischewski, M. Heitmann, G. Schembecker, C. Bramsiepe
  Design of equipment modules for flexibility
  Chemical Engineering Science 168, 271-288 (2017)

- L. Hohmann, K. Kössl, N. Kockmann, G. Schembecker, C. Bramsiepe
  Modules in process industry - A life cycle definition
  Chemical Engineering and Processing: Process Intensification 111, 115 - 126 (2017)

- T. Kleetz, G. Paetzold, G. Schembecker, K. Wohlgemuth
  Gassing Crystallization at Different Scales: Potential to Control Nucleation and Product Properties
  Crystal Growth & Design 17, 1028–1035 (2017)

- M. Eilermann, C. Post, D. Schwarz, (...), G. Schembecker, C. Bramsiepe
  Generation of an equipment module database for heat exchangers by cluster analysis of industrial applications
  Chemical Engineering Science 167, 278-287 (2017)

Publications 2018 - 2016

- M. Heitmann, T. Huhn, S. Sievers, G. Schembecker, C. Bramsiepe
  Framework to decide for an expansion strategy of a small scale continuously operated modular multi-product plant
  Chemical Engineering and Processing: Process Intensification 113, 74-85 (2017)

- S.Sievers, T. Seifert, M. Franzen, G. Schembecker, C. Bramsiepe
  Fixed capital investment estimation for modular production plants
  Chemical Engineering Science 158, 395-410 (2017)

- J. Krause, R. Krutz, G. Schembecker, J. Merz
  Whole cell immobilization and catalysis in a Centrifugal Partition Chromatograph
  Biochemical Engineering Journal 117 Part A, 188-197 (2017)

2016

- L. Hohmann, K. Kössl, N. Kockmann, G. Schembecker, C. Bramsiepe
  Modules in process industry - A life cycle definition
  Chemical Engineering and Processing: Process Intensification (2016) DOI: 10.1016/j.cep.2016.09.017

- M. Heitmann, T. Huhn, S. Sievers, G. Schembecker, C. Bramsiepe
  Framework to decide for an expansion strategy of a small scale continuously operated modular multi-product plant
  Chemical Engineering and Processing: Process Intensification (2016) DOI: 10.1016/j.cep.2016.09.004

- T. Kleetz, F. Funke, A. Sunderhaus, G. Schembecker, K. Wohlgemuth
  Influence of Gassing Crystallization Parameters on Induction Time and Crystal Size Distribution
  Crystal Growth & Design 16, 6797-6803 (2016)

- N. Wolters, C. Schabronath, G. Schembecker, J. Merz
  Efficient conversion of pretreated brewer's spent grain and wheat bran by submerged cultivation of Hericium erinaceus
  Bioresource Technology 222, 123-129 (2016)

- M. Lochmüller, G. Schembecker
  Simultaneous optimization of scheduling, equipment dimensions and operating conditions of sequential multi-purpose batch plants
  Computers and Chemical Engineering 94, 157-179 (2016)

- S. Sievers, T. Seifert, G. Schembecker, C. Bramsiepe
  Methodology for evaluating modular production concepts
  Chemical Engineering Science 155, 153-166 (2016)

- L. Holtmann, M. Lobedann, J. Magnus, G. Schembecker
  Disposables for continuous viral clearance for the production of monoclonal antibodies
  European Pharmaceutical Review 21 (2), 22-27 (2016)

- L.-M. Terdenge, K. Wohlgemuth
  Impact of agglomeration on crystalline product quality within the crystallization process chain
  Crystal Research & Technology 51513-523 (2016)

- L. Hohmann, R. Gorny, O. Klaas, J. Ahlert, K. Wohlgemuth, N. Kockmann
  Design of a Continuous Tubular Cooling Crystallizer for Process Development on Lab-scale
  Chemical Engineering & Technology 39, 1268-1280 (2016)

- S. Klutz, L. Holtmann, M. Lobedann, G. Schembecker
  Cost evaluation of antibody production processes in different operation modes
  Chemical Engineering Science141, 63-74 (2016)

- S. Klutz, M. Lobedann, C. Bramsiepe, G. Schembecker
  Continuous viral inactivation at low pH value in antibody manufacturing
  Chemical Engineering and Processing: Process Intensification 102, 88-101 (2016)

- T. Kleetz, F. Braak, N. Wehenkel, G. Schembecker, K. Wohlgemuth
  Design of Median Crystal Diameter Using Gassing Crystallization and Different Process Concepts
  Crystal Growth & Design 161320-1328 (2016)

- C. Dowidat, M. Kalliski, G. Schembecker, C. Bramsiepe
  Synthesis of batch heat exchanger networks utilizing a match ranking matrix
  Applied Thermal Engineering 100, 78–83 (2016)

- F. Thygs, J. Merz, G. Schembecker
  Automation of Solubility Measurements on a Robotic Platform
  Journal of Chemical and Engineering Technology 39 (6), 1049-1057 (2016)

- B. Dreisewerd, J. Merz, G. Schembecker
  Modeling the Quasi-Equilibrium of Multistage Phytoextractions
  Industrial & Engineering Chemistry Research 55, 1808–1812 (2016)

- K. Brandt, G. Schembecker
  Production Rate-Dependent Key Performance Indicators for a Systematic Design of Biochemical Downstream Processes Plants
  Chemical Engineering and Technology 39, 354-364 (2016)

- S. Klutz, J. Magnus, M. Lobedann, M. Temming, G. Schembecker
  Developing the biofacility of the future based on continuous processing and single-use technology
  Source of the Document Journal of Biotechnology 213, 120-130 (2015)

Proceedings & Book Chapters

- K. Wohlgemuth (editor)
  BIWIC 2017 - 24th International Workshop on Industrial Crystallization
  Verlag Dr. Hut, ISBN 978-3-8439-3247-9

- S. Heisel, L.-M. Terdenge, K. Wohlgemuth
  Eine Strategie Zur Charakterisierung und dem Design organischer kristalliner Produkte
  In: Produktgestaltung in der Partikeltechnologie, Band 8, pp. 33-40 Fraunhofer Verlag, ISBN 978-3-8396-1194-4

- S. Heisel, J. Schön, A.-L. Diekmann, G. Schembecker, K. Wohlgemuth
  Evolution of the agglomeration degree over time during batch cooling crystallization
  Proceedings of the 24th International Workshop on Industrial Crystallization "BIWIC" (2017) 60-65, Verlag Dr. Hut, ISBN 978-3-8439-3247-9

Publications 2018 - 2016

- M.-C. Ostermann, M. Termühlen, J. Timmermann, G. Schembecker, K. Wohlgemuth
  Nucleation and Growth Kinetic Measurements for the Design of a Novel MSMPR Cascade with Separated Zones of Crystallization Phenomena
  Proceedings of the 24th International Workshop on Industrial Crystallization "BIWIC" (2017) 155-160,
  Verlag Dr. Hut, ISBN 978-3-8439-3247-9

Biomaterials and Polymer Science (BMP)

Ciprofloxacin-POx Conjugates delay the Resistance Formation in Bacteria

Polymer-Antibiotic-Conjugates (PACs)

Martin Schmidt, Alina Romanowska, Joerg C. Tiller

The use of antibiotics is the only efficient weapon against bacterial infections, which is the number one killer world-wide. The abusive application of antibiotics has led to the formation of resistant bacterial strains, which represent a great threat even in industrialized countries. Thus modifying antibiotics that do not or only slowly cause bacterial resistance is an important research field. We have shown for the first time that conjugation of the antibiotic ciprofloxacin with poly(2-oxazoline)s (POx) can indeed delay the formation of resistance mechanism in bacterial strains.

As shown previously, conjugation of antibiotics such as penicillins and ciprofloxacin retains the activity of the antibiotics and can reduce the penicillinase induced hydrolysis in the case of the first class. However, the influence on the resistance formation of polymers attached to antibiotics is rarely investigated. In this study, ciprofloxacin (CIP) was conjugated to poly(2-methyl-2-oxazoline)s with an ethylene diamine end group (Me-PMOx$_{28}$-EDA) via two different spacers (CIP modified with α,α´-dichloro-p-xylene - xCIP, CIP modified with chloroacetyl chloride - eCIP) (see Figure 1).

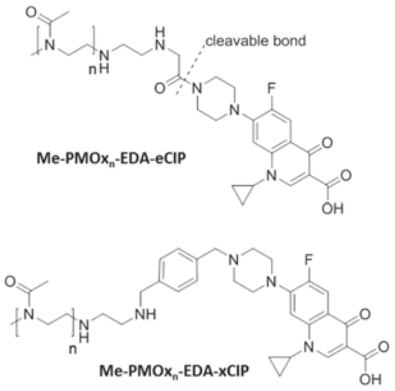

Figure 1: Structures of Poly(2-methyloxazoline) (PMOx)-Ciprofloxacin (CIP)-Conjugates with the two different linkers eCIP and xCIP.

The antibacterial activity of the conjugates against a number of bacterial strains shows a great dependence on the nature of the spacer. Me-PMOx$_{39}$-EDA-eCIP, containing a potentially cleavable linker, does not exhibit a molecular weight dependence on antibacterial activity in contrast to Me-PMOx$_{27}$-EDA-xCIP. The resistance formation of both conjugates against the Gram-positive bacterium *Staphylococcus aureus* and the Gram-negative bacterium *Escherichia coli* was investigated. This was done by letting the bacterial cells cultivate in the presence of half the concentration that inhibits their growth (MIC). The MIC value of the regrown cells was determined and the experiment was repeated. As seen in Figure 2, in the case of CIP the experiment leads to bacterial cells that are several orders of magnitude less susceptible to the antibiotic in only 9 days. Both conjugates showed potential of significantly delaying the formation of resistant bacteria compared to the unmodified CIP. While the xCIP linker was effective in the case of *S. aureus*, the eCIP linker afforded delay in resistance formation in case of *E. coli*. Closer inspection of a possible resistance mechanism by genome sequencing of the topoisomerase IV region of resistant *S. aureus* revealed that this bacterium mutates at the same position when building up resistance to CIP and to Me-PMOx$_{27}$-EDA-xCIP. However, the *S. aureus* cells that became resistant against the polymer conjugate are fully susceptible to CIP. Thus, conjugation of CIP with PMOx seems to alter the resistance mechanism.

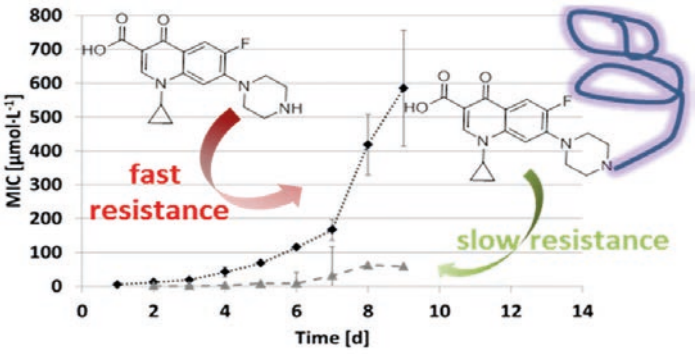

Figure 2: Resistance test for CIP and the conjugate Me-PMOx$_{27}$-EDA-xCIP for *S. aureus*.

This shows that polymer antibiotic conjugation is a tool to lower the resistance formation of antibiotics.

Contact:
martin.schmidt2@tu-dortmund.de
alina.romanowska@tu-dortmund.de
joerg.tiller@tu-dortmund.de

Publications:
M. Schmidt, A. Romanovska, Y. Wolf, T.-D. Nguyen, A. Krupp, H. L. Tumbrink, J. Lategahn, J. Volmer, D. Rauh, S. Luetz, C. Krumm, J. C. Tiller, Bioconjugate Chemistry 2018, 29 (8), 2671-2678.

Non-amphiphilic Polymers as Solubilizer for Enzymes in Organic Solvents

Cheap and reversible method to make enzymes organo-soluble

Montasser Hijazi, Christian Krumm, Joerg C. Tiller

Enzymes are highly active and selective biocatalysts in their natural solvent water. However, they also work in organic solvents, but are dramatically less active in their free form. An effective possibility to activate enzymes is to dissolve them in organic solvents. Surfactants and amphiphilic polymers suited for "dissolving" enzymes in organic solvents cover the whole protein surface by weak hydrophobic and/or ionic interactions, while polymers in covalent PECs are attached to the protein via their terminus. In this study, we combine both concepts by using hydrophilic polymers that reversibly bind to proteins only with one end group.

Goal of this work was to render enzymes "organo-soluble" by a reversible binding of poly(2-oxazoline)s to the biocatalysts. This is based on a previous study in which poly(2-methyl-2-oxazoline)s were equipped with a metal complexing 2,2'-iminodiacetate (IDA) end group in order to bind to the protein horseradish peroxidase (HRP) in water. The hypothesis of this study is that such conjugates should be more stable in organic solvents, i.e. they do not dissociate in aprotic solvents and thus they might be "organo-soluble". This was investigated by dissolving IDA-terminated poly(2-oxazoline)s (POx) and enzymes in water, lyophilizing this solution and adding the resulting solid to organic solvents. A series of enzymes that covers a wide range of molecular weights and isoelectric points was conjugated with POx-IDA of different molecular weights and with varying side groups. The proposed generical concept for polymer enzyme conjugates dissolved in organic solvents is shown in Figure 1.

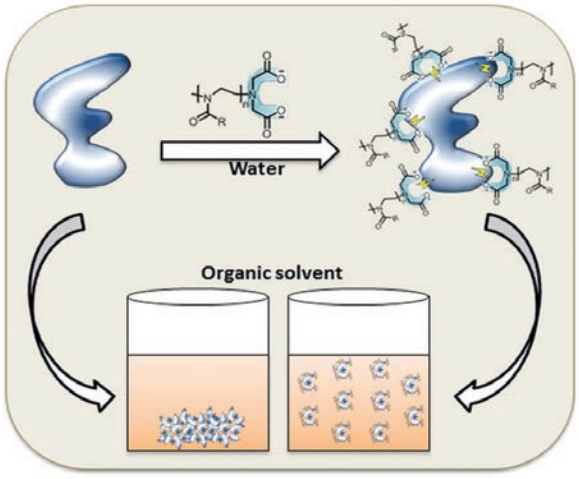

Figure 1: Schematic representation of the proposed generical concept of how polymer enzyme conjugates can be "dissolved" in chloroform.

POx-IDA were shown to form reversible, nano-sized non-covalent polymer enzyme conjugates (PECs). These PECs give clear solutions in organic solvents (see Figure 2). The enzymes Lysozyme, Horse Radish Peroxidase (HRP), Laccase, alpha-Chymotrypsin (CT), Catalase, and Alcohol Dehydrogenase could be solubilized in chloroform and toluene at concentrations of up to 2 mg protein per mL. The PECs of lysozyme with the size of 9.9 nm are comparable with the theoretically size of the single enzyme (D_h lysozyme = 3.94 nm) in the core and two polymers (D_h polymer = 2.9 nm).

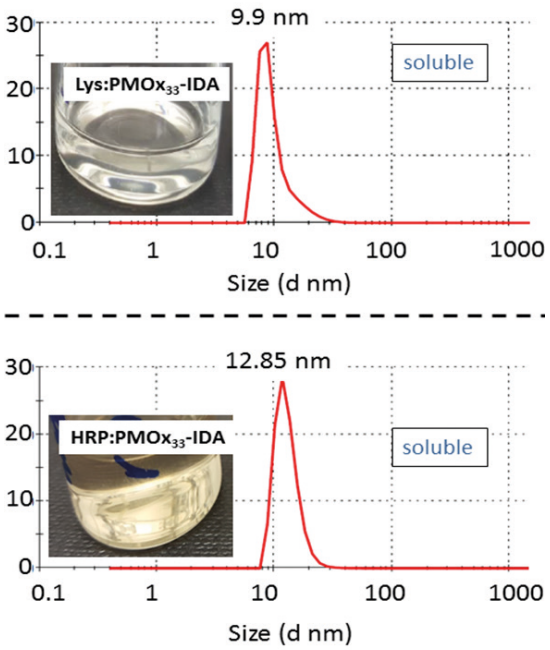

Figure 2: Dynamic light scattering (DLS) of solutions formed by adding PMOx-IDA / enzyme lyophilisates to chloroform. Top: Lysozyme, Bottom: HRP. The enzyme concentrations are 2 mg/ml. The inlets are photographs of the respective solution. The DLS curves are given as number plots.

Laccase, HRP, and CT were shown to survive the transfer into the organic medium and back to water in their active form. The distribution coefficient of the proteins between water and organic solvent was shown to be dependent on the nature of the POx backbone. All three biocatalysts exhibit greatly enhanced activity in the respective organic solvent.

Contact:
montasser.hijazi@tu-dortmund.de
christian.krumm@tu-dortmund.de
joerg.tiller@tu-dortmund.de

Publications:
M. Hijazi, P. Spiekermann, C. Krumm, J. C. Tiller, Biotechnology and Bioengineering 116, 272-282 (2019).

Critically Cross-Linked Syndiotactic Polypropylene

An Ultimate Shock- and Energy-Absorbing Material

Thomas Raidt, Panusa Santhirasegaran, Robin Hoeher, Joerg C. Tiller, Frank Katzenberg

Safety engineering concepts usually use energy dissipation via plastic deformation (e.g. in cars) or frictional loss (e.g. in climbing ropes) for controlled deceleration of fast moving objects. Spider webs master this task much more effective than any other material or established technical conception by using dragline silk. We found, that critically cross-linked syndiotactic polypropylene is capable of mimicking dragline silk, since it transforms itself from a fully amorphous rubber-like into a semicrystalline, high modulus and high strength state upon stretching to large elongations and retains the latter after removing the stretching force.

Syndiotactic polypropylene (x-sPP) was critically cross-linked right at the borderline between thermoplastic and elastomer, quenched to a fully amorphous state and, subsequently, tested using a falling weight experiment. We found, that x-sPP causes by far the lowest impact force (12.8 N) compared to the reference samples, Dyneema (33.6 N) and natural rubber (23.9 N) and that it is able to absorb more than 99% of the kinetic energy of the used deadweight within 2 s and only 4 oscillations (see Fig. 1).

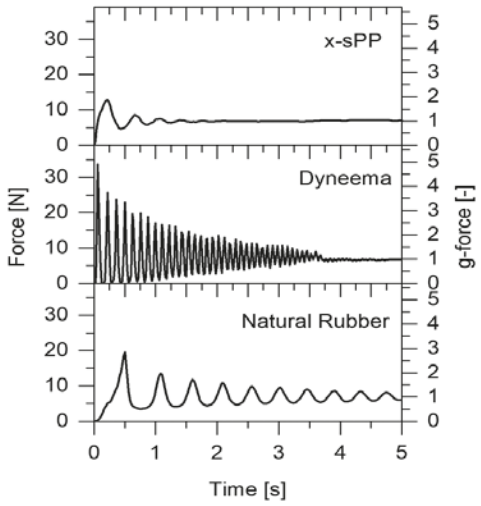

Figure 1: Force/g-force vs. time plots of the falling weight experiments with safety lines of x-sPP (top), Dyneema (middle) and NR (bottom). (Deadweight 0.7 kg, drop height 80 mm, sample length 90 mm).

Since it is known from aerospace and car crash tests, that the change of acceleration (jerk), to which a body is exposed to, is more dangerous than the magnitude of acceleration or impact force, the jerks of the first impact were determined. While the jerks of x-sPP (20.4 g/s) and natural rubber (17.0 g/s) are far below the critical value of 120 g/s, from which serious injuries to humans must be expected, the jerk of Dyneema (199.6 g/s) clearly exceeds this value.

Although the maximum jerk of x-sPP is slightly higher than that of the rubber reference for a deadweight of 0.7 kg and a drop height of 80 mm, this important quantity stays nearly constant or is even getting smaller for x-sPP with increasing mass of the deadweight or drop height. Thus, x-sPP is the more able to avoid harmful jerks the more it is loaded.

In summary, amorphous x-sPP merges the damping capability of high modulus, high strength materials such as Dyneema with the absorption potential of elastomeric materials such as natural rubber (see Fig. 2). Thus, x-sPP is able to compete with the excellent properties of spider drag-line silk and is well suited for applications such as safety lines.

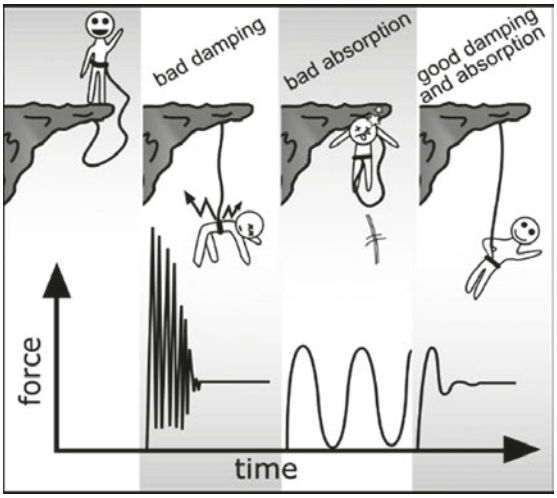

Figure 2: The combination of good impact damping and good energy absorption is required for an excellent safety-line.

Contact:
frank.katzenberg@tu-dortmund.de
joerg.tiller@tu-dortmund.de

Publications:
T. Raidt, P. Sanhirasegaran, R. Hoeher, F. Katzenberg, J. C. Tiller, Macromolecular Chemistry and Physic 220(2), 1800274 (2019).

High Strain Storing, High Temperature Shape Memory Polymers with Full Recovery

Thomas Raidt, Martin Schmidt, Joerg C. Tiller, Frank Katzenberg

Shape memory polymers (SMPs) became an inexpensive and efficient alternative to well-known metallic shape memory alloys, except for applications that require a sensory or actuatory shape change at temperatures exceeding 200 °C. The few known SMPs with trigger temperatures above 200 °C suffer from poor recovery ratios, low storable strains, or broad trigger temperature ranges. Now, we managed to realize the first high temperature SMPs with trigger temperatures distinctly above 200 °C, narrow trigger ranges and fully recoverable stored strains of up to 200%.

The capability of an SMP of storing fully recoverable high strains usually requires a covalently cross-linked network while a narrow trigger range can be realized by utilizing a narrow phase transition for the shape change. That is why we chose the semi-aromatic polyesters polyethylene terephthalate (PET) and polybutylene terephthalate (PBT) with melting temperatures of 254 °C and 225 °C, respectively. In order to avoid from viscous flow during programming/triggering of the SMPs and, thus, enable high recovery ratios and preferably high storable strains at temperatures above the respective crystal melting temperatures, we searched for an efficient cross-linking strategy.

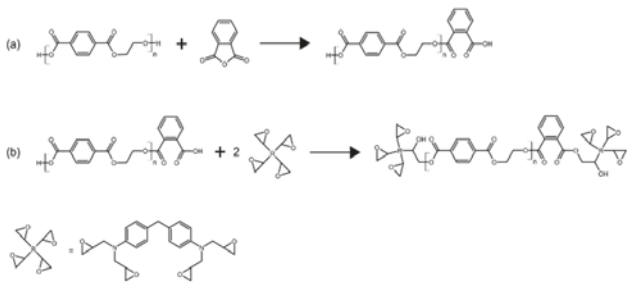

Figure 1: Cross-linking reaction using the example of PET.

Targeting an end-group cross-linking, the tetra-functional epoxy 4,4' methylenebis (*N,N* diglycidylaniline) (TGDDM) was used, which is a very reactive compound toward macromolecules containing carboxyl end-groups but not hydroxyl end-groups. Since in the case of PET and PBT both species are present, the residual hydroxyl end-groups were converted to carboxyl end-groups by the use of phthalic anhydride (PA). The reaction pathway is shown in Figure 1. PET and PBT were mixed with PA and TGDDM, extruded in a twin extruder, compression-molded to thin sheets, and thermally cured at 270 °C for 10 min under exclusion of air. In order to obtain highly stretchable networks the cross-linking agents were varied until the minimum amount was found that is required for critical cross-linking right at the borderline between thermoplastic and elastomer.

The shape memory properties of the critically cross-linked x-PET- and x-PBT were explored over ten shape memory cycles. It was found that both networks were capable of fixing the complete applied strain of 200% in a temporary shape, which indicates a fixity ratio of 100%. Since the samples fully recovered their original length after reheating to the previously applied programming temperature, both samples exhibit also a recovery ratio of 100%. These shape memory parameters were found to be unchanged even after 10 programming/triggering cycles.

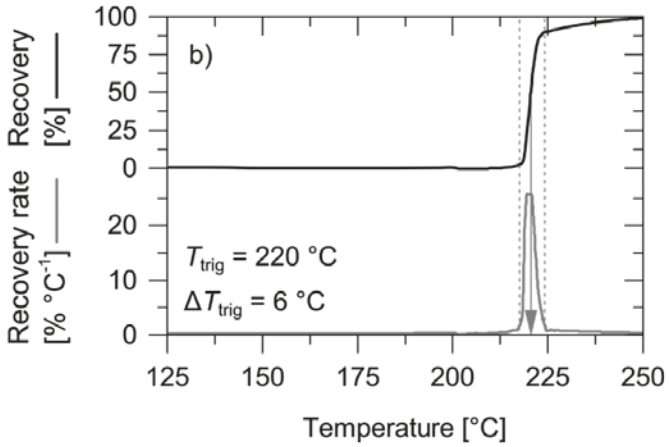

Figure 2: Trigger process shown exemplarily for x-PBT.

The average trigger temperatures T_{trig} were determined for x-PET to 236 °C and x-PBT to 220 °C. Investigation of the trigger process revealed for x-PET and x-PBT trigger ranges ΔT_{trig} of 22 °C and 6 °C, respectively, which are in good accordance with the melting ranges of the uncross-linked starting polymers.

Publications:
T. Raidt, M. Schmidt, J. C. Tiller, F. Katzenberg
Macromolecular Rapid Communications 39 (6), 1700768 (2018).

Contact:
frank.katzenberg@tu-dortmund.de
joerg.tiller@tu-dortmund.de

Artificial Metalloenzymes based on Acylated lysozyme and Bovine Serum Albumin

Artificial enzymes prepared from cheap proteins

Melanie Leurs, Sascha Wilhelm, Joerg C. Tiller

Efficient catalysts that lead to pure product is one important way make chemistry greener, and thus to save energy and CO_2 release by minimizing elaborate downstream processes. One possibility to obtain such catalysts is the reprogramming of enzymes to let them catalyze non-natural reactions and still use the chiral environment of proteins to obtain enantiopure products. Such, so-called artificial metalloenzymes (AMEs) are usually specific and expensive enzymes that are modified with metals in their active site. Here, we show that it is also possible to render cheap proteins into AMEs.

The objective of this work was to convert inexpensive proteins into AMEs for the enantioselective synthesis in organic solvents. The rational is that blocking the primary amino groups by acylation might block the outer non-chiral binding sites for heavy metal catalysts and force those into less accessible, but likely better chirality-controlling sites of the protein, (Figure 1).

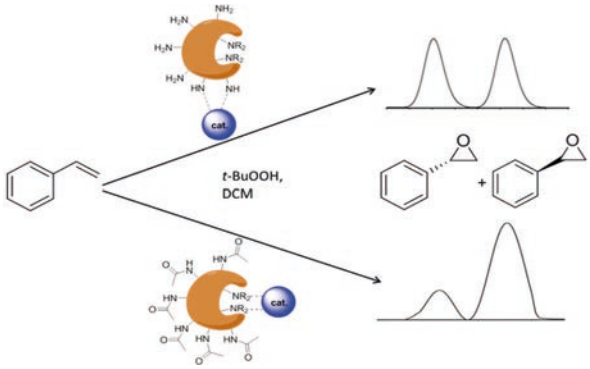

Figure 1: Concept of preparing artificial metalloenzymes from proteins by acylation of the surface amino groups followed by metallization and thus affording an enantioselective active center.

It was found that fully acylated lysozyme (LYS) and bovine serum albumin (BSA) could be modified with osmate to render these proteins into enantioselective catalysts for the dihydroxylation of styrene.

Taking a look at Figure 2, top shows that the best enantioselectivity in the dihydroxylation of styrene with lysozyme based AME's was achieved with some 98 %ee (*S*) by using Os-LYS acylated with hexanoic acid (HA) at 0 °C. The respective Os-LYS derivative with propionic acid (PA) also affords a high enantioselectivity with 95 %ee (*S*) under the same reaction conditions, but about 4-fold lower activity. In comparison to the latter Os-LYS modified with acetic acid (AA) shows the lowest enantioselectivity with 57 %ee (*S*) and also a lower activity. Increasing the temperature to 20 °C expectedly increases the activity by a factor of 2-5 and lowers the enantioselectivity. Os-LYS-HA and OS-LYS-PA retain enantioselectivities of 88 and 85 %ee (*S*), respectively.

Further increasing the reaction temperature to 40 °C leads to greatly enhanced activities, but the enantioselectivity drops to below 40 %ee (*S*) in both cases.

Similar results were found for the respective BSA derivatives (Figure 2, bottom).

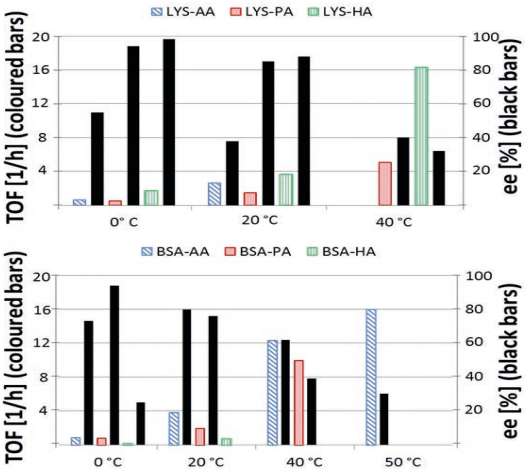

Figure 2: Comparison of turnover frequency (TOF, coloured bars) and enantiomeric excess (ee, (*S*)-enantiomer, black bars) of the asymmetric dihydroxylation catalyzed by osmate based AME's (pH 7, fully acylated) with an MPR of 1 at different temperatures. The reaction was carried out with 0.03 µmol/mL protein conjugate, 0.03 µmol/mL $K_2O_sO_2(OH)_4$, 110 µmol/mL *t*BuOOH and 100 µmol/mL styrene. The reaction times were adjusted to previously determined surviving times of a respective Os-laccase-PMOx under the used conditions and temperatures, being 7 d at 0 °C, 72 h at 20 °C, and 24 h at 40 °C. The TOF is defined as µmol product per µmol protein per hour.

It could also be shown that these new AMEs have potential to perform enantioselective epoxidations with high activity.

Contact:
melanie.leurs@tu-dortmund.de
sascha.wilhelm@tu-dortmund.de
joerg.tiller@tu-dortmund.de

Publications:
M. Leurs, B. Dorn, S. Wilhelm, M. Manisegaran, J. C. Tiller
Chemistry - A European Journal 24 (42), 10859-10867 (2018).

Publications 2018 - 2016

2018

Peer Reviewed Articles

- N. Rauner, C. Mueller, S. Ring, S. Boehle, A. Strassburg, C. Schoeneweiss, M. Wasner, J. C. Tiller
  A Coating that Combines Lotus-Effect and Contact-Active Antimicrobial Properties on Silicone
  Advanced Functional Materials 28 (29) 1801248 (2018)

- M. Leurs, B. Dorn, S. Wilhelm, M. Manisegaran, J. C. Tiller
  Multicore Artificial Metalloenzymes Derived from Acylated Proteins as Catalysts for the Enantioselective Dihydroxylation and Epoxidation of Styrene Derivatives
  Chemistry 24 (42) 10859 -10867 (2018)

- M. Schmidt, A. Romanovska, Y. Wolf, T. - D. Nguyen, A. Krupp, H. L. Tumbrink, J. Lategahn, J. Volmer, D. Rauh, S. Luetz, C. Krumm, J. C. Tiller
  Insights into the Kinetics of the Resistance Formation of Bacteria against Ciprofloxacin Poly(2-methyl-2-oxazoline) Conjugates
  Bioconjugate Chemistry 29 (8), 2671-2678 (2018)

- L. Richter, M. Hijazi, F. Arfeen, C. Krumm, J. C. Tiller
  Telechelic, Antimicrobial Hydrophilic Polycations with Two Modes of Action
  Macromolecular Bioscience 18 (4), 1700389 (2018)

- M. Hijazi, C. Krumm, S. Cinar, L. Arns, W. Alachraf, W. Hiller, W. Schrader, R. Winter, J. C. Tiller
  Entropically driven Polymeric Enzyme Inhibitors by End-Group directed Conjugation
  Chemistry A European Journal 24 (18), 4523-4527 (2018)

- T. Raidt, M. Schmidt, J. C. Tiller, F. Katzenberg
  Cross-Linking of Semi-Aromatic Polyesters Towards High Temperature Shape Memory Polymers with Full Recovery
  Macromolecular Rapid Communications 39 (6), 1700768 (2018)

- D. E. Apostolides, C. S. Patrickios, T. Sakai, M. Guerre, G. Lopez, B. Ame´duri, V. Ladmiral, M. Simon, M. Gradzielski, D. Clemens, C. Krumm, J. C. Tiller, B. Ernould, J. - F. Gohy
  Near-Model Amphiphilic Polymer Conetworks Based on Four-Arm Stars of Poly(vinylidene fluoride) and Poly(ethylene glycol): Synthesis and Characterization
  Macromolecules 51 (7), 2476-2488 (2018)

2017

Peer Reviewed Articles

- A. Strassburg, J. Petranowitsch, F. Paetzold, C. Krumm, E. Peter, M. Meuris, M. Köller, J. C. Tiller
  Cross-Linking of a Hydrophilic, Antimicrobial Polycation toward a Fast-Swelling, Antimicrobial Superabsorber and Interpenetrating Hydrogel Networks with Long Lasting Antimicrobial Properties
  Applied Materials & Interfaces 9 (42), 36573-36582 (2017)

- M. Leurs, J. C. Tiller
  Chapter 17 - Nanoarmored Enzymes for Organic Enzymology: Synthesis and Characterization of Poly(2-Alkyloxazoline)-Enzyme Conjugates
  Methods in Enzymology 590, 413-444 (2017)

- C. Krumm, H. Montasser, S. Trump, S. Saal, L. Richter, G. G. F. K. Noschmann, T.-D. Nguyen, K. Preslikoska, T. Moll, J. C. Tiller
  Highly active and selective telechelic antimicrobial poly(2-oxazoline) copolymers
  Polymer 118, 107-115 (2017)

- N. Rauner, M. Meuris, M. Zoric, J. C. Tiller
  Enzymatic mineralization generates ultrastiff and tough hydrogels with tunable mechanics
  Nature 543, 407-410 (2017)

- R. Plothe, I. Sittko, F. Lanfer, M. Fortmann, M. Roth, V. Kolbach, J. C. Tiller
  Poly(2-ethyloxazoline) as matrix for highly active electrospun enzymes in organic solvents
  Biotechnology and Bioengineering 114 (1), 39-45 (2017)

- C. Krumm, J. C. Tiller
  Chapter 15 Antimicrobial Polymers and Surfaces - Natural Mimics or Surpassing Nature?
  Bio-inspired Polymers, The Royal Society of Chemistry, 490-522 (2017)

- T. Raidt, R. Hoeher, F. Katzenberg, J. C. Tiller
  Multiaxial Reinforcement of Cross-Linked Isotactic Polypropylene upon Uniaxial Stretching
  Macromolecular Materials and Engineering 302, 1600308 (2017)

- M. Schmidt, T. Raidt, S. Ring, S. Gielke, C. Gramse, S. Wilhelm, F. Katzenberg, C. Krumm, J. C. Tiller
  Investigations on "near perfect" poly(2-oxazoline) based amphiphilic polymer conetworks with a crystallizable block
  European Polymer Journal 88, 562-574 (2017)

Publications 2018 - 2016

2016

Peer Reviewed Articles

- T. Raidt, R. Hoeher, M. Meuris, F. Katzenberg, J. C. Tiller
  Ionically Cross-Linked Shape Memory Polypropylene
  Macromolecules 49 (18), 6918-6927 (2016)

- R. Plothe, I. Sittko, F. Lanfer, M. Fortmann, M. Roth, V. Kolbach, J. C. Tiller
  Poly(2-ethyloxazoline) as matrix for highly active electrospun enzymes in organic solvents
  Biotechnology and Bioengineering 114 (1), 39-45 (2016)

- R. Hoeher, T. Raidt, F. Katzenberg, J. C. Tiller
  Heating Rate Sensitive Multi-Shape Memory Polypropylene: A Predictive Material
  ACS Applied Materials & Interfaces 8, 13684-13687 (2016)

- F. Katzenberg, J. C. Tiller
  Shape Memory Natural Rubber
  Journal of Polymer Science Part B: Polymer Physics 54, 1381-1388 (2016)

- M. Leurs, P. S. Spiekermann, J. C. Tiller
  Optimization of and Mechanistic Considerations for the Enantioselective Dihydroxylation of Styrene Catalyzed by Osmate-Laccase-Poly(2-Methyloxazoline) in Organic Solvents
  ChemCatChem 8 (3), 593-599 (2016)

- N. Gushterov, F. Doghieri, D. Quitmann, E. Niesing, F. Katzenberg, J. C. Tiller, G. Sadowski
  VOC Sorption in Stretched Cross-Linked Natural Rubber
  Industrial & Engineering Chemistry Research 55 (26), 7191-7200 (2016)

- W. Tillmann, L. Hagen, F. Hoffmann, M. Dildrop, A. Wibbeke, V. Schöppner, V. Resonnek, M. Pohl, C. Krumm, J. C. Tiller, M. Paulus, C. Sternemann
  The detachment behavior of polycarbonate on thin films above the glass transition temperature
  Polymer Engineering & Science 56 (7), 786-797 (2016)

- S. Sommer, T. Raidt, B. M. Fischer, F. Katzenberg, J. C. Tiller, M. Koch
  THz-Spectroscopy on High Density Polyethylene with Different Crystallinity
  Journal of Infrared, Millimeter, and Terahertz Waves 37 (2), 189-197 (2016)

- A. Drahten, J. Reiber, C. Krumm, M. Meuris, J. C. Tiller, C. M. Niemeyer, S. Brakmann
  Genetic Engineering of Silaffin-Like Peptides for Binding and Precipitating Siliceous Materials
  Chemistry Select 1 (15), 4765-4771 (2016)

Patents

- J. C. Tiller, F. Katzenberg, R. Hoeher, T. Raidt
  Method for producing an oriented polymer
  Eur. Pat. Appl. (2016), EP 3098059 A1 20161130

- J. C. Tiller, C. Mueller, N. Rauner
  Derivatized silicon dioxide nanoparticles coated with quaternary ammonium salts contg. a silane group and long alkyl chain exhibiting biocidal action
  Ger. Offen. (2015), DE 102014108278 A1 20151217

- J. C. Tiller, D. Quitmann, F. Katzenberg
  Polymer network comprising shape memory polymers used as a sensor or force element
  Eur. Pat. Appl. (2014), EP 2783834 A1 20141001

Bioprocess Engineering (BPT)

Catalytic Promiscuity of cGAS

Enzymatic synthesis of novel compounds

Katrin Rosenthal, Martin Becker, Markus Nett, Stephan Lütz

The cyclic dinucleotide 2'3'-cGAMP activates the production of type I interferons and is part of the innate immune system in mammalians. 2'3'-cGAMP and derivatives of this important second messenger are highly valuable for pharmaceutical applications. However, the production of these compounds requires complex, multistep synthesis. Therefore, the enzymatic synthesis of cyclic dinucleotide derivatives was studied. In the cytosol of human cells, cyclic GMP-AMP synthase (cGAS) catalyzes the synthesis of 2'3'-cGAMP. This enzyme was used in order to synthesize a series of non-natural cyclic dinucleotides. Most tested substrates were accepted demonstrating the promiscuity of cGAS.

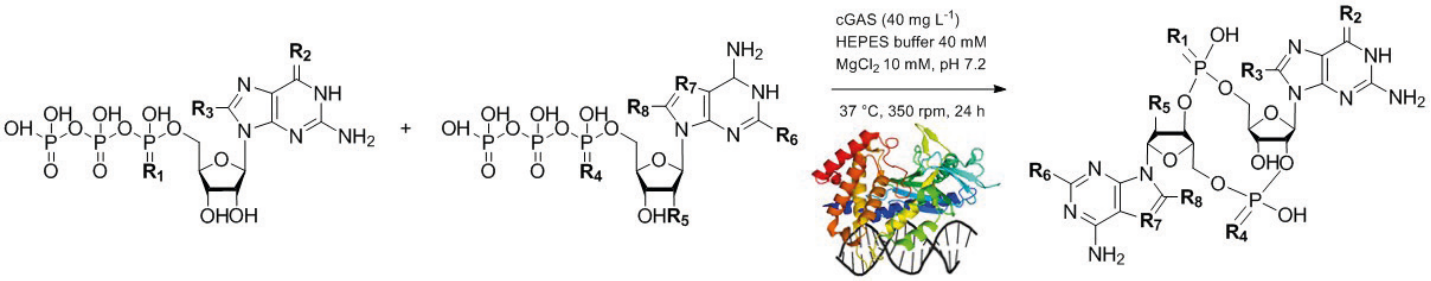

R_1 = O, S; R_2 = O, S, H; R_3 = H, Br; R_4 = O, S; R_5 = OH, F, NH_2, H; R_6 = H, Cl, SMe, NH_2; R_7 = N, C; R_8 = H, Br, Cl, NH_2, N_3

Figure 1: cGAS catalyzed conversion of substrate derivatives into cyclic dinucleotide derivatives.

The enzyme cGAS was produced by heterologous expression in *E. coli* BL21 (DE3) pLysS pET28(a) *SUMO thscGAS* and was used *in vitro* for the synthesis of 2'3'-cGAMP and various analogs (Figure 1). The substrate derivatives were chosen with modifications at different positions in the base, ribose or phosphate. Each of the 16 substrate derivatives was tested with its natural counterpart to evaluate the individual effect of any position-dependent variation.

The specific activities and conversions within 24 h were calculated for all reactions (Figure 2). No products were synthesized for the substrates 2'd-7-CH-ATP, 2'-NH_2-ATP and Thio-ATP. Specific activities between 40 and 43 mU mg^{-1} were determined for the derivatives 8-Br-dATP, 8-Br-ATP and Thio-GTP with conversions between 56 and 93 %. These values are in the range of 2'3'-cGAMP synthesis (52 mU mg^{-1}). The highest specific activity of 136 mU mg^{-1} for the product synthesis from 8-Br-GTP was significantly higher compared to the natural product synthesis. The addition of a bromide at the 8' position of the base seems to be preferred for both, ATP and GTP, substrates.

These results show the substrate promiscuity of cGAS which can be applied to obtain 2'3'-cGAMP analogs. In future, the availability of cyclic dinucleotide derivatives might enable to get a more detailed insight into the meaning of cyclic dinucleotides as second messenger.

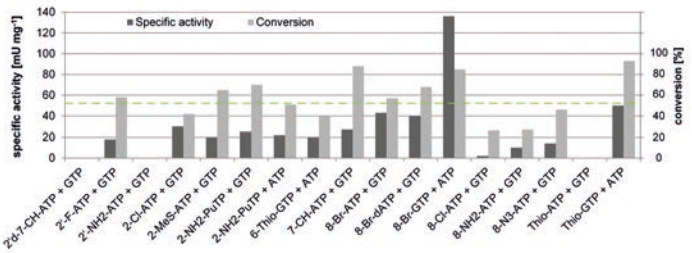

Figure 2: Specific activities and conversions of cGAS catalyzed reactions of 16 derivatives with their natural counterpart. Dark grey bars represent the specific activities [mU mg^{-1}], light grey bars represent conversions after 24 h [%], green dashed line represents the specific activity of cGAS catalyzed conversion of ATP and GTP into 2'3'-cGAMP as reference reaction.

Contact:
katrin.rosenthal@tu-dortmund.de
stephan.luetz@tu-dortmund.de

Publications:
K. Rosenthal, M. Becker, M. Nett, S. Lütz, Catalytic promiscuity of cGAS: A facile enzymatic synthesis of 2'3' linked cyclic dinucleotides, submitted manuscript.

Publications 2018 - 2016

2018

Proceedings & Book Chapters

- K. Rosenthal, S. Lütz
  Recent developments and challenges of biocatalytic processes in the pharmaceutical industry
  Current Opinion in Green and Sustainable Chemistry 11, 58-64 (2018)

- A. Worsch, F. K. Eggimann, M. Girhard, C. J. von Bühler, F. Tieves, R. Czaja, A. Vogel, C. Grumaz, K. Sohn, S. Lütz, M. Kittelmann, V. B. Urlacher
  A novel cytochrome P450 monooxygenase from Streptomyces platensis resembles activities of human drug metabolizing P450s
  Biotechnology & Bioengineering 115 (9), 2156-2166 (2018)

- M. Schmidt, A. Romanovska, Y. Wolf, T. - D. Nguyen, A. Krupp, H. Tumbrink, J. Lathgahn, J. Volmer, D. Rauh, S. Lütz, C. Krumm, J. C. Tiller
  Insights into the kinetics of the resistance formation of bacteria against ciprofloxacin poly(2-methyl-2-oxazoline) conjugates
  Bioconjugate Chemistry 29 (8), 2671-2678 (2018)

Books & Booksarticles

- J. Schwarz, J. Volmer, S. Lütz
  Enzyme in der chemischen und pharmazeutischen Industrie
  In: K.E. Jäger, A. Liese, C. Syldatk (eds), Einführung in die Enzymtechnologie. Springer Spektrum, Berlin, Heidelberg (2018)

Presentations & Poster

- J. Schwarz, S. Lütz
  Influence of Nutrient Limitation on the Production Profile of Bacteria with High Biosynthetic Potential
  European Conference on Natural Products, 02.-05. September 2018, Frankfurt am Main

- K. Rosenthal, M. Becker, J. Rolf, S. Lütz
  Enzymatic synthesis of cyclic dinucleotides
  Emerging Trends in Natural Product Biotechnology, 20.-21. September 2018, Dortmund

- A. Steinmann, C. Dickmeis, A. Kohl, D. Decembrino, S. Wohlgemuth, M. Girhard, S. Lütz
  Development of an Analytical Method for Metabolic Profiling of Monolignol- and Lignan-Producing *Escherichia coli*
  Emerging Trends in Natural Product Biotechnology, 20.-21. September 2018, Dortmund

- J. Rolf, M. Julsing, S. Lütz
  Biotechnological monoterpene production in *Escherichia coli*
  ProcessNet-Jahrestagung, 10.-13. September 2018, Aachen

- K. Rosenthal, M. Becker, J. Rolf, S. Lütz
  Enzymatic synthesis of cyclic dinucleotides
  ProcessNet-Jahrestagung, 10.-13. September 2018, Aachen

2017

Peer Reviewed Journal Papers

- S. Lütz
  The First Biocatalytic Carbon-Silicon Bond Formation
  Angewandte Chemie 56 (12), 3140-3141 (2017)

- C. Grumaz, Y. Vainshtein, P. Kirstahler, S. Lütz, M. Kittelmann, K. Schroer, F. K. Eggimann, R. Czaja, A. Vogel, T. Hilberath, A. Worsch, M. Girhard, V. B. Urlacher, M. Sandberg, Kai Sohn
  Draft Genome Sequences of Three Actinobacteria Strains Presenting New Candidate Organisms with High Potentials for Specific P450 Cytochromes.
  Genome Announcements 5 (28), e00532-17 (2017)

- K. Rosenthal, V. Oehling, C. Dusny, A. Schmid
  Beyond the bulk: disclosing the life of single microbial cells
  FEMS Microbiology Reviews 41 (6), 751-780 (2017)

- E. Theodosiou, M. Breisch, M. K. Julsing, F. Falcioni, B. Bühler, A. Schmid
  An artificial TCA cycle selects for efficient α-ketoglutarate dependent hydroxylase catalysis in engineered *Escherichia coli*
  Biotechnology and Bioengineering 114 (7), 1511-1520 (2017)

- R. Kourist, J. Gonzalez-Sabin, B. Siebers, M. Julsing
  Editorial: Applied microbiology for chemical synthesis
  Frontiers in Microbiology 8,1931 (2017)

- M. Kadisch, M. K. Julsing, M. Schrewe, N. Jehmlich, B. Scheer, M. von Bergen, A. Schmid, B. Bühler
  Maximization of cell viability rather than biocatalyst activity determines whole-cell ω-oxyfunctionalization performance.
  Biotechnology and Bioengineering 114 (4), 874-884 (2017)

- C. Willrodt, B. Halan, L. Karthaus, J. Rehdorf, M. K. Julsing, K. Bühler, A. Schmid
  Continuous multistep synthesis of perillic acid from limonene by catalytic biofilms under segmented flow
  Biotechnology and Bioengineering 114 (2), 281-290 (2017)

- J. Volmer, A. Schmid, B. Bühler
  The application of constitutively solvent-tolerant P. taiwanensis VLB120ΔCΔttgV for stereospecific epoxidation of toxic styrene alleviates carrier solvent use
  Biotechnology Journal 12,1600558 (2017)

- L. M. Schmitz, K. Rosenthal, S. Lütz
  Enzyme-Based Electrobiotechnological Synthesis
  In: F. Harnisch, D. Holtmann (eds), Advances in biochemical engineering/ biotechnology, Springer Nature Switzerland, Cham (2017)

Publications 2018 - 2016

2016

Peer Reviewed Journal Papers

- M. Antunes, F. Eggimann, M. Kittelmann, S. Lütz, S. P. Hanlon, B. Wirz, T. Bachler, M. Winkler
  Human xanthine oxidase recombinant in *E. coli*: A whole cell catalyst for preparative drug metabolite synthesis
  Journal of Biotechnology 235, 3-10 (2016)

- K. Lange, A. Schmid, M. K. Julsing
  Δ9-Tetrahydrocannabinolic acid synthase: the application of a plant secondary metabolite enzyme in biocatalytic chemical synthesis
  Journal of Biotechnology 233, 42-48 (2016)

- C. Willrodt, A. Hoschek, B. Bühler, A. Schmid, M. K. Julsing
  Decoupling production from growth by magnesium sulfate limitation boosts de novo limonene production
  Biotechnology and Bioengineering 113 (6), 1305-1314 (2016)

- N. Ladkau, M. Aßmann, M. Schrewe, M. K. Julsing, A. Schmid, B. Bühler
  Efficient production of the Nylon 12 monomer ω-aminododecanoic acid methyl ester from renewable dodecanoic acid methyl ester with engineered *Escherichia coli*
  Metabolic Engineering, 36, 1-9 (2016)

Chemical Reaction Engineering (CVT)

Slug Velocity in Multiphase Capillary Flows

David Hellmann, David W. Agar

Micro process engineering offers the potential to increase the efficiency of different small scale processes, consequently reducing resource consumption and waste production. The most promising multiphase flow in micro process engineering is slug flow where the different phases form small bubbles in a regular sequence. The development of such microstructured devices faces various challenges, among those the slug velocity in the microreactor which is crucial to determine the performance of the system for reaction and extraction.

Multiphase flow is not a new concept in the field of micro process engineering. Biphasic systems either gas-liquid or liquid-liquid are well understand and used for reaction or extraction. Particle handling on small scales is also possible either for particle synthesis or catalytic purposes. Triphasic flow, where a gas slug and a liquid slug are present in an additional liquid phase is a relatively new field, which offers the potential to combine reaction and extraction or complex reaction networks in one apparatus, further increasing the overall process efficiency. An example of a triphasic slug flow is shown in figure 1.

Figure 1: Gas-liquid-liquid triphasic slug flow from right to left in a 1 mm inner diameter capillary. Hexanol (red), Water (blue), Nitrogen (with).

Slug flow in capillaries can occur in two different ways, as wetting flow where a small liquid film of the wetting phase covers the capillary wall and as nonwetting flow where every phase has contact to the wall. In the nonwetting case, the velocity of each phase is equal to the average velocity in the capillary. In contrast to this, the slug velocity in the wetting case differs from the average velocity as shown in figure 2.

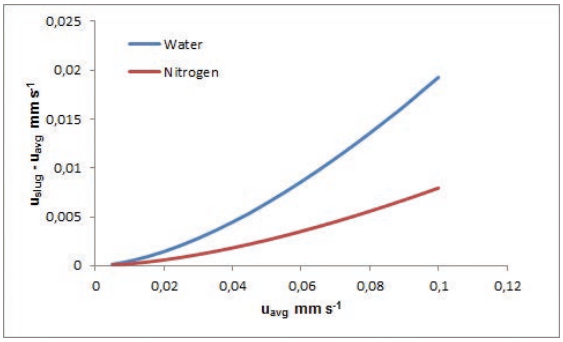

Figure 2: Comparison of nitrogen and water slug velocity derivation from average velocity for the hexanol, water and nitrogen system.

A new calculation method for the triphasic system was developed based on existing biphasic models. In contrast to the biphasic case, the triphasic slug velocity can differ depending on the ratio of gas and disperse liquid phase which normally have different biphasic velocities (Fig. 2). The new model takes this into account and has good accuracy with different systems and different disperse phase ratios (Fig. 3). The good velocity determination allows a accurate determination of the mass transfer and residence time and thus allowing a better prediction of the reactor performance.

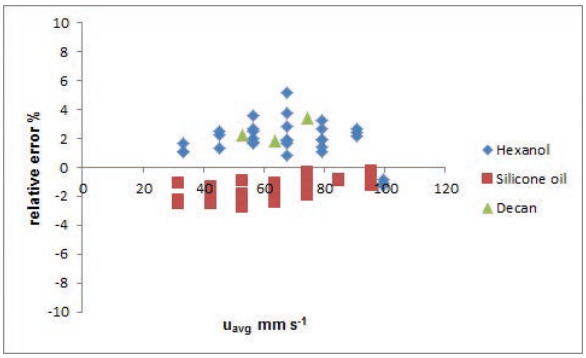

Figure 3: Relative error between experiment and calculated triphasic velocity over the nitrogen to water volume flow ratio.

Contact:
david.hellmann@tu-dortmund.de
david.agar@tu-dortmund.de

Highly Heat Integrated Adsorber Concepts for use in Direct Air Capture Applications

Carsten Drechsler, David W. Agar

The development of human based technologies to reduce the carbon dioxide content in ambient air, summarized under the name direct air capture (DAC), can become a new, strong measure to reach the targets formulated in the Paris Agreement on climate change. However, reasoned in the low carbon dioxide mole fraction in ambient air (~400 ppm) the realization of these technologies faces various challenges, among those especially the high carbon dioxide-specific energy demand of thermally driven ab- and adsorption processes can be named. Consequently, the design of concepts which allow for a high recovery of energy integration might enable a large scale realization of DAC.

Various energy integration concepts to recover the sorbent's sensible heat, required to change its temperature in thermally driven adsorption processes, have been investigated under the constraints holding for direct air capture applications. Among the latter, especially the concept of a belt and moving bed absorber seems promising. Transforming the cyclic steady state of the adsorption process from the time to the spatial domain, more than 90 % of the sorbent's sensible heat can be recovered. Moreover, the designs proposed ensure high open contact areas to the ambient air, avoiding an energy intensive compression of the latter.

With an high heat integrated adsorber concept at hand the question remains how to process the stream of concentrated carbon dioxide. In contrast to carbon capture and storage concepts (CCS), this work focusses on a chemical conversion of the carbon dioxide (carbon capture and utilization, CCU). In this context, the integration of the highly heat integrated DAC unit in a Power-to-Gas (PtG) concept allows for the production of methane based on carbon dioxide from ambient air and hydrogen, generated by renewable energy sources. Besides, the high heat of reaction, released in the PtG concept can be used to drive the adsorption process, so that the design of an overall autothermal process might be possible.

Detailed numerical simulations show that under idealized conditions an autothermally operating process can be designed. However, the high content of water in ambient air which might favor a co-adsorption of water can have a significant influence on the overall energy balance. Thus, the application of tailor-made sorbents or the design of process based solutions seems required to allow for an application of the proposed concepts.

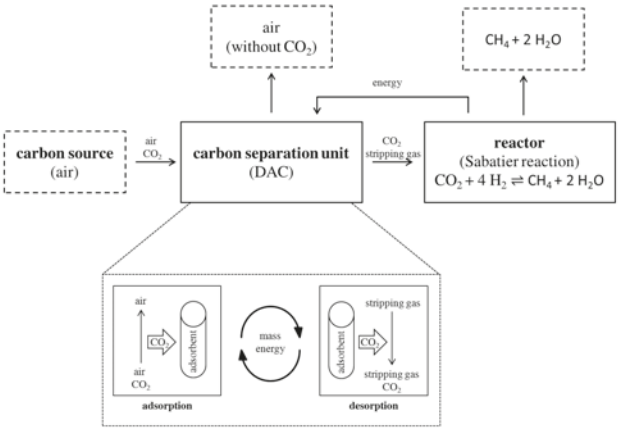

Figure 1: Basic process design of an integrated DAC-PtG concept.

Publications:
C. Asmanoglo, D.W. Agar, Entwicklung wärmeintegrierter Adsorber / Desorber-Konzepte für eine Anwendung in Direct Air Capture (DAC) Technologien, 1. Statuskonferenz zur BMBF Fördermaßnahme CO2Plus, Berlin, Germany (2018).

Contact:
carsten.drechsler@tu-dortmund.de
david.agar@tu-dortmund.de

Publications 2018 - 2016

2018

Proceedings & Book Chapters

- J. González Rebordinos, F. Saki, F. Matulla, D. W. Agar
  Experimental Study on Thermal and Catalytic Hydrogen Bromide Oxidation
  Industrial & Engineering Chemistry Research 2018, 57, 50, 17111-17118

- J. González Rebordinos, R. Tian, N. Robert, D. W. Agar
  Carbon retrieval and purification in the BrOx cycle for CO2-free energy
  Chemical Engineering Research & Design 2018, 140, 283-291

- M. Hussainy, D. W. Agar
  Modeling and optimization of the cyclic steady state operation of adsorptive reactors
  Chinese Journal of Chemical Engineering 2018, 26(6), 1321-1329

- A. A. Munera Parra, C. Asmanoglo, D. W. Agar
  Modelling and Optimization of a Moving-Bed Adsorptive Reactor for the Reverse Water-Gas Shift Reaction
  Computers & Chemical Engineering, 2018, 109, 203–215

- M. G. Gelhausen, D. Lenz, F. Krull, V. Korkmaz, D. W. Agar
  3D Printing for Chemical Process Laboratories II: Measuring Liquid-Solid Mass Transfer Coefficients
  Chemical Engineering Technology 2018, 41(4), 798–805

- M. G. Gelhausen, T. Feuerbach, A. Schubert, D. W. Agar
  3D Printing for Chemical Process Laboratories I: Materials and Connection Principles
  Chemical Engineering Technology 2018, 41(3), 618–627

Presentations & Poster

- C. Drechsler, J. M. Alava, D. W. Agar
  MATLAB Unit Operation potential improvements for academic use
  CAPE-OPEN 2018 annual meeting, Ludwigshafen, Germany, October 2018

- C. Asmanoglo, D. W. Agar
  Entwicklung wärmeintegrierter Adsorber/Desorber-Konzepte für eine Anwendung in Direct Air Capture (DAC) Technologien
  1. Statuskonferenz zur BMBF Fördermaßnahme CO2Plus, Berlin, Germany, April 2018

- C. Schwarz, D. W. Agar
  Reduzierung räumlicher Diskretisierungsfehler in der Volume-of-Fluid-Methode durch analytische Integration der Grenzflächenformfunktion
  Jahrestreffen Bremen der ProcessNet-Fachgruppen MPH & WSUE & CFD, HTT & AuW, KRI, PMT, Bremen, Germany, März 2018

- D. Hellmann, T. Krell, D. W. Agar
  Calculation of slug velocity and pressure drop in multiphase Slug Flow
  International Conference on Micro Reaction Technology - IMRET, Karlsruhe, Germany, Oktober 2018

- D. Hellmann, I. de Oliveira-Goncalves, A. Thierfelder, D. W. Agar
  Generation of uniform gas-liquid-liquid slug flow for micro suspension catalysis
  9th Workshop "Chemical and Biological Micro Laboratory Technology", Ilmenau, Germany, Februar 2018

- M. Wiesehahn, D. W. Agar
  Selective partial oxidation via the BrOx cycle
  Jahrestreffen Reaktionstechnik, Würzburg, Germany Mai, 2018

2017

Proceedings & Book Chapters

- A. A. Munera Parra, D. W. Agar
  Molten metal capillary reactor for the high-temperature pyrolysis of methane
  International Journal of Hydrogen Energy, 42 (19), 13641-13648 (2017)

- A. A. Munera Parra, C. Asmanoglo, D. W. Agar
  Cyclic Steady-State Behavior of a Fixed-Bed Adsorptive Reactor for Reverse Water-Gas Shift Reaction
  Chemical Engineering and Technology, 40 (5), 915-926 (2017)

- J. González Rebordinos, A. H. J. Salten, D. W. Agar
  BrOx cycle: A novel process for CO2-free energy production from natural gas
  BrOx cycle: A novel process for CO2-free energy production from natural gas

- J. González Rebordinos, J. Kampwerth, D. W. Agar
  Flowsheeting and optimisation of the BrOx cycle for CO_2-free energy production from natural gas
  Energy, 133, 327-337 (2017)

- M. G. Gelhausen, S. Yang, M. Cegla, D. W. Agar
  Cyclic mass transport phenomena in a novel reactor for gas–liquid–solid contacting
  AIChE Journal, 63 (1), 208-215 (2017)

Publications 2018 - 2016

2016

Proceedings & Book Chapters

- N. Antweiler, S. Gatberg, G. Jestel, J. Franzke, D. W. Agar
  Noninvasive Sensor for the Detection of Process Parameters for Multiphase Slug Flows in Microchannels
  ACS Sensors, (2016)

- M. G. Gelhausen, S. Yang, M. Cegla, D. W. Agar
  Cyclic mass transport phenomena in a novel reactor for gas–liquid–solid contacting
  AIChe Journal 63(1), 208-215 (2016)

- N. Antweiler, Z. Wang, D. W. Agar
  Evaluation of Ion Exchange Resins for the Esterification of Acrylic Acid with n-Butanol by Polytropic Kinetic Measurement
  Chemie Ingenieur Technik 88 (8), 1095-1101 (2016)

- L. Arsenjuk, F. Kaske, J. Franzke, D. W. Agar
  Experimental investigation of wall film renewal in liquid–liquid slug flow
  International Journal of Multiphase Flow 85, 117-185 (2016)

- J. F. Horstmeier, A. Gomez Lopez, D. W. Agar
  Performance improvement of vacuum swing adsorption processes for CO_2 removal with integrated phase change material
  International Journal of Greenhouse Gas Control 47, 364-375 (2016)

- F. Kaske, S. Dick, S. Aref Pajoohi, D. W. Agar
  The influence of operating conditions on the mass transfer performance of a micro capillary contactor with liquid–liquid slug flow
  Chemical Engineering and Processing: Process Intensification 108, 10-16 (2016)

- A. A. Munera Parra, F. Platte, D. W. Agar
  Multiplicity Regions in a Moving-Bed Reactor: Bifurcation Analysis, Model Extension, and Application for the High-Temperature Pyrolysis of Methane
  Chemie Ingenieur Technik 88(11), 1703-17 (2016)

- A. A. Munera Parra, D. W. Agar
  Molten Metal Capillary Reactor for the High Temperature Pyrolysis of Methane
  International Journal of Hydrogen Energy, (2016)

- A. Behr, D. W. Agar, J. Jörissen, A. J. Vorholt
  Einführung in die Technische Chemie
  2. Aufl., Springer: Berlin. (2016)

Conference Proceedings

- M. Hussainy, D. W. Agar
  Structural and Operational Optimality of Adsorptive Reactors
  Chemical Engineering & Technology 39(11), 2135-2141 (2016)

Process Dynamics and Operations (DYN)

Tube-enhanced Multi-stage Model Predictive Control

A new framework for improved trade-off between complexity and performance

Sankaranarayanan Subramanian, Sergio Lucia, Seyed Ali Baradaran Birjandi, Radoslav Paulen, Sebastian Engell

Model Predictive Control (MPC) is an advanced control technique that is used increasingly in the process industries to handle plants with many controlled and manipulated variables with state and input constraints. MPC uses a model of the system to optimize the future behavior from which a sequence of control inputs over a finite prediction horizon result. However, models are only approximate descriptions of reality, and the presence of model uncertainties may make the approach fail. Robust model predictive control approaches deal with the presence of uncertainties in the model. The multi-stage NMPC approach that was developed in our group gives good performance but becomes computationally expensive when the number of uncertain parameters and the optimization horizon grow. Recently, a new robust MPC scheme called "Tube-enhanced multi-stage MPC" was developed to reduce the computational effort without giving up too much performance. It was shown to provide an improved trade-off between complexity and performance compared to the existing approaches.

Tube-enhanced multi-stage (TEMS) MPC combines two promising ideas from robust MPC approaches namely tube-based MPC and multi-stage MPC schemes. In the proposed TEMS MPC scheme, the large uncertainties are handled using a multi-stage primary controller whereas the small disturbances are dealt with by the ancillary controller which tracks the predictions of the primary controller. Multi-stage MPC handles the significant uncertainties that are present in the model by formulating the decision problem on a scenario-tree where at each time-step different states are predicted for different possible realizations of the uncertainties. For linear systems, a proportional feedback ancillary controller is used and for nonlinear systems, a multi-stage ancillary controller is employed to reject the small disturbances. The goal of the ancillary controller is to keep the state and control trajectories of the real system close to those that the primary controller has computed.

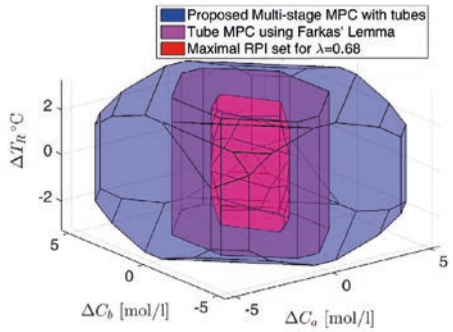

Figure 1: Comparison of feasible domains obtained using the proposed combined MPC scheme with the schemes that use affine and linear feedback policyies for the linearized CSTR example.

The proposed combined scheme has the following advantages compared to the multi-stage and tube-based MPC schemes independently:

1. The growth in problem complexity is limited because the small uncertainties are not considered in the scenario tree.
2. The recourse (i.e. the fact that the future control inputs can be adapted to the observed evolution of the process) that is included in the predictions for the realizations of the large uncertainties in the scenario tree can reduce the conservatism compared to pure tube-based MPC.

The proposed scheme results in an enlarged feasible domain as shown in Figure 1 when compared to the tube-based MPC scheme and significant reduction in computational complexity when compared to the multi-stage MPC scheme when applied to a linearized CSTR example. The scheme is also applied to an industrial fed-batch polymerization reactor example and the resulting plant trajectories are shown in Figure 2.

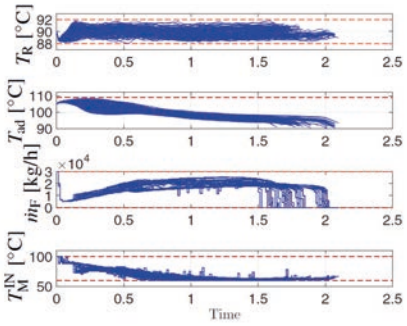

Figure 2: Reactor temperature, adiabatic safety temperature, monomer Feed, jacket inlet temperature trajectories of the fed-batch polymerization reactor obtained for 100 batch runs when controlled by the proposed TEMS scheme.

For this case, the tube-based MPC scheme was not able to satisfy the constraints while the proposed scheme results in rigorous constraint satisfaction. The TEMS scheme required only 9 scenarios while a standard multi-stage MPC scheme would require 59049 scenarios to achieve robustness. This exemplifies the drastic reduction in the computational complexity. The proposed scheme handled parametric uncertainties, additive disturbances and estimation errors using a fraction of the computational resources of a standard multi-stage MPC that includes all uncertainties.

Contact:
sankaranarayanan.subramanian@tu-dortmund.de
sebastian.engell@tu-dortmund.de

Publications:
S. Subramanian, S. Lucia, S. A. B. Birjandi, R. Paulen, S. Engell, A Combined Multi-stage and Tube-based MPC Scheme for Constrained Linear Systems. IFAC-PapersOnLine, 51(20), 481-486 (2018).

S. Subramanian, S. Lucia, S. Engell, A Synergistic Approach to Robust Output Feedback Control: Tube-based Multi-stage NMPC. IFAC-PapersOnLine, 51(18), 500-505 (2018).

Optimization of a Hydroformulation Process in a Thermomorphic Solvent System using a Commercial Steady-state Process Simulator and a Memetic Algorithm

Tim Janus, Maximilian Cegla, Sabine Barkmann, Sebastian Engell

Chemical process design is usually done by an interdisciplinary team in an iterative process. In many companies, such design studies are performed using block-oriented flowsheet simulators as e.g. Aspen Plus. This is convenient from a modelling point of view because many preconfigured modules and physical property calculations are available. The drawback from an optimization perspective is the lack of derivative information which is essential for fast local convergence.
We developed an optimization procedure that employs a memetic algorithm (MA) which couples an evolution strategy (ES) with a derivative free local optimization (DFO) and additionally make use of in-built optimization capabilities of Aspen Plus. We show the improvement of the performance of the algorithm for a well-investigated case study of a hydroformylation process in a thermomorphic solvent system (TMS).

As a case study, the homogeneously catalyzed hydroformulation of 1-dodecene in a thermomorphic solvent system (TMS) is considered. This case study has been investigated by various groups within the TR SFB InPROMPT. We optimize the total annual costs (TAC) of the process. Figure 1 shows the cost distribution. The raw material costs have the biggest impact on the TAC. The heat exchangers and the column are the cause of the main equipment costs. Although the catalyst and solvent makeup costs are only a small fraction of the TAC, they represent the part of the costs that are most influenced by the design of the plant due to the high cost of the catalyst.

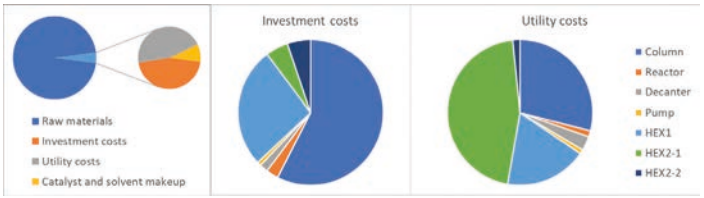

Figure 1: Cost distribution for the best-found solution.

We compared the performance of the MA for different local solvers. Figure 2 shows the convergence of three runs for each MA variant, i.e. lines of the same type represent different runs of the MA variant that is identified in the legend. Both variants EOOPT and EOSPEC use the finite difference approximations of the derivatives of the equation-oriented Aspen Plus simulation. EOOPT minimizes the catalyst loss of the process by using the Aspen Plus internal SQP solver. EOSPEC tries to reach the product purity constraint by adapting the equation-system in Aspen Plus, i.e. the type of the variable representing the purity is changed from calculated to constant and the type of the variable representing the columns reflux ratio from constant to calculated such that the underlying equation-system remains determined. The SM variant uses the sequential-modular simulation mode of Aspen Plus and does not make use of any local optimization, i.e. it is a standard evolution strategy. Nonetheless it performs better than the DFO variants NOMAD and CMAES that also use the sequential-modular mode of Aspen Plus. This means that the function evaluations that are invoked when using the DFO methods are not worth the effort in the early stages of the optimization, using these function evaluations directly in the ES leads to a faster convergence.

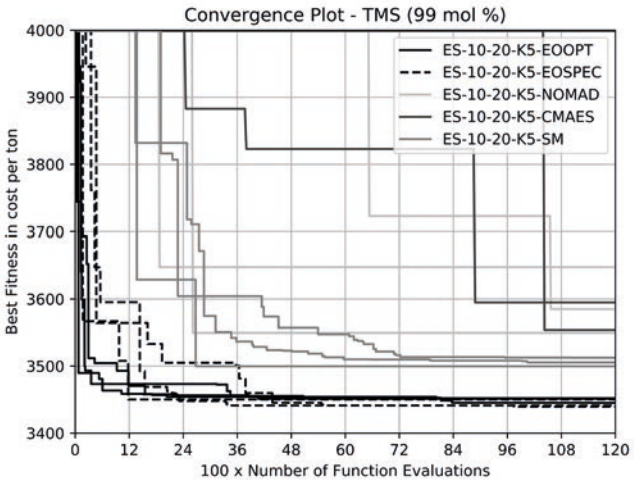

Figure 2: Overview of the results of optimization runs.

Contact:
tim.janus@tu-dortmund.de
sebastian.engell@tu-dortmund.de

Optimal Planning of the Operation of a NH_3 Network

Site-wide optimization at the integrated petrochemical production site of INEOS in Köln

Simon Wenzel[1], Yannik-Noel Misz[1], Keivan Rahimi-Adli[1,2], Benedikt Beisheim[1,2], Sebastian Engell[1]

Many companies in the process industries face an increasingly tough competition and increasing pressure for reducing the consumption of fossil fuels and thus are forced to continuously improve their production with respect to resource and energy efficiency, to become greener, and to remain competitive. Often, production plants in the process industries are situated on large production sites where multiple streams of material and energy couple the processes, which gives rise to complex dynamic networks of plants and utility systems with tight interactions. The optimization of such systems is very demanding, especially if external influences like the supply raw materials has to be embedded, which is inherently uncertain (see Figure 1). Mathematical modeling of the interconnected plants, storage systems and logistics and mixed-integer optimization techniques help to find a plan for the operation of the site and its networks that is feasible and optimal with respect to cost and efficiency.

The integrated petrochemical production site of INEOS in Köln is a complex system of systems, where more than 20 processing plants are coupled via different networks of shared resources such as steam on different pressure levels, electric power, or intermediate products. The site imports and exports raw materials as well as products over the boundaries of the system via trucks, train vessels, or barges on the river Rhine.

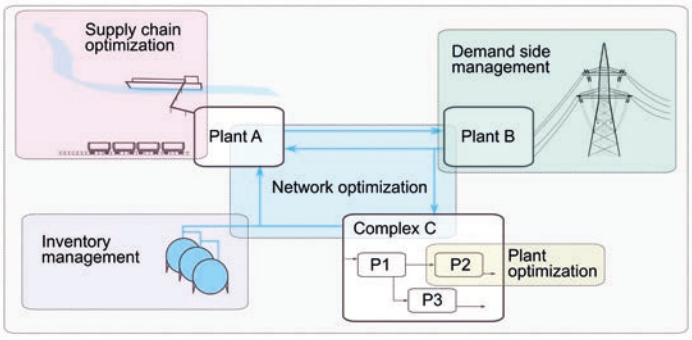

Figure 1: Scope of the different domains that need to be incorporated in the optimization scope.

The supply chain logistics over the boundaries of the system is inherently uncertain and disturbances like the low river level in the Summer of 2018 can have a significant impact on the operation of the processes on site. In the European Horizon 2020 research and innovation action “CoPro”, the problem of finding a feasible and optimal plan for the operation of the site is tackled with mathematical modeling of the production site and mixed-integer programming methods. The use of a site-wide optimization helps to reveal previously unknown bottlenecks in the infrastructure and it helps to suggest optimal reactions to events like plant shutdowns or maintenance activities. A holistic view of the site enables the site management to increase the use of the demand side management potential, where, e. g., the operation of large energy consumers can be scheduled according to daily prices on the electricity market. First results for the optimization of the ammonia network (see Figure 2) show that INEOS in Köln could for instance save electricity by a better planning of the liquefaction of gaseous ammonia and by taking smarter decisions on when and how to operate the compressors, tanks, and processes that are part of the subnetwork.

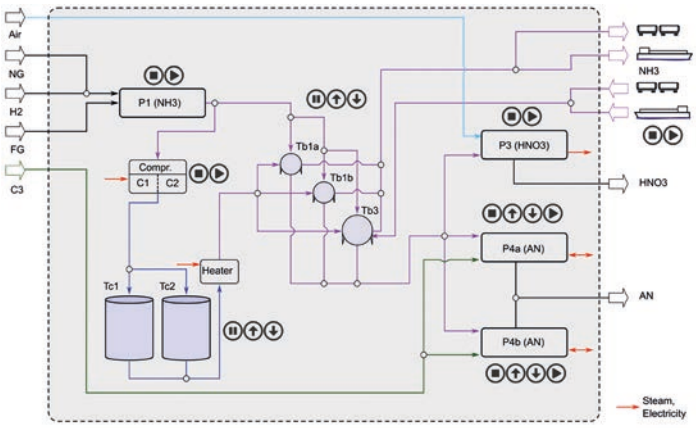

Figure 2: Schematic overview of the ammonia network at INEOS in Köln.

Acknowledgement:
The project leading to this publication has received funding from the European Union’s Horizon 2020 research and innovation programme under grant agreement No 723575 (CoPro) in the framework of the SPIRE PPP (www.copro-project.eu).

[1] TU Dortmund University, Biochemical and Chemical Engineering, Process Dynamics and Operations Group, Emil-Figge-Straße 70, 44227 Dortmund, Germany.

[2] INEOS Manufacturing Deutschland GmbH, Alte Straße 201, 50769 Köln, Germany.

Contact:
simon.wenzel@tu-dortmund.de
sebastian.engell@tu-dortmund.de

Publications:
S. Wenzel, Y.-N. Misz, K. Rahimi-Adli, B. Beisheim, R. Gesthuisen, S. Engell, An optimization model for site-wide scheduling of coupled production plants with an application to the ammonia network of a petrochemical site, Optim. Eng. 2019. https://doi.org/10.1007/s11081-019-09429-2.

S. Wenzel, Y.-N. Misz, K. Rahimi-Adli, B. Beisheim, S. Engell, Optimal Site-Wide Planning of a NH3 Network – A Study on Uncertain Logistic Constraints –. In ECCE12 - The 12th European Congress of Chemical Engineering; Florence, Italy, 2019; pp 1–2.

S. Wenzel, S. Engell, Coordination of Coupled Systems of Systems with Quadratic Approximation. In 15th IFAC Symposium on Large Scale Complex Systems (LSS 2019); IFAC: Delft, The Netherlands, 2019; pp 1–6.

Publications 2018 - 2016

2018

Conference Papers

- T. Janus, M. Cegla, S. Barkmann, S. Engell
  Optimization of a hydroformulation process in a thermomorphic solvent system using a commercial steady process simulator and a memetic algorithm
  Proceedings of 29th European Symposium on Computer-Aided Process Engineering, accepted for publication (2019)

- T. Ebrahim, S. Subramanian, S. Engell
  Hybrid NMPC for switching Systems Applied to a Supermarket Refrigeration System
  Proceedings of ECC18, European Control Conference, Limassol, Cyprus, 2018, IEEE 813-818

- S. Subramanian, S. Nazari, M. A. Alvi, S. Engell
  Robust NMPC Schemes for the Control of Mobile Robots in the Presence of Dynamic Obstacles
  Proceedings of MMAR 2018, Methods and Models in Automation and Robotics, Miedzyzdroje, Poland, IEEE 768-773

- R. Hernandez, J. Dreimann, S. Engell
  Reliable Iterative RTO of a Continuously Operated Hydroformylation Process
  Proceedings of ADCHEM18, 10th IFAC Symposium of Chemical Processes, Shenyang, China, IFAC-PapersOnLine 51(18), 61-66

- S. Subramanian, S. Lucia, S. Engell
  A Synergistic Approach to Robust Output Feedback Control: Tube-based Multi-stage NMPC
  Proceedings of ADCHEM18, 10th IFAC Symposium of Chemical Processes, Shenyang, China, IFAC-PapersOnLine 51(18), 500-505

- A. R. Gottu Mukkula, S. Wenzel, S. Engell
  Active Perturbations Around Estimated Future Inputs in Modifier Adaptation to Cope with Measurement Delays
  Proceedings of ADCHEM18, 10th IFAC Symposium of Chemical Processes, Shenyang, China, IFAC-PapersOnLine 51(18), 839-844

- E. Leo, S. Engell
  Multi-stage integrated electricity procurement and production scheduling
  Proceedings of PSE18, 13th Symposium on Process System Engineering, Computer Aided Chemical Engineering 44, 1291-1296

- E. Leo, S. Engell
  A two-stage stochastic programming approach to integrated day-ahead electricity commitment and production scheduling
  Proceedings of CAPE18, 28th Symposium on Computer Aided Process Engineering, Computer Aided Chemical Engineering 43, 1009-1014

- L. S. Maxeiner, S. Wenzel, S. Engell
  Price-based coordination of interconnected systems with access to external markets
  Proceedings of PSE18, 13th Symposium on Process System Engineering, Computer Aided Chemical Engineering 44, 877-882

- A. Ahmad, W. Gao, S. Engell
  Modifier Adaptation with Model Adaptation in Iterative Real-Time Optimization
  Proceedings of PSE18, 13th Symposium on Process System Engineering, Computer Aided Chemical Engineering 44, 691-696

- G. D. Ave, I. Harjunkoski, S. Engell
  Industrial Demand Side Management Formulation for Simultaneous Electricity Load Commitment and Future Load Prediction
  Proceedings of PSE18, 13th Symposium on Process System Engineering, Computer Aided Chemical Engineering 44, 1237-1242

- S. Wenzel, L. S. Maxeiner, S. Engell
  Virtual splitting of shared resource networks for price-based coordination with portfolio tariffs
  Proceedings of ESCAPE18, 28th European Symposium on Computer Aided Process Engineering, Computer Aided Chemical Engineering 43, 301-306

- A. R. Gottu Mukkula, S. Wenzel, S. Engell
  Active Perturbation in Modifier Adaptation for Real Time Optimization to Cope with Measurement Delays
  Proceedings of ACODS2018, 5th IFAC Conference on Advances in Control and Optimization of Dynamical Systems, IFAC-PapersOnLine 51(1), 124-129

- S. Thangavel, S. Subramanian, S. Lucia, S. Engell
  Handling Structural Plant-model Mismatch using a Model-error Model in the Multi-stage NMPC framework
  Proceedings of SYSID2018, 18th IFAC Symposium on System Identification, Stockholm, Sweden, IFAC-PapersOnLine 51(15), 1074-1079

- G. D. Ave, X. Wang, I. Harjunkoski, S. Engell
  A heuristic neighbourhood search-based algorithm for the solution of resource-task network scheduling problems
  Proceedings of ESCAPE18, 28th European Symposium on Computer Aided Process Engineering, Computer Aided Chemical Engineering 43, 907-912

- S. Subramanian, S. Lucia, B. Baradaran, A. Seayed, R. Paulen, S. Engell
  A Combined Multi-stage and Tube-based MPC Scheme for Constrained Linear Systems
  Proceedings of NMPC2018, 6th Conference on Nonlinear Model Predictive Control, Madison, Wisconsin, USA, IFAC-PapersOnLine 51(20), 481-486

- S. Thangavel, M. Aboelnour, S. Lucia, R. Paulen, S. Engell
  Robust Dual Multi-stage NMPC using Guaranteed Parameter Estimation
  Proceedings of NMPC2018, 6th Conference on Nonlinear Model Predictive Control, Madison, Wisconsin, USA, IFAC-PapersOnLine 51(20), 72-77

- A. Ahmad, M. Singhal, W. Gao, D. Bonvin, S. Engell
  Enforcing Model Adequacy in Real-Time Optimization via Dedicated Parameter Adaptation
  Proceedings of ADCHEM 2018, 10th Symposium on Advanced Control of Chemical Processes, Shenyang, China, IFAC-PapersOnLine 51(18), 49-54

- D. Haßkerl, C. Lindscheid, S. Subramanian, S. Markert, A. Gorák, S. Engell
  Application of Economics Optimizing Control to a Two-Step Transesterification Reaction in a Pilot-Scale Reactive Distillation Column
  Proceedings of ADCHEM 2018, 10th Symposium on Advanced Control of Chemical Processes, Shenyang, China, IFAC-PapersOnLine 51(18), 67-72

Publications 2018 - 2016

- S. Wenzel, L. S. Maxeiner, S. Engell
  Steigerung der Energie- und Ressourceneffizienz durch bessere Koordinierung der Produktion in der Prozessindustrie
  Proceedings of ProcessNet 2018, 33. DECHEMA-Jahrestagung der Biotechnologen, Aachen, Germany, Chemie Ingenieur Technik 90(9), 1162-1163

- A. R. Gottu Mukkula, S. Engell, S. Kern, S. Guhl, K. Mayer, M. Maiwald
  PAT-basierte iterative Optimierung der Fahrweise eines kontinuierlichen organischen Syntheseprozesses
  Proceedings of ProcessNet 2018, 33. DECHEMA-Jahrestagung der Biotechnologen, Aachen, Germany, Chemie Ingenieur Technik 90(9), 1237-1237

- D. Haßkerl, C. Lindscheid, S. Markert, S. Engell
  Dynamische Echtzeitoptimierung einer zweistufigen Umesterungsreaktion in einer Mehrprodukt-Pilotanlage für Reaktivrektifikation
  Proceedings of ProcessNet 2018, 33. Jahrestagung der Biotechnologen, Aachen, Germany, Chemie Ingenieur Technik 90(9), 1236-1236

- C. Linscheid, P. Shakthihasan, S. Engell
  An Ecological Interface Design Based Visualization of the Energy Balance of Chemical Reactors
  Proceedings of CPHS18, 2nd IFAC Conference on Cyber-Physical & Human Systems, Miami, USA

- S. Wenzel, Y.-N. Misz, K. Rahimi-Adli, R. Gesthuisen, S. Engell
  Optimale standortweite Produktionsplanung am Beispiel des NH3-Netzwerkes der INEOS in Köln
  Jahrestreffen der Fachgemeinschaft Prozess-, Apparate- und Anlagentechnik, Köln, Germany

- M. Rantanen Modeer, S. Engell
  Integration of Partial Models of Multi-Agent Systems through Abstraction
  21st Euromicro conference on Digital System Design, Praque, Czech Republic, 2018

- M. Rantanen Modeer, C. Sonntag, S. Engell
  Towards enabling heterogeneous model inter-operation across abstraction levels
  MATHMOD2018; 9th Vienna Conference on Mathematical Modelling, Vienna, Austria, 2018

- T. Janus, C. Foussette, M. Urselmann, S. Tlatlik, A. Gottschalk, M. Emmerich, T. Bäck, S. Engell
  Optimierungsbasierte Prozesssynthese auf Basis eines kommerziellen Flowsheet-Simulators
  Chemie Ingenieur Technik, 89(5), 655–664 (2017)

Journal Papers

- D. Haßkerl, S. Subramanian, S. Markert, S. Kaiser, S. Engell
  Multi-rate state estimation applied to a pilot-scale reactive distillation process
  Chemical Engineering Science 185, 256-281 (2018)

- S. Thangavel, S. Lucia, R. Paulen, S. Engell
  Dual robust nonlinear model predictive control: A multi-stage approach
  Journal of Process Control 72, 39-51 (2018)

- E. Leo, S. Engell
  Integrated day-ahead energy procurement and production scheduling
  at-Automatisierungstechnik 66(11), 950-963 (2018)

- D. Haßkerl, C. Lindscheid , S. Subramanian, A. Tatulea-Codrean, S. Engell
  Economics optimizing control of a multi-product reactive distillation process under uncertainty
  Computers and Chemical Engineering 118, 25-48 (2018)

- D. Haßkerl, C. Lindscheid, S. Subramanian, A. Górak, S. Engell
  Dynamic Optimization of a Pilot-Scale Distillation Process by Economics Optimizing Control
  Industrial and Engineering Chemistry Research 57(36), 12165–12181 (2018)

- R. Hernandez, J. Dreimann, A. J. Vorholt, A. Behr, S. Engell
  Iterative Real-Time Optimization Scheme for Optimal Operation of Chemical Processes under Uncertainty: Proof of Concept in a Miniplant
  Industrial and Engineering Chemistry Research 57(26), 8750-8770 (2018)

- A. Ahmad, W. Gao, S. Engell
  A study of model adaptation in iterative real-time optimization of processes with uncertainties
  Computer Aided Chemical Engineering, Article in Press

Proceedings & Book Chapters

- T. Ebrahim, S. Subramanian, S. Engell
  Hybrid NMPC for switching Systems Applied to a Supermarket Refrigeration System
  Proceedings of ECC 2018, European Control Conference, Limassol, Cyprus, 2018, IEEE 813-818 (2018)

- S. Subramanian, S. Nazari, M. A. Alvi, S. Engell
  Robust NMPC Schemes for the Control of Mobile Robots in the Presence of Dynamic Obstacles
  Proceedings of MMAR 2018, Methods and Models in Automation and Robotics, Miedzyzdroje, Poland, IEEE 768-773 (2018)

- R. Hernandez, J. Dreimann, S. Engell
  Reliable Iterative RTO of a Continuously Operated Hydroformylation Process
  Proceedings of ADCHEM 2018, 10th IFAC Symposium of Chemical Processes, Shenyang, China, IFAC-PapersOnLine 51(18), 61-66 (2018)

Publications 2018 - 2016

- S. Subramanian, S. Lucia, S. Engell
  A Synergistic Approach to Robust Output Feedback Control: Tube-based Multi-stage NMPC
  Proceedings of ADCHEM 2018, 10th IFAC Symposium of Chemical Processes, Shenyang, China, IFAC-PapersOnLine 51(18), 500-505 (2018)

- A. R. Gottu Mukkula, S. Wenzel, S. Engell
  Active Perturbations Around Estimated Future Inputs in Modifier Adaptation to Cope with Measurement Delays
  Proceedings of ADCHEM 2018, 10th IFAC Symposium of Chemical Processes, Shenyang, China, IFAC-PapersOnLine 51(18), 839-844 (2018)

- E. Leo, S. Engell
  Multi-stage integrated electricity procurement and production scheduling
  Proceedings of PSE 2018, 13th Symposium on Process System Engineering, Computer Aided Chemical Engineering 44, 1291-1296 (2018)

- E. Leo, S. Engell
  A two-stage stochastic programming approach to integrated day-ahead electricity commitment and production scheduling
  Proceedings of ESCAPE 2018, 28th Symposium on Computer Aided Process Engineering, Computer Aided Chemical Engineering 43, 1009-1014 (2018)

- L. S. Maxeiner, S. Wenzel, S. Engell
  Price-based coordination of interconnected systems with access to external markets
  Proceedings of PSE 2018, 13th Symposium on Process System Engineering, Computer Aided Chemical Engineering 44, 877-882 (2018)

- A. Ahmad, W. Gao, S. Engell
  Modifier Adaptation with Model Adaptation in Iterative Real-Time Optimization
  Proceedings of PSE 2018, 13th Symposium on Process System Engineering, Computer Aided Chemical Engineering 44, 691-696 (2018)

- G. D. Ave, I. Harjunkoski, S. Engell
  Industrial Demand Side Management Formulation for Simultaneous Electricity Load Commitment and Future Load Prediction
  Proceedings of PSE 2018, 13th Symposium on Process System Engineering, Computer Aided Chemical Engineering 44, 1237-1242 (2018)

- S. Wenzel, L. S. Maxeiner, S. Engell
  Virtual splitting of shared resource networks for price-based coordination with portfolio tariffs
  Proceedings of ESCAPE18, 28th European Symposium on Computer Aided Process Engineering, Computer Aided Chemical Engineering 43, 301-306 (2018)

- A. R. Gottu Mukkula, S. Wenzel, S. Engell
  Active Perturbation in Modifier Adaptation for Real Time Optimization to Cope with Measurement Delays
  Proceedings of ACODS 2018, 5th IFAC Conference on Advances in Control and Optimization of Dynamical Systems, IFAC-PapersOnLine 51(1), 124-129 (2018)

- S. Thangavel, S. Subramanian, S. Lucia, S. Engell
  Handling Structural Plant-model Mismatch using a Model-error Model in the Multi-stage NMPC framework
  Proceedings of SYSID 2018, 18th IFAC Symposium on System Identification, Stockholm, Sweden, IFAC-PapersOnLine 51(15), 1074-1079 (2018)

- G. D. Ave, X. Wang, I. Harjunkoski, S. Engell
  A heuristic neighbourhood search-based algorithm for the solution of resource-task network scheduling problems
  Proceedings of ESCAPE 2018, 28th European Symposium on Computer Aided Process Engineering, Computer Aided Chemical Engineering 43, 907-912 (2018)

- S. Subramanian, S. Lucia, B. Baradaran, A. Seayed, R. Paulen, S. Engell
  A Combined Multi-stage and Tube-based MPC Scheme for Constrained Linear Systems
  Proceedings of NMPC 2018, 6th Conference on Nonlinear Model Predictive Control, Madison, Wisconsin, USA, IFAC-PapersOnLine 51(20), 481-486 (2018)

- S. Thangavel, M. Aboelnour, S. Lucia, R. Paulen, S. Engell
  Robust Dual Multi-stage NMPC using Guaranteed Parameter Estimation
  Proceedings of NMPC 2018, 6th Conference on Nonlinear Model Predictive Control, Madison, Wisconsin, USA, IFAC-PapersOnLine 51(20), 72-77 (2018)

- A. Ahmad, M. Singhal, W. Gao, D. Bonvin, S. Engell
  Enforcing Model Adequacy in Real-Time Optimization via Dedicated Parameter Adaptation
  Proceedings of ADCHEM 2018, 10th Symposium on Advanced Control of Chemical Processes, Shenyang, China, IFAC-PapersOnLine 51(18), 49-54 (2018)

- D. Haßkerl, C. Lindscheid, S. Subramanian, S. Markert, A. Gorák, S. Engell
  Application of Economics Optimizing Control to a Two-Step Transesterification Reaction in a Pilot-Scale Reactive Distillation Column
  Proceedings of ADCHEM 2018, 10th Symposium on Advanced Control of Chemical Processes, Shenyang, China, IFAC-PapersOnLine 51(18), 67-72 (2018)

- C. Lindscheid, P. Shakthihasan, S. Engell
  An Ecological Interface Design Based Visualization of the Energy Balance of Chemical Reactors
  Proceedings of CPHS 2018, 2nd IFAC Conference on Cyber-Physical & Human Systems, Miami, USA (2018)

- M. Rantanen Modeer, C. Sonntag, S. Engell
  Towards enabling heterogeneous model inter-operation across abstraction levels
  MATHMOD 2018; 9th Vienna Conference on Mathematical Modelling, Vienna, Austria, 105-106 (2018

Publications 2018 - 2016

Presentations / Posters

- S. Wenzel, L. S. Maxeiner, S. Engell
  Steigerung der Energie- und Ressourceneffizienz durch bessere Koordinierung der Produktion in der Prozessindustrie
  Proceedings of ProcessNet 2018, 33. DECHEMA-Jahrestagung der Biotechnologen, Aachen, Germany, Chemie Ingenieur Technik 90(9), 1162-1163 (2018)

- A. R. Gottu Mukkula, S. Engell, S. Kern, S. Guhl, K. Mayer, M. Maiwald
  PAT-basierte iterative Optimierung der Fahrweise eines kontinuierlichen organischen Syntheseprozesses
  Proceedings of ProcessNet 2018, 33. DECHEMA-Jahrestagung der Biotechnologen, Aachen, Germany, Chemie Ingenieur Technik 90(9), 1237-1237 (2018)

- D. Haßkerl, C. Lindscheid, S. Markert, S. Engell
  Dynamische Echtzeitoptimierung einer zweistufigen Umesterungsreaktion in einer Mehrprodukt-Pilotanlage für Reaktivrektifikation
  Proceedings of ProcessNet 2018, 33. Jahrestagung der Biotechnologen, Aachen, Germany, Chemie Ingenieur Technik 90(9), 1236-1236 (2018)

- S. Wenzel, Y.-N. Misz, K. Rahimi-Adli, R. Gesthuisen, S. Engell
  Optimale standortweite Produktionsplanung am Beispiel des NH3-Netzwerkes der INEOS in Köln
  Jahrestreffen der Fachgemeinschaft Prozess-, Apparate- und Anlagentechnik, Köln, Germany (2018)

- M. Rantanen Modeer, S. Engell
  Integration of Partial Models of Multi-Agent Systems through Abstraction
  21st Euromicro conference on Digital System Design, Praque, Czech Republic (2018)

2017

Journal Papers

- R. Hernández, S. Engell
  Stochastic Approximation in Online Steady State Optimization under noisy measurements
  Computer Aided Chemical Engineering 40, 1747-1752 (2017)

- A. R. Gottu Mukkula, R. Paulen
  Model-based design of optimal experiments for nonlinear systems in the context of guaranteed parameter estimation
  Computers & Chemical Engineering 99, 198 - 213 (2017), ISBN 0098-1354

- T. Janus, C. Foussette, M. Urselmann, S. Tlatlik, A. Gottschalk, M. Emmerich, T. Bäck, S. Engell
  Optimierungsbasierte Prozesssynthese auf Basis eines kommerziellen Flowsheet Simulators
  Chemie Ingenieur Technik 89 (5), Special Issue: Prozessoptimierung, 655-664 (2017)

- S. Lucia, A. Tatulea-Codrean, C Schoppmeyer, S. Engell
  Rapid Development of Modular and Sustainable Nonlinear Model Predictive Control Solutions
  Control Engineering Practice, 51-62 (2017)

- S. Wenzel, R. Paulen, B. Beisheim, S. Krämer, S. Engell
  Market-Based Coordination of Shared Resources in Cyberphysical Production Sites
  Chemie Ingenieur Technik 89, 636-644 (2017)

- M. Kalliski, S. Engell
  Real-time resource efficiency indicators for monitoring and optimization of batch-processing plants
  Canadian Journal of Chemical Engineering, 95 (2), 265-280 (2017)

- A. Sharma, M. Jelemenský, R. Paulen, M. Fikar
  Modeling and optimal operation of batch closed-loop diafiltration processes
  Chem Eng Res Des 122, 198-210 (2017)

- F. Lamnabhi-Lagarrigue, A. Annaswamy, S. Engell, A. Isaksson, P. Khargonekar, RM. Murray, et al.
  Systems & Control for the future of humanity, research agenda: Current and future roles, impact and grand challenges
  Annual Reviews in Control 43, 1-64 (2017)

Proceedings & Book Chapters

- D. Haßkerl, S. Subramanian, R Hashemi, M. Arshad, S. Engell
  State estimation using a multi-rate particle filter for a reactive distillation column de-scribed by a DAE model
  Proceedings of the 25th IEEE Mediterranean Conference on Control and Automation (MED), Valetta/Malta, 876- 881 (2017)

- T. Siwczyk, S. Engell
  Solving Two-Stage Stochastic MILP Chemical Batch Scheduling Problems by Evolu-tionary Algorithms and Ordinal Optimization
  Proceedings of FOCAPO, Foundations of Computer Aided Process Operations / Chemical Process Control, Tucson, Arizona USA (2017)

- S. Wenzel, R. Paulen, S. Engell
  Quadratic approximation in price-based coordination of constrained systems-of-systems
  Proceedings of FOCAPO, Foundations of Computer Aided Process Operations / Chemical Process Control, Tucson, Arizona, 1-6 (2017)

- S. Thangavel, S. Subramanian, S. Engell
  Offset-free NMPC with robust constraint satisfaction using model-error modeling
  Proceedings of FOCAPO, Foundations of Computer Aided Process Operations / Chemical Process Control, Tucson, Arizona USA (2017)

- S. Subramanian, S. Lucia, S. Engell
  A novel tube-based output feedback MPC for constrained linear systems
  Proceedings of American Control Conference (ACC) IEEE, Seattle, WA, 3060-3065 (2017)

Publications 2018 - 2016

- S. Subramanian, S. Lucia, S. Engell
  An Improved Output Feedback MPC scheme for Constrained Linear Systems
  Proceedings of IFAC International Federation of Automatic Control World Congress, Toulouse, France, IFAC-PapersOnLine 50 (1), 15506- 15511 (2017)

- W. Gao, R. Hernandez, S. Engell
  Real-time optimization of a novel hydroformylation process by using transient measurements in modifier adaptation
  Proceedings of IFAC International Federation of Automatic Control World Congress, Toulouse, France, 2017, IFAC-PapersOnLine 50 (1), 5731-5736 (2017)

- A.R. Gottu Mukkula, R. Paulen
  Model-Based Optimal Experiment Design for Nonlinear Parameter Estimation Using Exact Confidence Regions
  Proceedings of IFAC International Federation of Automatic Control World Congress, Toulouse, France, IFAC-PapersOnLine,50 (1), 13760 - 13765 (2017)

- Nazari, S. Wenzel, L. Maxeiner, C. Sonntag, S. Engell
  A Framework for the Simulation and Validation of Distributed Control Architectures for Technical Systems of Systems
  Proceedings of IFAC International Federation of Automatic Control World Congress, Toulouse, France, IFAC-PapersOnLine,50 (1), 12458-12463 (2017)

- S. Wenzel, R. Paulen, B. Beisheim, S. Krämer, S. Engell
  Adaptive pricing for optimal resource allocation in industrial production sites
  Proceedings of IFAC International Federation of Automatic Control World Congress, Toulouse, France, IFAC-PapersOnLine,50 (1), 12446 – 12451 (2017)

- J. Cadavid, R. Hernández, S. Engell
  Speed-up of Iterative Real-Time Optimization by Estimating the Steady States in the Transient Phase using Nonlinear System Identification
  Proceedings of IFAC International Federation of Automatic Control World Congress, Toulouse, France, IFAC-PapersOnLine,50 (1), 1269-11274 (2017)

- M. Jelemenský, M. Fikar, R. Paulen
  Time-Optimal Operation of Membrane Processes in the Presence of Fouling with Set-membership Parameter Estimation
  Proceedings of IFAC International Federation of Automatic Control World Congress, Toulouse, France, IFAC-PapersOnLine,50 (1), 4690-4695 (2017)

- W. Gao, S. Engell
  Dynamic MAWQA: Towards Efficient Real-time Optimization of Slow Dynamic Processes
  Proceedings of 36th IEEE Chinese Control Conference, Dalian, China (2017)

- S. Thangavel, S. Lucia, R. Paulen, S. Engell
  Robust Nonlinear Model Predictive Control with Reduction of Uncertainty via Dual Control
  Proceedings of 21st IEEE International Conference on Process Control (PC), Štrbské Pleso, Slovakia, 48-53 (2017)

- R. Hernandez, M. Buckova, S. Engell
  An efficient RTO scheme for the optimal operation of chemical processes under uncertainty
  Proceedings of 21st IEEE International Conference on Process Control (PC), Štrbské Pleso, Slovakia, 364-369 (2017)

- A. Sharma, M. Jelemensky, M. Fikar, R. Paulen
  Optimal operation of nanofilter based diafiltration processes using experimental per-meation models
  Proceedings of 21st IEEE International Conference on Process Control (PC), Štrbské Pleso, Slovakia, 185-190 (2017)

- A. Ahmad, W. Gao, S. Engell
  Effective Model Adaptation in Iterative RTO
  Proceedings of ESCAPE-27, European Symposium on Computer Aided Process Engineering, Barcelona Spain, Computer-Aided Chemical Engineering 40, 1717-1722 (2017)

- F. Benski, C. Nentwich, S. Engell
  Optimization-based early phase design of a homogeneously catalysed process in a thermomorphic solvent system
  Proceedings of ESCAPE-27, European Symposium on Computer Aided Process Engineering, Barcelona Spain, Computer-Aided Chemical Engineering 40, 715-720 (2017)

- T. Keßler, N. Mertens, S. Kunde, C. Nentwich, D. Michaels, S. Engell, A. Kienle
  Efficient global optimization of a novel hydroformylation process
  Proceedings of ESCAPE-27, European Symposium on Computer Aided Process Engineering, Barcelona Spain, Computer-Aided Chemical Engineering 40, 2113-2118 (2017)

- S. Wenzel, V. Yfantis, W. Gao
  Comparison of regression data selection strategies for quadratic approximation in RTO
  Proceedings of ESCAPE-27, European Symposium on Computer Aided Process Engineering, Barcelona Spain, Computer-Aided Chemical Engineering 40, 1711-1716 (2017)

- A. R. Gottu Mukkula, R. Paulen
  Robust model-based design of experiments for guaranteed parameter estimation
  Proceedings of ESCAPE-27, European Symposium on Computer Aided Process Engineering, Barcelona Spain, Computer-Aided Chemical Engineering 40, 1639-1644 (2017)

Publications 2018 - 2016

Presentations/ Posters

- T. Goerke, S. Engell
  Batch–to–Conti Transfer of the Production of a Highly Viscous Copolymer System
  Proceedings of International Process Intensification Conference IPIC1, Barcelona (2017)

- T. Goerke, S. Engell
  Übertragung einer Copolymerisation vom Batch Prozess in eine kontinuierliche Produktion: Von der Modellierung über Prozessentwicklung zur Prozessführung
  ProcessNet Fachgemeinschaft Jahrestreffen "Prozess-, Apparate- und Anlagentechnik" 2017, Würzburg (2017)

- D. Haßkerl, C. Lindscheid, S. Markert, S. Engell
  Dynamische Echtzeitoptimierung einer Umesterung in einer Pilotanlage für Reaktivrektifikation
  ProcessNet Fachgemeinschaft Jahrestreffen "Prozess-, Apparate- und Anlagentechnik" 2017, Würzburg (2017)

- T. Siwczyk, S. Engell
  A Fast Hybrid Evolutionary Algorithm with Inexact Fitness Evaluation for Solving Two-Stage Stochastic Scheduling Problems
  GECCO '17 Proceedings of the Genetic and Evolutionary Computation Conference Companion, 307-308 (2017)

2016

Journal Papers

- D. Ackerschott, B. Beisheim, S. Engell
  Decision support for optimised cooling tower operation using weather forecasts
  Chemical Engineering Transactions 52, AIDIC, 1009-1014 (2016)

- C. Dowidat, M. Kalliski, G. Schembecker, C. Bramsiepe
  Synthesis of batch heat exchanger networks utilizing a match ranking matrix
  Applied Thermal Engineering 100, 78-83 (2016)

- T. Goerke, D. Kohlmann, S. Engell
  Transfer of Semibatch Processes to Continuous Processes with Side Injections - Opportunities and Limitations, Macromolecular Reaction Engineering
  Macromolecular Reaction Engineering 10 (4), Special Issue: Batch to Conti Transfer of Polymer Production Processes, 364–388 (2016)

- R. Hashemi, D. Kohlmann, S. Engell
  Optimizing Control and State Estimation of a Continuous Polymerization Process in a Tubular Reactor with Multiple Side-streams
  Macromolecular Reaction Engineering 10 (4), Special Issue: Batch to Conti Transfer of Polymer Production Processes, 415-434 (2016)

- D. Kohlmann, M.C. Chevrel, S. Hoppe, D. Meimaroglou , D. Chapron, P. Bourson, C. Schwede, W. Loth, S. Engell, F. Durand
  Modular, Flexible, and Continuous Plant for Radical Polymerization in Aqueous Solution
  Macromolecular Reaction Engineering 10 (4), Special Issue: Batch to Conti Transfer of Polymer Production Processes, 339-353 (2016)

- C. Schoppmeyer, H. Vermue, S. Subbiah, D. Kohlmann, P. Ferlin, S. Engell
  Operation of Flexible Multiproduct Modular Continuous Polymerization Plants
  Macromolecular Reaction Engineering 10 (4), Special Issue: Batch to Conti Transfer of Polymer Production Processes, 435-457 (2016)

- W. Gao, S. Wenzel, S. Engell
  A reliable modifier-adaptation strategy for real-time optimization
  Computers & Chemical Engineering 91, 318-328 (2016)

- H. Hadera, R. Labrik, S. Engell, I. Harjunkoski
  An Improved Energy-awareness Formulation for General Precedence Continuous-time Scheduling Models
  Industrial and Engineering Chemistry Research 55, 1336-1346 (2016)

- M. Kalliski, S. Engell
  Real-Time Resource Efficiency Indicators for Monitoring and Optimization of Batch-Processing Plants
  Canadian Journal of Chemical Engineering 95 (2), 265-280 (2016)

- S. Wenzel, R. Paulen, G. Stojanovski, S. Krämer, B. Beisheim, S. Engell
  Optimal resource allocation in industrial complexes by distributed optimization and dynamic pricing
  at – Automatisierungstechnik 64, 428-442 (2016)

- R. Hernándes, S. Engell
  Modelling and iterative Real-time Optimization of a homogeneously catalyzed hydroformylation process
  Computer Aided Chemical Engineering 38, Elsevier, 1-6 (2016)

- H. Hadera, R. Labrik, J. Mäntysaari, G. Sand, I. Harjunkoski, S. Engell
  Integration of Energy-cost Optimization and Production Scheduling Using Multiparametric Programming
  Computer Aided Chemical Engineering 38, Elsevier, 559-564 (2016)

- F. Shamim, R. Hernández, R. Paulen, S. Engell
  A hierarchical coordination approach to the optimal operation of a sugar crystallization process
  Computer Aided Chemical Engineering 38, Elsevier, 703-708 (2016)

- L. Maxeiner, S. Engell
  Distributed minimum batch time optimization for batch reactors with shared resources
  Computer Aided Chemical Engineering 38, Elsevier, 1593-1598 (2016)

- M. Urselmann, T. Janus, C. Foussette, S. Tlatlik, A. Gottschalk, M. Emmerich, T. Bäck, S. Engell
  Derivative-Free Chemical Process Synthesis by Memetic Algorithms Coupled to Aspen Plus Process Models
  Computer-Aided Chemical Engineering 38, Elsevier, 187-192 (2016)

Publications 2018 - 2016

- J. Steimel, S. Engell
  Optimization-based support for process design under uncertainty: A case study
  AIChE Journal 62(9), 3404-3419 (2016)

Proceedings & Book Chapters

- R. Paulen, M. Fikar
  Optimal Operation of Batch Membrane Processes
  Springer, ISBN 978-3-319-20475-8, (2016)

- W. Gao, S. Engell
  Using Transient Measurements in Iterative Steady-State Optimizing Control
  Computer Aided Chemical Engineering 38511-516 (2016)

- A. Gottu Mukkula, R. Paulen
  Optimal dynamic experiment design for guaranteed parameter estimation
  Computer Aided Chemical Engineering 38, 757-762 (2016)

- R. Hernández, S. Engell
  Modelling and iterative Real-time Optimization of a homogeneously catalyzed hydroformylation process
  Computer Aided Chemical Engineering. 38, 1-6 (2016)

- A. Gottu Mukkula, R. Paulen
  Optimal design of dynamic experiments for guaranteed parameter estimation
  Proceedings of American Control Conference, 1826-1831 (2016)

- D. Haßkerl, M. Arshad, R. Hashemi, S. Subramanian, S. Engell
  Simulation Study of the Particle Filter and the EKF for State Estimation of a Large-scale DAE-system with Multi-rate Sampling
  Proceedings of 11th IFAC Symposium on Dynamics and Control of Process Systems, including Biosystems, IFAC PapersOnline 49 (7), Elsevier, 490-496 (2016)

- L. Hebing, T. Neymann, T. Thüte, A. Jockwer, S. Engell
  Effcient Generation of Models of Fed-Batch Fermentations for Process Design and Control
  Proceedings of 11th IFAC Symposium on Dynamics and Control of Process Systems, including Biosystems, IFAC PapersOnline 49 (7), Elsevier, 621-626 (2016)

- R. Hashemi, S. Engell
  Effect of Sampling Rate on the Divergence of the Extended Kalman Filter for a Continuous Polymerization Reactor in Comparison with Particle Filtering
  Proceedings of 11th IFAC Symposium on Dynamics and Control of Process Systems, including Biosystems, IFAC PapersOnLine 49 (7), Elsevier, 365-370 (2016)

- S. Subramanian, A. Ahmad, S. Engell
  Robust control of a supermarket refrigeration system using multi-stage
  NMPC 11th Proceedings of IFAC Symposium on Dynamics and Control of Process Systems, including Biosystems, IFAC-PapersOnLine Bd. 49 (7), Elsevier, 2016, 901-906 (2016)

- T. Ebrahim, R. Hernandez, S. Subramanian, M. Kalliski, S. Krämer, S. Engell
  NCO-Tracking with Changing Set of Active Constraints using Multiple Solution Models
  Proceedings of 11th IFAC Symposium on Dynamics and Control of Process Systems, including Biosystems IFAC PapersOnLine 49 (7), Elsevier, 79-84 (2016)

- R. Paulen, S. Nazari, S.A. Shahidi, C. Sonntag, S. Engell
  Primal and Dual Decomposition for Distributed MPC – Theory, Implementation, and Comparison in a Tailored Validation Framework
  Proceedings of 24th Mediterranean Conference on Control and Automation, 286-291 (2016)

- D. Haßkerl, S. Markert, S. Engell
  Application of Model-based Experimental Design for the Calibration of Online Composition Measurement by Near-infrared Spectroscopy
  Proceedings of 24th IEEE Mediterranean Conference on Control and Automation, 967- 972 (2016)

- D. Haßkerl, S. Markert, S. Engell
  Application of Model-based Experimental Design for the Calibration of Online Composition Measurement by Near-infrared Spectroscopy
  Proceedings of 24th IEEE Mediterranean Conference on Control and Automation, 967- 972 (2016)

- C. Nentwich, S. Engell
  Application of surrogate models for the optimization and design of chemical processes
  Proceedings of IEEE World Congress of Computational Intelligence, International Joint Conference on Neural Networks (IJCNN), 1291-1296 (2016)

- T. Siwczyk, S. Engell
  Solving two-stage stochastic mixed-integer linear problems by ordinal optimization and evolutionary algorithms
  Proceedings of IEEE Congress on Evolutionary Computation, CEC 2016, 2836- 2843 (2016)

- A. Tatuela-Codrean, D. Haßkerl, M. Urselmann, S. Engell
  Steady-state Optimization and Nonlinear Model-predictive Control of a Reactive Distillation Process using the Software Platform do-mpc1
  Proceedings of IEEE Conference on Control Applications (CCA), 1513-1518 (2016)

- C. Lindscheid, D. Haßkerl, A. Meyer, A. Potschka, H.-G. Bock, S. Engell
  Parallelization of modes of the Multi-Level Iteration Scheme for Nonlinear Model-Predictive Control of an Industrial Process
  Proceedings of IEEE Conference on Control Applications (CCA), 1506-1512 (2016)

Publications 2018 - 2016

- T. Goerke, S. Engell
  Application of evolutionary algorithms in guaranteed parameter estimation
  Proceedings of IEEE Congress on Evolutionary Computation (CEC), 5100-5105 (2016)

- M. Urselmann, C. Foussette, T. Janus, S. Tlatlik, A. Gottschalk, M.T.M. Emmerich, S. Engell, T. Bäck
  Selection of a DFO Method for the Efficient Solution of Continuous Constrained Sub-Problems within a Memetic Algorithm for Chemical Process Synthesis
  Proceedings of Genetic and Evolutionary Computation Conference (GECCO), 1029- 1036 (2016)

- S. Wegerhoff, S. Engell
  Control of the production of Saccharomyces cerevisiae on the basis of a reduced metabolic model
  Proceedings of 6th IFAC Conference on Foundations of Systems Biology in Engineering, 49(26), Elsevier 201-206 (2016)

Presentations/ Posters

- D. Ackerschott, S. Engell
  Multi-kriterielle Optimierung zur Verbesserung der Ressourceneffizienz
  ProcessNet-Jahrestagung, September 2016, Aachen

- C. Nentwich, J. Steimel, S. Engell
  Entwicklung und Optimierung chemischer Prozesse unter Verwendung von datenbasierten Modellen
  ProcessNet Jahrestagung, September 2016, Aachen

Solids Process Engineering (FSV)

Development of a Scale-Up Model for the Spheronization of Wet Extrudates

Maria Evers, Markus Thommes

Extrusion-Spheronization is a technique commonly used to produce spherical pellets with narrow size distributions for pharmaceutical use. In this process, a wet mass is extruded and the wet extrudates are immediately rounded in a spheronizer, which consists of a rotating bottom plate surrounded by a stationary cylindrical wall. The rounding process of extrudates to pharmaceutical pellets is based on deformation, attrition, agglomeration and breakage of the extrudate strands, which can proceed simultaneously.

Previously described scaling models for the spheronization process of wet extrudates suggest keeping the peripheral speed constant [1], but give no guideline on adjustment of the load. For the scaling of the loads, a constant ratio of used extrudate mass to the plate diameter cubed was proposed. The validity of the assumption was tested using a 2x2x2 design of experiments, using spheronizers with plate diameters of 12 cm and 25 cm, two different peripheral speeds and two different loads, respectively. Three repetitions were conducted at medium speeds and loads for each spheronizer to prove repeatability. By evaluating the particle size and shape of the pellets after various residence times, the evolution of the shape over time as well as final particle shape could be evaluated.

The equivalent diameter of the pellets varies during spheronization, as can be seen in Figure 1. No significant effect of the load or the plate diameter can be observed.

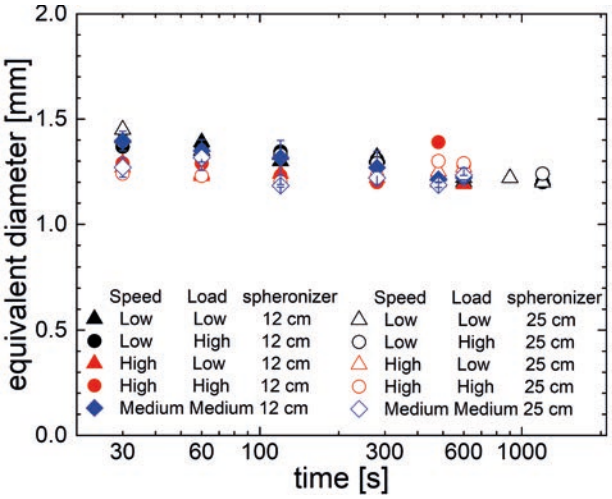

Figure 1: Change of equivalent diameter over time, n=1. Medium settings shown with standard deviations, n=3.

As shown in Figure 2, the median aspect ratio (AR) decreases over time, until a minimum is reached and spheronization is complete. This final aspect ratio was lower than 1.2 for all investigated parameter sets. The load did not affect the final aspect ratio. However, particles rounded at high speeds and with a larger plate diameter seem to show a wider shape distribution than those rounded at low speeds and smaller plate diameters.

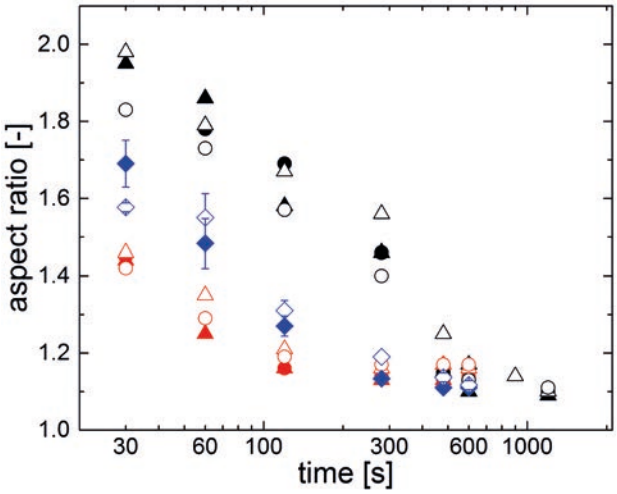

Figure 2: Change of aspect ratio over time, n=1. Medium settings shown with standard deviations, n=3.

Therefore, it was found that keeping the peripheral speed constant is a simple and effective way to ensure comparable results when using spheronizers with different diameters. The spheronizer load has only minor influence. For a wide range of ratios of extrudate mass to the diameter cubed, m/d^3, the influence of the load on the pellet size and shape, as well as the rounding kinetic can be neglected. Residence times should be chosen with regard to spheronization kinetic, because short residence times may result in unfinished rounding, but long spheronization times can lead to an increase in equivalent diameter.

Contact:
maria.evers@tu-dortmund.de
markus.thommes@tu-dortmund.de

Publications:
M. Evers, D. Weis, S. Antonyuk, M. Thommes, 11th world meeting on pharmaceutics, biopharmaceutics and pharmaceutical technology, Granada, March 2018.

Quality by Design for Fused Deposition Modeling 3D Printing: Extrudate Mass Flow Control

Uniform mass flow independent of filament diameter variations

Tim Feuerbach, Markus Thommes

Fused Deposition Modeling (FDM) is considered to be a promising manufacturing method for customized pharmaceutical products, such as patient-specific implants. In FDM, thermoplastics in form of a filament are used as a feedstock material. Filaments are produced via hot-melt extrusion in a preceding step and require a uniform diameter. Deviations of the filament diameter from the nominal value directly translate into inconsistent flowrates during the printing process and can lead to altered object geometry, porosity and mechanical strength. The aim of this study was the adjustment of the filament feed velocity based on the measured filament diameter in order to compensate the filament diameter deviations and obtain consistent extrudate mass flow.

During the printing process, constant extrudate mass flow is required to obtain a product with the desired properties and quality. Due to the missing feedback control in FDM printers, variations of the filament diameter directly translate into inconsistent flowrates, as indicated in Figure 1.

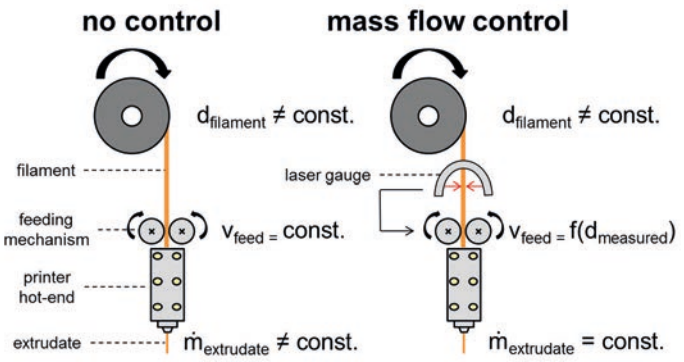

Figure 1: Schematic of the printing process with and without mass flow control.

This effect was demonstrated by discretizing an acrylonitrile butadiene styrene filament into 1 mm compartments and by printing a pattern, in which each pattern element correlates to one filament compartment (see Figure 2).

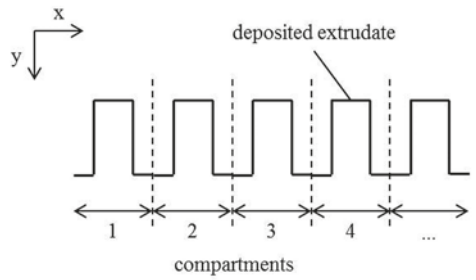

Figure 2: Schematic top view of the printing pattern on the build platform (x, y: horizontal coordinates).

By cutting the pattern at the positions indicated by the dashed lines, it was possible to evaluate the influence of the filament diameter on the extrudate mass flow gravimetrically. As shown in Figure 3, the variations in the filament diameter were similarly introduced into the extrudate mass flow.

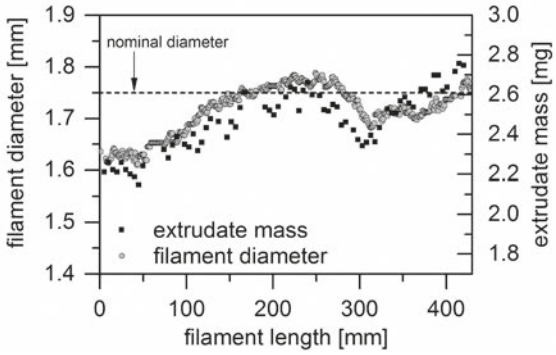

Figure 3: Measured filament diameter and corresponding extrudate mass.

For the experiments with mass flow control, a filament piece with a diameter of 1.699 ± 0.021 mm (arithmetic mean ± standard deviation, n = 7) was used. The pattern elements were collected to groups of 20 and analyzed gravimetrically. Based on the deviation from the nominal diameter of 1.75 mm, a theoretical mean sample weight of $m_{no\ control}$ = 45.33 mg was expected for each group, which is similar to a mass deviation of approximately -5.8% to the set value of 48 mg. The applied control strategy led to an improved mean sample weight of $m_{controlled}$ = 47.31 mg, which is similar to a mass deviation of only -1.6%.

m_{set} [mg]	$m_{no\ control}$ [mg]	$m_{controlled}$ [mg]
48.1	45.33 ± 1.11	47.31 ± 0.90

Table 1: Comparison of the expected extrudate mass with the measured extrudate mass with feed velocity compensation (arithmetic mean ± standard deviation, n = 7).

The results showed the suitability of the presented control strategy for precise material extrusion, which is particularly important for 3D printing of pharmaceutical products to control the drug dosage. The control strategy can be integrated as a Quality by Design tool into the printing process and allows the application of a wider range of filaments as well as a wider range of materials for which the production of filaments with low diameter tolerances is difficult.

Publications:
T. Feuerbach, M. Thommes, 3rd European Conference on Pharmaceutics, Bologna, March 2019.

Contact:
tim.feuerbach@tu-dortmund.de
markus.thommes@tu-dortmund.de

Modelling the Filtration Performance of Fibrous Depth Filters considering Tomographic Data

Kevin Hoppe, Michail Maricanov, Gerhard Schaldach, Reiner Zielke, Dirk Renschen, Wolfgang Tillmann, Damian Pieloth, Markus Thommes

The pollution of air with fine dust (Particles smaller than 10 µm), so-called particulate matter (pm), is actually in the focus of social political discussion. This is reasoned by the harmfulness of the fine dust particles since they are suspected to be carcinogenic or to cause respiratory diseases. Since the emission of pm is strictly controlled by governmental regulations, there is a rising demand for efficient systems for separating particles from gas streams in the (bio-) chemical industry. For separating particles from gas streams with low to medium loadings fibrous depth filters are frequently used. To optimize filter media, broadening of the knowledge about the relation between microscopic properties (porosity, fiber diameter) and their macroscopic effects (filtration efficiency, pressure drop) is essential. The development of a model for dealing with these issues and the investigation of particle separation inside the filter media is the aim of this study.

Particle separation within fibrous depth filters occurs based on diffusional deposition, inertial impaction and interception. Those mechanisms can be described by different model equations. However, these equations are usually not able to deal with the high structural heterogeneity of filter media. To deal with this issue, a model was derived, which divides the filter into several sub-filters having known structural data (Figure 1).

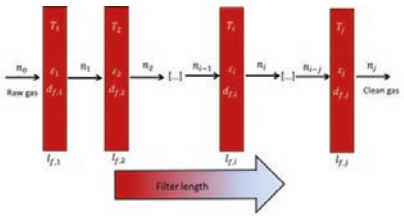

Figure 1: Schematic drawing of the proposed filter model.

Test filters are characterized using an X-ray microscope (XRM) which allows to visualize the 3D-structure and to extract the porosity distribution along the filter length via image analysis of cross-sectional images. A descending porosity of the filter material along its length was expected which can be proofed by the data from XRM. This is desired by the manufacturer to obtain a uniform loading of the filter material. Since the image analysis is a crucial step and prone to error, the porosity distribution measured by XRM is compared to a gravimetrically determined porosity. A good agreement between both methods is found (Table 1).

ε_{grav} [-]	ε_{XRM} [-]
0.988 ± 0.0006	0.981

Table 1: Comparison of obtained porosity by gravimetric (arithmetic mean ± standard deviation, n = 3) and tomographic measurement.

These data were implemented into the model, and the filtration efficiency is calculated. Especially the local deposition is of particular interest and can be calculated with the proposed model (Figure 2).

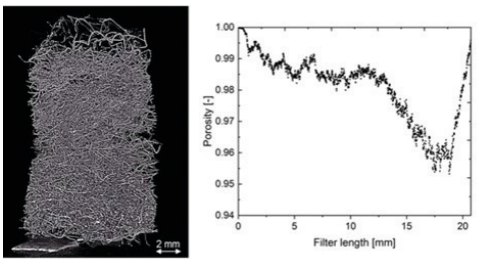

Figure 2: Measured 3D-structure of test filter with a voxel resolution of 15 µm (left) and via image analysis (1444 images with a thickness of 14.35 µm) determined porosity distribution (right).

For testing a filtration with a face velocity of 0.5 m/s and test dust Pural NF ($d_{p50,3}$=9.93µm), a dust load of air of 2.5mg/l was considered and the local distribution of the mass in the initial state is calculated (Figure 3).

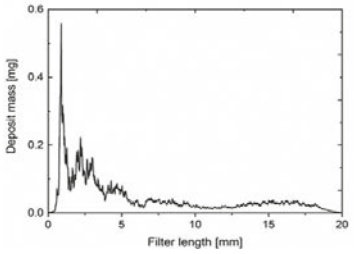

Figure 3: Calculated local distribution of deposit mass inside the filter media.

In this particular case a mayor amount of deposited mass is separated within the first layers of the filter media. This is reasoned by the coarse test dust, and high inertial forces expired to the dust appearing in the filter media. A desired uniform loading of the material couldn't be observed based on that calculated data.
However, the proposed strategy for modeling the filtration performance seems to be promising since it is possible to predict filtration efficiency considering structural inhomogeneity and to investigate local phenomena inside the material.

Contact:
kevin.hoppe@tu-dortmund.de
damian.pieloth@tu-dortmund.de

Publications:
K. Hoppe, M. Maricanov, G. Schaldach, R. Zielke, D. Renschen, W. Tillmann, M. Thommes, D. Pieloth, ProcessNet Abgasreinigung, Presentation, Bamberg, March 2019.

K. Hoppe, L. Wischemann, G. Schaldach, R. Zielke, D. Renschen, W. Tillmann, M. Thommes, D. Pieloth, International Conference on Particle Technology (Partec), Presentation, Nuremberg, April 2019.

Using the Phase Field Approach for Simulating Particle Dissolution

Dominik Sleziona, David R. Ely, Markus Thommes

The aim of this work is to describe the dissolution behavior of single crystals with a numerical model. Already existing analytical approaches for the description of crystal dissolution like Fick's law of diffusion, the Nernst-Brunner equation, the Hixson-Crowell cubic root law and the Higuchi equation are suitable. However they do not take into account the anisotropy or the particle shape. The motivation of this work is to model the dissolution behavior of single crystal particles by using a finite volume method. Dissolution is understood as the transformation of a solid (crystalline state) in a liquid environment in a solution. This process is divided into two parts. The phase transition and diffusion.

The phase transition can be modelled numerically with the so called phase field simulation. In this numerical tool a partial differential equation is used to replace boundary conditions at the interface. This leads to an evolving auxiliary field. The time evolution of the phase (phase transition) of one substance could be described according to the Beckermann approach. The corresponding concentration field (diffusion) for the binary system was modelled using the equation below. It shows that the concentration change over space and time is related to the phase averaged diffusivity and the concentration gradient.

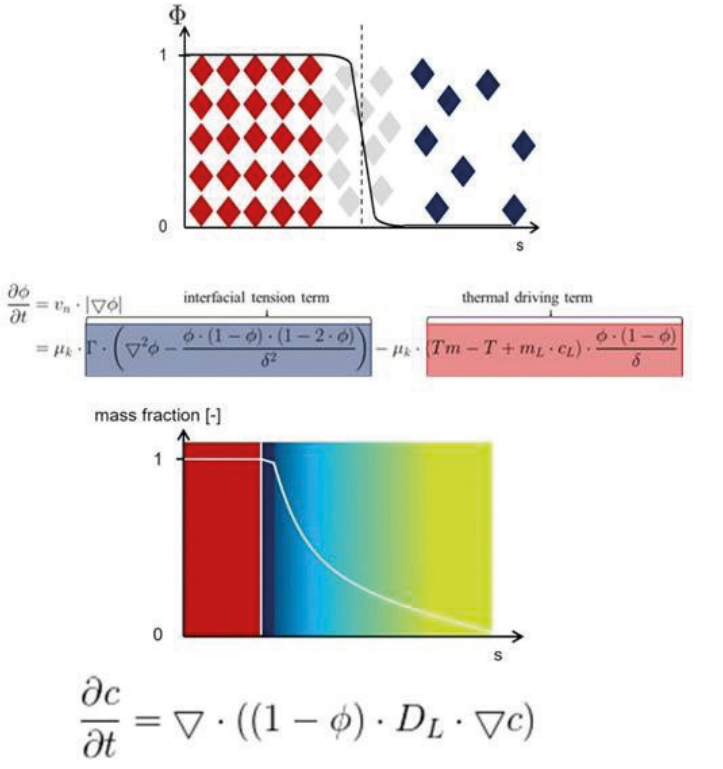

$$\frac{\partial \phi}{\partial t} = v_n \cdot |\nabla \phi| = \mu_k \cdot \Gamma \cdot \left(\nabla^2 \phi - \frac{\phi \cdot (1-\phi) \cdot (1-2 \cdot \phi)}{\delta^2} \right) - \mu_k \cdot \left(Tm - T + m_L \cdot c_L \right) \cdot \frac{\phi \cdot (1-\phi)}{\delta}$$

$$\frac{\partial c}{\partial t} = \nabla \cdot ((1-\phi) \cdot D_L \cdot \nabla c)$$

Figure 1: Schematic and formula of the phase field (top), Schematic and formula of the concentration field (bottom).

$$r = r_0 - \frac{D \cdot (c_s - c)}{\delta \cdot \rho} \cdot t$$

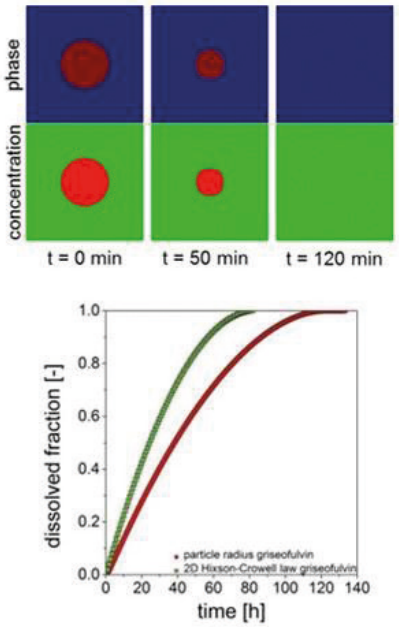

Figure 2: Dissolving isotropic, two dimensional 2,5 µm griseofulvin particle in water at 37°C (top), dissolved fraction over the simulation time (bottom).

An isotropic, circular, two-dimensional griseofulvin particle dissolving in water (37 °C) was simulated as a model system. In the simulation a simultaneously evolving phase and concentration field could be observed. Because of the isotropic properties of the simulated, two dimensional particle a comparison of the numerical results based on the previous mentioned Hixson-Crowell law is possible.

The system was solved numerically to obtain the phase transition and diffusion (concentration field) as a function of time. Due to the fact that the Hixson-Crowell law describes the dissolution behaviour of a three dimensional, isotropic spherical particle, a new equation for a circular two dimensional, isotropic, crystal was derived.

Publications:
D. Sleziona, David R. Ely, M. Thommes, 11th World Meeting on Pharmaceutics, Biopharmaceutics and Pharmaceutical Technology, Granada, March 2018.

Contact:
dominik.sleziona@tu-dortmund.de
markus.thommes@tu-dortmund.de

Correlation of Powder Performance on a Rotary Tablet Press and Standardized Methods for Flowability

Maren Zimmermann, Kalaiarasi Sathiyaseelan, Markus Thommes

In tablet manufacturing powder flow is frequently the rate limiting step as it directly influences weight and dose uniformity. In addition, an insufficient powder flow may cause variations in several product quality attributes (e.g. mechanical strength). Various methods are known for the measurement of powder flowability, which are standardized in the European pharmacopeia to ensure comparability. Nevertheless, the methods are mainly used to qualitatively rank powder flowability and rather investigate the performance of powder in tablet manufacturing. The aim of this study is the determination of a correlation between standardized measurement procedures for the evaluation of powder flowability and the flow behavior of pharmaceutical powder in a rotary tablet press.

In most rotary tablet presses a feed frame with rotating paddles is used in order to overcome the challenges in powder flow. Powder flow of three different pharmaceutical powder from the feed frame (see Figure 1) is compared with static (ring shear cell) and dynamic (powder flow from a funnel) measurement methods.

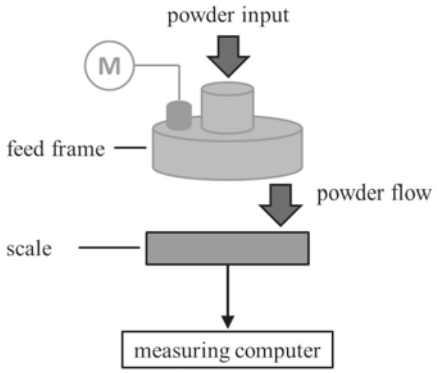

Figure 1: Schematic of the experimental set-up to determine powder flow rate through a feed frame of a rotary tablet press.

As shown in Figure 2 the results of the measurements with the ring shear cell are as expected: Emcocel 90M could be classified as “free flowing” powder ($4 < ff_c < 10$). Di-Cafos A150 offers a higher flowability ($ff_c > 10$) due to a high and regular particle size. GranuLac 200 is a cohesive powder and features low powder flowability ($1 < ff_c < 2$).
Variations could be seen by measuring the flow rate through an orifice (see Figure 2): The mass flow of Emcocel 90M is the smallest one due to a various flow behavior.

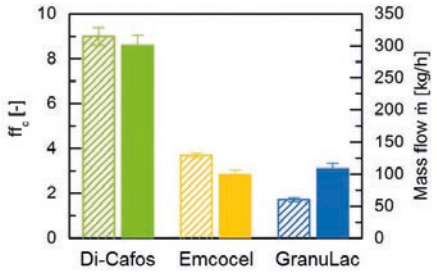

Figure 2: Comparison of the flowability index ff_c (hatched, arithmetic mean ± standard deviation, n = 3) and the flow rate through an orifice (filled, arithmetic mean ± standard deviation, n = 6) of three model substances.

By determining the powder mass flow through a rotary tablet press feed frame a similar order can be found than in the experiments with the ring shear cell (see Table 1): The mass flow of Di-Cafos A150 is the highest one while the flow rates of Emcocel 90M and GranuLac 200 are lower due to the cohesion of the powders.

	Di-Cafos A150	**Emocel 90M**	**GranuLac 200**
ṁ [kg/h]	**5.66 ± 0.82**	**1.73 ± 0.21**	**0.39 ± 0.20**

Table 1: Mass flow rate through the feed frame of a rotary tablet press of three model substances (arithmetic mean ± standard deviation, n = 10).

Contrary to the expectations and the recommendations of the European pharmacopeia, powder flowability determined by the flow rate through an orifice does not correlate with the mass flow from the feed frame of a rotary tablet press. As this standardized method considers both particle-related and dynamic process-related factors, it should represent the conditions in a rotary tablet press feed frame best.
Next to the evaluation of powder flowability by standardized methods and the comparison to heuristic ranges, the mass flow through a feed frame of a rotary tablet press was measured in order to investigate transferability. Determining powder flowability with a ring shear cell resulted in the same order than measuring the flow rate through the feed frame. Unexpectedly, powder flow through an orifice cause a different ranking.

Contact:
maren.zimmermann@tu-dortmund.de
markus.thommes@ tu-dortmund.de

Publications:
M. Zimmermann, K. Sathiyaseelan, M. Thommes, 3rd European Conference on Pharmaceutics, Bologna, March 2019.

Publications 2018 - 2016

2018

- D. Weis, M. Evers, M. Thommes, S. Antonyuk
  DEM simulation of the mixing behavior in a spheronization process
  Chemical Engineering Science 192, 803-815 (2018)

- J. Wesholowski, S. Prill, A. Berghaus, M. Thommes
  Inline UV/Vis spectroscopy as PAT tool for hot-melt extrusion
  Drug Delivery and Translational Research 8 (6), 1595-1603 (2018)

- J. Wesholowski, A. Berghaus, M. Thommes
  Investigations concerning the residence time distribution of twin-screw-extrusion processes as indicator for inherent mixing
  Pharmaceutics 10 (4), 207 (2018)

- R. Strob, A. Dobrowolski, D. Pieloth, G. Schaldach, H. Wiggers, P. Walzel, M. Thommes
  Preparation and characterization of spray-dried submicron particles for pharmaceutical application
  Advanced Powder Technology, 29 (12), 2920-2927 (2018)

- T. Feuerbach, S. Kock, M. Thommes
  Characterisation of fused deposition modeling 3D printers for pharmaceutical and medical applications
  Pharmaceutical Development and Technology, 23 (10), 1136-1145 (2018)

- Ł. Pałkowski, M. Karolak, B. Kubiak, J. Błaszczyński, R. Słowiński, M. Thommes, P. Kleinebudde, J. Krysiński
  Optimization of pellets manufacturing process using rough set theory
  European Journal of Pharmaceutical Sciences, 124, 295-303 (2018)

- R. Strob, A. Dobrowolski, G. Schaldach, P. Walzel, M. Thommes
  Preparation of spray dried submicron particles: Part A – Particle generation by aerosol conditioning
  International Journal of Pharmaceutics, 548 (1), 423-430 (2018)

- A. Dobrowolski, R. Strob, J. Nietfeld, D. Pieloth, H. Wiggers, M. Thommes
  Preparation of spray dried submicron particles: Part B – Particle recovery by electrostatic precipitation
  International Journal of Pharmaceutics, 548 (1), 237-243 (2018)

- J. Wesholowski, A. Berghaus, M. Thommes
  Inline determination of residence time distribution in hot-melt-extrusion
  Pharmaceutics, 10 (2), 49 (2018)

- J. Kamplade, I. Hohlfeld, M. Kelz, M. Thommes, P. Walzel
  Effect of Coandă-deflection-openings on the spray behavior of pressure swirl nozzles
  Atomization and Sprays, 28 (3), 281-297 (2018)

2017

- D. Weis, M. Niesing, M. Thommes, S. Antonyuk
  Particle Kinematics in Spheronization of Pharmaceutical Pellets
  Chemie Ingenieur Technik 89 (8), 1083-1091 (2017)

- D. Weis, M. Niesing, M. Thommes, S. Antonyuk
  Effect of the particle shape on the particle dynamics in a spheronization process
  EPJ Web of Conferences 140, 15005 (2017)

- D. Hegyesi, M. Thommes, P. Kleinebudde, P. Jr. Kása, A. Kelemen, K. Pintye-Hódi, G. Jr. Regon
  Preparation and physicochemical characterization of matrix pellets containing APIs with different solubility via extrusion process
  Drug Development and Industral Pharmacy 43 (3), 458-464 (2017)

Proceedings & Book Chapters

- M. Thommes, P. Kleinebudde
  The Science and Practice of Extrusion-Spheronization in: A. R. Rajabi-Siahboomi (Editor), Multiparticulate Drug Delivery Formulation, Processing and Manufacturing
  New York: Springer Science+Buisness Media LLC, 37-63 (2017)

2016

- D. T. Hegyesi, M. Thommes, P. Kleinebudde, T. Sovány, P. Jr Kása, A. Kelemen, K. Pintye-Hódi, G. Jr Regdon
  Preparation and Physicochemical Characterization of Matrix Pellets Containing APIs with Different Solubility via Extrusion Process
  Drug Development and Industrial Pharmacy dx.doi.org/10.1080/03639045.2016.1261150 (2016)

- E. J. Laukamp, K. Knop, M. Thommes, J. Breitkreutz
  Micropellet-Loaded Rods with Dose-Independent Sustained Release Properties for Individual Dosing via the Solid Dosage Pen
  International Journal of Pharmaceutics 499, 271-279 (2016)

- R. Meier, M. Thommes, N. Rasenack, K.P. Moll, M. Krumme, P. Kleinebudde
  Granule Size Distributions after Twin-Screw Granulation - Do Not Forget the Feeding Systems
  European Journal of Pharmaceutics and Biopharmaceutics 106, 59-69 (2016)

Fluid Separations (FVT)

Efficient Design of Solvent-based Separation Processes

Kai Fabian Kruber, Mirko Skiborowski

Solvent-based separation processes, such as extraction or extractive-distillation, show large potential for the purification of highly diluted components from fermentation broths and waste streams or for the separation of azeotropic mixtures. While the overall process performance inherently depends on the choice of an optimal solvent, common methods for solvent selection rely on simple performance indicators, potentially resulting in suboptimal processes. In order to connect solvent selection and process performance more closely, a hierarchical approach with successive model refinement is developed, which builds on the prediction of thermodynamic properties by COSMO-RS, avoiding the need for experimental data in early conceptual design phases. The approach allows for optimized massive screening of solvents while finally providing a rigorous process optimization.

Liquid-liquid extraction is one of the most promising techniques for the separation of components with similar molecular sizes, boiling and melting points. It is of specific importance for the processing of bio-renewables, especially highly diluted fermentation broths. One of the most important steps in designing a liquid-liquid extraction process is selecting a suitable solvent. This selection is commonly based on heuristic guidelines, expert knowledge and simplified process performance indicators, such as distribution coefficients at infinite dilution, selectivity and the capacity of the solvent. These indicators are usually considered simultaneously in order to characterize the solvent performance. Modern computer-aided molecular design (CAMD) methods can automatically generate solvent candidates and rate them based on the mentioned indicators, e.g. by group-contribution based estimations. In order to avoid heuristic weighting of these indicators, process performance should rather be considered directly including process economics.

For this purpose, a hierarchical design approach has been developed, which can be divided into four stages according to Figure 1. The approach builds on the prediction of thermodynamic properties based on COSMO-RS followed by two screening steps [1]. The feasibility screening removes solvent candidates according to pre-defined constraints, such as boiling temperature and the formation of azeotropes. For the remaining candidates, the minimal energy demand and operational costs are evaluated automatically using thermodynamic sound pinch-based process models. The most promising solvent candidates are further investigated regarding the overall economics of the hybrid process utilizing a rigorous superstructure optimization. This builds on equilibrium-stage models in combination with sizing and costing equations. The resulting approach facilitates the efficient selection of a solvent for an extraction-distillation hybrid process with a hierarchical model refinement to manage the trade-off between detailed results and minimal effort.

The proposed approach was successfully applied to the purification of the platform chemical γ-Valerolactone from an aqueous solution. For the investigated case study, more than 4600 solvent candidates were evaluated. The results of the revised screening and rigorous optimization demonstrate the capability of the approach to determine a cost-optimal solvent based on the overall process design. The presented approach is highly flexible and computationally efficient and thus the application to other solvent-based separation processes as well as more complex process configurations will be subject to future work.

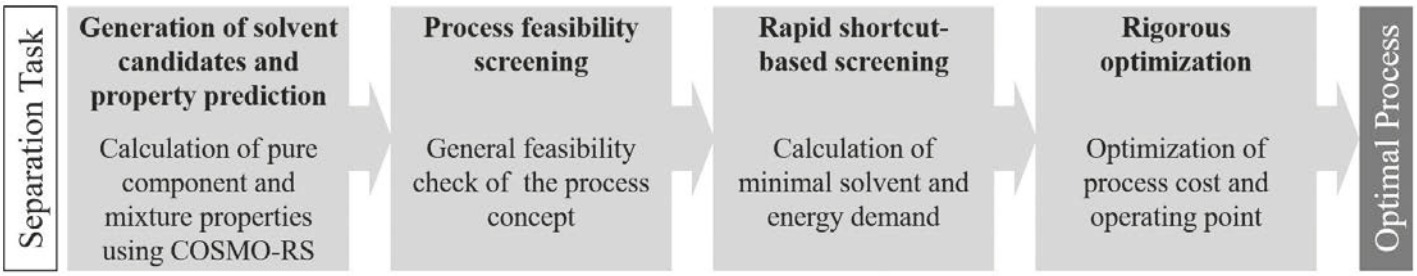

Figure 1: Schematic representation of hierarchical design approach.

Contact:
kai.kruber@tu-dortmund.de
mirko.skiborowski@tu-dortmund.de
andrzej.gorak@tu-dortmund.de

Publications:
[1] K. F. Kruber, J. Scheffczyk, K. Leonhard, A. Bardow, M. Skiborowski, Comp. Aided Chem. Eng. 43, 325-330 (2018).

Automatic Model Development for Organic Solvent Nanofiltration

Rebecca Goebel, Mirko Skiborowski

Organic solvent nanofiltration (OSN) is a promising technology for an energy-efficient separation of organic mixtures. Currently, a quantitative prediction of the separation performance of a specific membrane in different chemical systems is not possible, since there is a lack of suitable models. Thus, an extensive experimental effort is needed to determine the feasibility of OSN for a specific separation task. In the current work an automatic method for the determination of a suitable data-driven model with predictive power for a given membrane was developed, which allows for performance predictions based on a number of thermodynamic and transport properties.

Pressure-driven membrane processes like OSN offer a high potential for improving the energy efficiency of classical separation processes, since they operate without phase transition at low operating temperatures. However, OSN is rarely considered during conceptual process design, since models for reliable quantitative predictions of the separation performance in different chemical systems are currently missing. To overcome this limitation, appropriate models with some predictive power are essential. Common models for OSN like solution-diffusion or pore-flow models, require membrane and component specific parameters, such that they are not applicable for predictions of different substances. Hence, the evaluation of OSN is requiring tedious screening experiments. So far a number of different models have been developed, which allow for the predictive evaluation of the solvent flux, by correlating molecular descriptors of the solvents and membrane-specific parameters in a fixed model structure. Such models were developed for a limited set of different membranes, already showing strong variations in the quality of the prediction for the different membranes. However, since the number of available OSN membranes is yet limited, tailored model structures for each membrane type are a feasible option. Models for the prediction of solute rejection have not been reported at all.

In order to facilitate the development of predictive membrane-specific models, an optimization-based data-driven approach is proposed [1]. The method utilizes a combination of genetic programming (GP) and deterministic global optimization for the identification of optimal parameters, in order to automatically identify suitable model structures and parametrization. For flux and rejection models for OSN, different descriptors that account for physical and chemical properties of the solutes and the solvents are correlated to experimentally measured data of different solutes and solvents. Whereas the GP approach is used for the identification of the model structure, the identification of the best parameter values for each model candidate is performed by means of global deterministic optimization. A considerable feature of the approach, which stands out in comparison to other automated model learning algorithms, is the ability to generate models that are nonlinear in the parameters and rate them on the basis of accuracy and parameter precision.

The method was successfully applied to the prediction of mixed solvent flux through ceramic membranes [2] and rejection of various components (homologous series of even numbered linear alkanes, a branched isomer and different aromatic components) solved in different organic solvents by polymeric membranes [1]. Figure 1 illustrates the results for the components solved in toluene. Only for one of the components, a deviation of ±5% between measured and predicted rejection is exceeded.

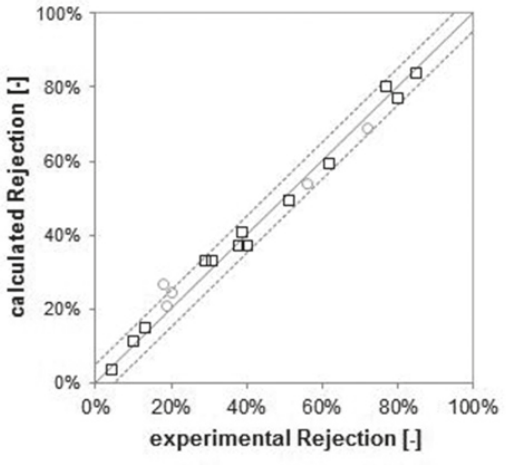

Figure 1: Calculated vs. experimental Rejection of various components solved in toluene (black symbols: components used for model development, green symbols: predicted components, dashed lines: deviation of ±5%) [1].

Publications:
[1] R. Goebel, T. Glaser, I. Niederkleine, M. Skiborowski, Computer Aided Chemical Engineering 43, 115-120 (2018).
[2] R. Goebel, M. Skiborowski, Proceedings 17th Aachener Membran Kolloqium (2018).

Contact:
rebecca.goebel@tu-dortmund.de
stefan2.schlueter@tu-dortmund.de
mirko.skiborowski@tu-dortmund.de
andrzej.gorak@tu-dortmund.de

Developing Rotating Packed Beds for Application in Distillation

Hina Qammar, Konrad Gladyszewski, Mirko Skiborowski, Andrzej Górak

Rotating packed beds (RPBs) have gained considerable attention as flexible and modular equipment for process intensification. However, the characterization of mass transfer performance in various RPB packings was most often characterized based on the overall mass transfer in the RPB without differentiation between mass transfer in the casing and the packing. To avoid these mistakes and derive reliable design correlations, a systematic investigation of the mass transfer performance w.r.t. the packing and the casing is performed. It is further shown that a newly developed ZickZack (ZZ) packing provides better separation efficiency compared to conventional RPB packings.

In an RPB, liquid and vapor streams are contacted counter currently in an annular shaped rotating packing. Phase contacting is intensified through the generation of thin films and fine droplets due to the applied centrifugal force resulting in a reduced equipment size compared to conventional columns. After the first patent for an RPB more than 50 years ago, a few hundred studies have been published on various separation processes, while also several industrial applications of RPBs are recognized [1]. Almost all published studies measure concentration differences between inlet and outlet of the RPB and contribute overall mass transfer to the packing. However, the liquid droplets leave the packing at high speed into the casing that is filled with the vapor phase, such that considerable mass-transfer takes place.

To develop generally applicable design correlations, a systematic investigation was initiated to determine the mass transfer distribution in an RPB. The evaluation was done in terms of total reflux distillation experiments with an ethanol-water system at atmospheric pressure. Temperature measurements for the binary system at the vapor inlet, outlet and in the casing validate that the casing contributes to the overall mass transfer equivalent to almost one theoretical stage [2], as shown in Figure 1.

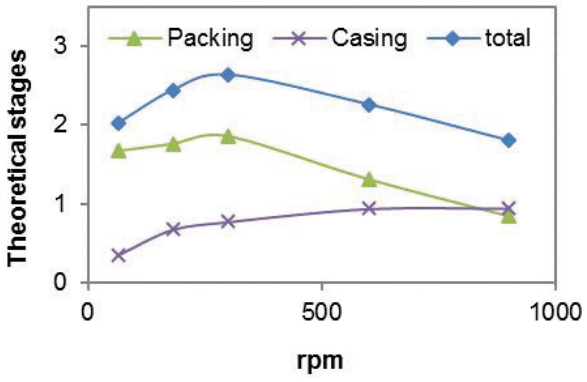

Figure 1: Distribution of mass transfer between casing and packing in an RPB; F_{eye} = 0.6 $Pa^{0.5}$, Knitted mesh [2].

The rotational speed represents an additional degree of freedom in the RPB, which affects the separation efficiency. Experimental results show however that this relationship is not necessarily linear. At a certain rotational speed, a trade-off between the beneficial effect of high shear forces and reduced residence time results in a maximum in separation performance. Therefore, an improvement in mass transfer particularly inside the packing can lead to an improvement in the overall separation efficiency of the RPB. This can be achieved by either increasing the wettability of the packing to provide a higher interfacial area and/or by improving the phase contacting time. In this regard, a single block stage-type packing, called ZickZack (ZZ) packing, was developed using additive manufacturing [3] to provide higher residence time and more homogeneous hydrodynamic conditions compared to conventional RPB packings. Figure 2 shows the performance evaluation of different packings in conventional distillation column e.g. Raschig super ring metal (RSRM), Intalox metal tower packing (IMTP) and HOLPACK, compared to knitted mesh (KM) and ZZ packing in an RPB. The obtained results show the potential benefits that can be achieved by improved packing design in an RPB.

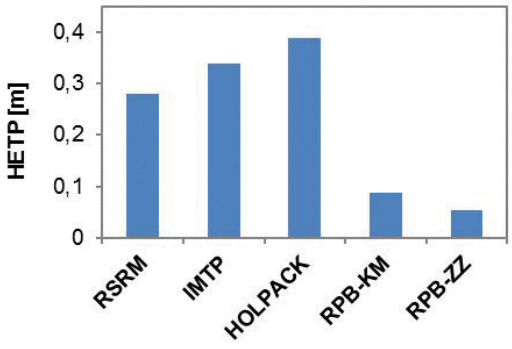

Figure 2: Comparison of different packings for conventional distillation column and RPB; F_{eye} = 0.6 $Pa^{0.5}$.

Contact:
hina.qammar@tu-dortmund.de
konrad.gladyszewski@tu-dortmund.de
mirko.skiborowski@tu-dortmund.de
andrzej.gorak@tu-dortmund.de

Publications:
[1] K. Neumann, K. Gladyszewski, K. Groß, H. Qammar, D. Wenzel, A. Górak, M. Skiborowski, Chemical Engineering Research and Design, 134, 443 (2018).
[2] H. Qammar, F. Hecht, M. Skiborowski, A. Górak, Chemical Engineering Transactions 69, 655 (2018).
[3] K. Gładyszewski, M. Skiborowski, Chemical Engineering and Processing: Process Intensification 127, 1 (2018).

Publications 2018 - 2016

2018

Peer Reviewed Journal Papers

- Blatkiewicz, M.; Antecka, A.; Górak, A.; Ledakowicz, S.
  Continuous laccase concentration in an aqueous two-phase system
  Chemical Papers 72, 3, 555-566 (2018)

- Skiborowski, M.
  Process synthesis and design methods for process intensification
  Current Opinion in Chemical Engineering 22, 216-225 (2018)

- Thiermeyer, Y.; Blumenschein, S.; Skiborowski M.
  Solvent dependent membrane-solute sensitivity of OSN membranes
  Journal of Membrane Science 567, 7-17 (2018)

- Goetsch, T.; Zimmermann, P.; Scharzec, B.; Enders, S.; Zeiner, T.
  Adsorption Isotherms of Liquid Isomeric Mixtures
  Industrial & Engineering Chemistry Research 57, 11210–11218

- Bertleff, B.; Goebel, R.; Claußnitzer, J.; Korth, W.; Skiborowski, M.; Wasserscheid, P.; Jess, A.; Albert, J.
  Investigations on Catalyst Stability and Product Isolation in the Extractive Oxidative Desulfurization of Fuels Using Polyoxometalates and Molecular Oxygen
  Chem. Cat. Chem. 10, 20, 4602–4609 (2018)

- Jaworska, M.; Stępniak, I.; Galiński, M.; Kasprzak, D.; Biniaś, D.; Górak, A.
  Modification of chitin structure with tailored ionic liquids
  Carbohydrate Polymers 202, 397–403 (2018)

- Haßkerl, D.; Lindscheid, C.; Subramanian, S.; Markert, S.; Górak, A.; Engell, S.
  Dynamic Performance Optimization of a Pilot-Scale Reactive Distillation Process by Economics Optimizing Control
  Industrial & Engineering Chemistry Research 57, 12165-12181 (2018)

- Wenzel, D.; Assirelli, M.; Rossen, H.; Lopattschenko, M.; Górak, A.
  On the reactant concentration and the reaction kinetics in the Villermaux-Dushman protocol
  Chemical Engineering and Processing - Process Intensification 130, 332–341 (2018)

- Wenzel, D.; Assirelli, M.; Rossen, H.; Lopattschenko, M.; Górak, A.
  On the reactant concentration and the reaction kinetics in the Villermaux-Dushman protocol
  Chemical Engineering and Processing - Process Intensification 130, 332–341 (2018)

- Neumann, K.; Gladyszewski, K.; Groß, K.; Qammar, H.; Wenzel, D.; Górak, A.; Skiborowski, M.
  A guide on the industrial application of rotating packed beds
  Chemical Engineering Research and Design 134, 443–462 (2018)

- Kuhlmann, H.; Veith, H.; Möller, M.; Nguyen, K.-P.; Górak, A.; Skiborowski, M.
  Optimization-Based Approach to Process Synthesis for Process Intensification
  Industrial & Engineering Chemistry Research 57, 10, 3639–3655 (2018)

- Gładyszewski, K.; Skiborowski, M.
  Additive manufacturing of packings for rotating packed beds
  Chemical Engineering and Processing - Process Intensification 127, 1–9 (2018)

- Blatkiewicz, M.; Antecka, A.; Boruta, T.; Górak, A.; Ledakowicz, S.
  Partitioning of laccases derived from Cerrena unicolor and Pleurotus sapidus in polyethylene glycol – phosphate aqueous two–phase systems
  Process Biochemistry 67, 165–174 (2018)

- Wenzel, D.; Górak, A.
  Review and analysis of micromixing in rotating packed beds
  Chemical Engineering Journal 345, 492–506 (2018)

- Jaworska, M.; Górak, A.
  New ionic liquids for modification of chitin particles
  Research on Chemical Intermediates 164, 341–341 (2018)

- Skiborowski, M.; Recker, S.; Marquardt, W.
  Shortcut-based optimization of distillation-based processes by a novel reformulation of the feed angle method
  Chemical Engineering Research and Design 132, 135–148 (2018)

- Neumann, K.; Hunold, S.; Beer, M. de; Skiborowski, M.; Górak, A.
  Mass Transfer Studies in a Pilot Scale RPB with Different Packing Diameters
  Ind. Eng. Chem. Res. 57, 6 , 2258–2266 (2018)

- Kiss, A.; Geertman, R.; Wierschem, M.; Skiborowski, M.; Gielen, B.; Jordens, J.; John, J.; van Gerven, T.
  Ultrasound-assisted emerging technologies for chemical processes
  Journal of Chemical Technology & Biotechnology 93, 1219-1227 (2018)

- Wierschem, M.; Langen, A.; Lins, J.; Spitzer, R.; Skiborowski, M.
  Model validation for enzymatic reactive distillation to produce chiral compounds
  Journal of Chemical Technology & Biotechnology 93, pp. 498–507 (2018)

- Leimbrink, M.; Nikoleit, K.; Spitzer, R.; Salmon, S.; Bucholz, T.; Górak, A.; Skiborowski, M.
  Enzymatic reactive absorption of CO_2 in MDEA by means of an innovative biocatalyst delivery system
  Chemical Engineering Journal 334, 1195–1205 (2018)

Peer Reviewed Conference Papers

- Skiborowski, M.
  Fast screening of energy and cost efficient intensified distillation processes
  Chemical Engineering Transactions 69, 199-204 (2018)

- Skiborowski, M.; Temmann, P.; Brandenbusch, C.
  Analyzing the link between GE-model parameter regression and optimal process design
  Computer Aided Chemical Engineering 43, 103-108 (2018)

- Haßkerl, D.; Lindscheid, C.; Subramanian, S.; Markert, S.; Górak, A., Engell, S.
  Application of Economics Optimizing Control to a Two-step Transesterification Reaction in a Pilot-Scale Reactive Distillation Column
  IFAC-PapersOnLine 51, 18, 67-72 (2018)

Publications 2018 - 2016

- Mackowiak, J. F.; Syring, K.; Thomas, A.; Leimbrink, M.; Skiborowski, M.; Górak, A.; Mackowiak, J.
Absorption of carbon dioxide using enzyme activated amine solution in columns with random packings
Chemical Engineering Transactions 69, 115-120 (2018)

- Waltermann, T.; Benfer, R.; Schlueter, S.; Reinhardt, A.; Knoesche, C.; Górak, A.; Skiborowski, M.
Choosing the right model for distillation processes in packed columns: theory and experiments
Chemical Engineering Transactions 69, 367–372 (2018)

- Waltermann, T.; Grueters, T.; Skiborowski, M.
Optimization of extractive distillation - integrated solvent selection and energy integration
Computer Aided Chemical Engineering 44, 187–192 (2018)

- Kruber, K.; Scheffczyk, J.; Leonhard, K.; Bardow, A.; Skiborowski, M.
A hierarchical approach for solvent selection based on successive model refinement
Computer Aided Chemical Engineering 43, 325–330 (2018)

- Goebel, R.; Glaser, T.; Niederkleine, I.; Skiborowski, M.
Towards predictive models for organic solvent nanofiltration
Computer Aided Chemical Engineering 43, 115–120 (2018)

- Qammar, H.; Hecht, F.; Skiborowski, M.; Górak, A.
Experimental Investigation and Design of Rotating Packed Beds for Distillation
Chemical Engineering Transactions 69, 655–660 (2018)

- Groß, K.; Neumann, K.; Skiborowski, M.; Górak, A.
Analyzing the Operating Limits in High Gravity Equipment
Chemical Engineering Transactions 69, 661–666 (2018)

- Groß, K.; Bieberle, A.; Gladyszweski, K.; Schubert, M.; Skiborowski, M.; Hampel, U.; Górak, A.
Evaluation of Liquid Hold-up in a Rotating Packed Bed for High Gravity Fluid Separation using Process-Synchronized Gamma-Ray Computed Tomography
Proceedings of the 9th World Congress on Industrial Process Tomography 831–838 (2018)

Book Chapters

- Mitsos, A.; Lee, U.; Recker, S.; Skiborowski, M.
Conceptual Process Design and Process Optimization
In: Green Chemical Engineering, Volume 12 (Eds. Anastas P. T., Lapkin A.) Wiley, 2018

- Werth, K.; Skiborowski, M.
Organic Solvent Nanofiltration for an Intensified Processing of Renewable Raw Materials
In: Intensification of Bio-Based Processes (Eds. Górak, A.; Stankiewicz, A.) Royal Society of Chemistry, 2018

- Wierschem, M.; Leimbrink, M.; Skiborowski, M.; Heils, R.; Smirnova, I.; Górak, A.
Enzymatic Reactive Absorption and Distillation
In: Intensification of Bio-Based Processes (Eds. Górak, A.; Stankiewicz, A.) Royal Society of Chemistry, 2018

- Górak, A.; Stankiewicz, A.
Preface
In: Intensification of Bio-Based Processes (Eds. Górak, A.; Stankiewicz, A.) Royal Society of Chemistry, 2018

- Barecka, M.; Skiborowski, M.; Górak A.
Process Intensification in practice: ethylene glycol case study
In: Practical aspects of Chemical Engineering (Eds.: M. Ochowiak, S. Woziwodzki, M. Doligalski, P. Mitkowski) Springer, 2018

- Wierschem, M.; Górak, A.
Reactive Distillation
In: Reference Module in Chemistry, Molecular Sciences and Chemical Engineering (Ed. Reedijk, J.) Elsevier, 2018

2017

Peer Reviewed Journal Papers

- I. Aspras, M. Jaworska, A. Górak
Kinetics of chitin deacetylase activation by the ionic liquid [Bmim][Br]
Journal of biotechnology 251, 94–98 (2017)

- A. Górak, C. Gourdon, F. Spits, A. Stankiewicz
Importance of Knowledge and Technology Transfer in PI
NPT Procestechnologie 4, 18–19 (2017)

- M. Leimbrink, S. Sandkämper, L. Wardhaugh, D. Maher, P. Green, G. Puxty, W. Conway, R. Bennett, H. Botma, P. Feron, A. Górak, M. Skiborowski
Energy-efficient solvent regeneration in enzymatic reactive absorption for carbon dioxide capture
Applied Energy 208, 263–276 (2017)

- T. Waltermann, M. Skiborowski
Conceptual Design of Highly Integrated Processes – Optimization of Dividing Wall Columns
Chemie Ingenieur Technik 89 (5), 562–581 (2017)

- K. Neumann, S. Hunold, M. Skiborowski, A. Górak
Dry pressure drop in rotating packed beds – systematic experimental studies
Industrial & Engineering Chemistry Research 56 (43), 12395–12405 (2017)

- J. Dreimann, F. Hoffmann, M. Skiborowski, A. Behr, A. Vorholt
Merging Thermomorphic Solvent Systems and Organic Solvent Nanofiltration for Hybrid Catalyst Recovery in a Hydroformylation Process
Industrial & Engineering Chemistry Research 56 (5), 1354-1359 (2017)

- H. Kuhlmann, M. Skiborowski
Optimization-Based Approach To Process Synthesis for Process Intensification: General Approach and Application to Ethanol Dehydration

Publications 2018 - 2016

Industrial & Engineering Chemistry Research 56 (45), 13461–13481 (2017)

- B. Scharzec, T. Waltermann, M. Skiborowski
  A Systematic Approach towards Synthesis and Design of Pervaporation-Assisted Separation Processes
  Chemie Ingenieur Technik 89 (11), 1534-1549 (2017)

- K. Neumann, S. Hunold, K. Groß, A. Górak
  Experimental investigations on the upper operating limit in rotating packed beds
  Chemical Engineering and Processing: Process Intensification 121, 240–247 (2017

- M. Wierschem, M. Skiborowski, A. Górak, R. Schmuhl, A. Kiss
  Techno-economic evaluation of an ultrasound-assisted Enzymatic Reactive Distillation process
  Computers & Chemical Engineering 105, 123-131 (2017)

- M. Barecka, M. Skiborowski, A. Górak
  A novel approach for process retrofitting through process intensification
  Chemical Engineering Research and Design 123, 295–316 (2017)

- M. Jaworska, A. Górak, J. Zdunek
  Modification of Chitin Particles with Ionic Liquids Containing Ethyl Substituent in a Cation
  Advances in Materials Science and Engineering 2017, 1–9 (2017)

- M. Leimbrink, S. Tlatlik, S. Salmon, A.-K. Kunze, T. Limberg, R. Spitzer, A. Gottschalk, A. Górak, M. Skiborowski
  Pilot scale testing and modeling of enzymatic reactive absorption in packed columns for CO_2 capture
  International Journal of Greenhouse Gas Control 62 (3), 100–112 (2017)

- K. Werth, P. Kaupenjohann, M. Skiborowski
  The potential of organic solvent nanofiltration processes for oleochemical industry
  Separation and Purification Technology 182 (3), 185–196 (2017)

- K. Werth, P. Kaupenjohann, M. Knierbein, M. Skiborowski
  Solvent recovery and deacidification by organic solvent nanofiltration
  Journal of Membrane Science 528 (3), 369–380 (2017)

- K. Kruber, M. Krapoth, T. Zeiner
  Interfacial mass transfer in ternary liquid-liquid systems
  Fluid Phase Equilibria 440, 54–63 (2017)

- J.-C. de Hemptinne, J.-H. Ferrasse, A. Górak, S. Kjelstrup, F. Maréchal, O. Baudouin, R. Gani
  Energy efficiency as an example of cross-discipline collaboration in chemical engineering
  Chemical Engineering Research and Design 119, 183–187 (2017)

- M. Wierschem, S. Schlimper, R. Heils, I. Smirnova, A.A. Kiss, M. Skiborowski, P. Lutze
  Pilot-Scale Validation of Enzymatic Reactive Distillation for Butyl Butyrate Production
  Chemical Engineering Journal 312, 106–117 (2017)

- M. Wierschem, O. Walz, A. Mitsos, M. Termuehlen, A.L. Specht, K. Kissing, M. Skiborowski
  Enzyme kinetics for the transesterification of ethyl butyrate with enzyme beads, coated packing and ultrasound assistance
  Chemical Engineering and Processing: Process Intensification 111, 25–34 (2017)

Peer Reviewed Conference Papers

- T. Waltermann, D. Muenchrath, M. Skiborowski
  Efficient optimization-based design of energy-intensified azeotropic distillation processes
  Computer Aided Chemical Engineering 40 (5), 1045–1050 (2017)

- M. Leimbrink, K. Neumann, K. Kupitz, A. Górak, M. Skiborowski
  Enzyme accelerated carbon capture in different contacting equipment - a comparative study
  Energy Procedia 114C, 795–812 (2017)

- M. Leimbrink, T.-L. Limberg, A.-K. Kunze, M. Skiborowski
  Different strategies for accelerated CO_2 absorption in packed columns by application of the biocatalyst carbonic anhydrase
  Energy Procedia 114C, 781–794 (2017)

- T.-J. Kim, A. Lang, A. Chikukwa, E. Sheridan, P. Dahl, M. Leimbrink, M. Skiborowski, J. Roubroeks
  Enzyme Carbonic Anhydrase Accelerated CO_2 Absorption in Membrane Contactor
  Energy Procedia 114C, 17–24 (2017)

Book Chapters

- M.H. Barecka, M. Skiborowski, A. Górak
  Process Intensification in Practice: Ethylene Glycol Case Study
  In: Lecture Notes on Multidisciplinary Industrial Engineering (Eds. M. Ochowiak, S. Woziwodzki, M. Doligalski, P. Mitkowski) Springer (2017)

Publications 2018 - 2016

2016

- J. Dreimann, P. Lutze, M. Zagajewski, A. Behr, A. Górak, A. J. Vorholt
  Highly integrated reactor–separator systems for the recycling of homogeneous catalysts
  Chemical Engineering and Processing: Process Intensification. 99, 124-131 (2016)

- T. Goetsch, P. Zimmermann, S. Enders, T. Zeiner
  Tuneable extraction systems based on hyperbranched polymers
  Chemical Engineering and Processing: Process Intensification. 99 (3), 175-182 (2016)

- T. Goetsch, P. Zimmermann, R. van den Bongard, S. Enders, T. Zeiner
  Superposition of Liquid–Liquid and Solid–Liquid Equilibria of Linear and Branched Molecules: Binary Systems
  Industrial & Engineering Chemistry Research. 55 (42), 11167-11174 (2016)

- M. M. Jaworska, A. Górak
  Modification of chitin particles with chloride ionic liquids
  Materials Letters. 164, 341-343 (2016)

- A. Kubiczek, W. Kamiński, A. Górak
  Modeling of single- and multi-stage extraction in the system of water, acetone, butanol, ethanol and ionic liquid
  Fluid Phase Equilibria. 425, 365-373 (2016)

- H. Kuhlmann, M. Skiborowski
  Synthesis of Intensified Processes from a Superstructure of Phenomena Building Blocks
  Computer Aided Chemical Engineering. 38, 697-702 (2016)

- K. Neumann, K. Werth, A. Martín, A. Górak
  Biodiesel production from waste cooking oils through esterification: Catalyst screening, chemical equilibrium and reaction kinetics
  Chemical Engineering Research and Design. 107, 52-62 (2016)

- R. Schulz, R. van den Bongard, J. Islam, T. Zeiner
  Purification of Terpenyl Amine by Reactive Extraction
  Industrial & Engineering Chemisty Research. 55 (19), 5763-5769 (2016)

- T. Waltermann, M. Skiborowski
  Efficient optimization-based design of energetically intensified distillation processes
  Computer Aided Chemical Engineering. 38, 571-576 (2016)

- M. Wierschem, S. Boll, P. Lutze, A. Górak
  Evaluation of the Enzymatic Reactive Distillation for the Production of Chiral Compounds
  Chem. Ing. Tech. 88 (1-2), 147-157 (2016)

- K. Groß, K. Neumann, K. Kupitz, M. Skiborowski, A. Górak
  HiGee-Technologie – Untersuchung von Hydrodynamik und Stofftransport
  Chemie-Ingenieur-Technik, 88 (9), p. 1283 (2016)

- J. Dreimann, P. Lutze, M. Zagajewski, A. Behr, A. Górak, A.J. Vorholt
  Highly integrated reactor-separator systems for the recycling of homogeneous catalysts
  Chemical Engineering and Processing: Process Intensification, 99, pp. 124-131 (2016)

- C. Kunde, D. Michaels, J. Micovic, P. Lutze, A. Górak, A. Kienle
  Deterministic global optimization in process design of distillation and melt crystallization
  Chemical Engineering and Processing: Process Intensification, 99,pp. 132-142 (2016)

Fluid Mechanics (SM)

Release of a Droplet entering a Shear Flow through a Pore

Droplet release similar to Rayleigh-Plateau instability

Konrad Boettcher, Daniel Becker, Peter Ehrhard

Fuel cells consist of an anode, cathode, and an electrolyte, mostly a non-wettable polymer-membrane. Usually, water is formed and the emerging droplets or liquid films may increase the pressure drop, which may cause an undersupply of the reactive materials in the reactive areas. Therefore, water management in fuel cells is still a big issue and can be improved, if the release of a droplet into and the transport in the gas flow is well understood. In the published literature, a droplet-release model is developed by using CFD. Due to numerical issues, the droplet wets the non-wettable channel, which changes the overall behavior of the droplet in the gas flow.

To get insight into the physical mechanism of droplet release, the general approach is to reduce the problem to a liquid flowing through a single pore into a gas shear-flow in a non-wettable channel. Hitherto, existing theoretical models try to predict the release by assuming a rupture in the liquid bridging the droplet with the pore, but this does not work well.

FLUENT is used to perform the CFD simulations. The VOF method is engaged in combination with a PLIC surface-reconstruction scheme for calculating the surface forces in a CSF-model. As the wettability is prohibited by a mass-conservation scheme, the simulations give a phenomenological insight into the flow structure.

Thereby, the liquid pressed through the pore forms a growing spherical cap. The liquid partly blocks the cross-sectional area of the channel, increasing the velocity of the gas due to continuity reasons. The stream-up stagnation pressure and the resulting pressure drop on top of the droplet force the droplet to move into the channel. The upper part is affected by higher shear forces, accelerating the droplet to move with a higher speed. Due to this, the liquid bridge thins.

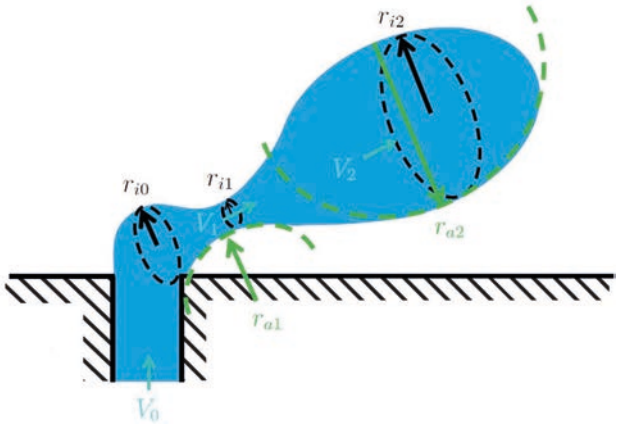

Figure 1: Scheme of release mechanism: The volumetric flow rate V_2 exceeds V_0 due to the shear forces acting on the upper part of the kidney-shaped droplet. Whilst in the pore-sided droplet and the kidney-shaped droplet the curvature radii ($r_{i0} \sim r_{a1}$ and $r_{i2} \sim r_{a2}$) are of the same magnitude, the azimuthal curvature exceeds the outer radius in the thinned region.

This corresponds to a shear-induced Rayleigh-Plateau instability: in the thinned region, the inner azimuthal curvature radius (r_{i1}) of the interface gets dominant in the Laplacian pressure jump across the interface (Figure 1). Therefore, the highest pressure appears in the constricting region (Figure 2), forcing the liquid to flow into the pore-sided droplet or into the kidney-shaped droplet. Knowing this release mechanism, simple mathematical criteria for the release is obtained.

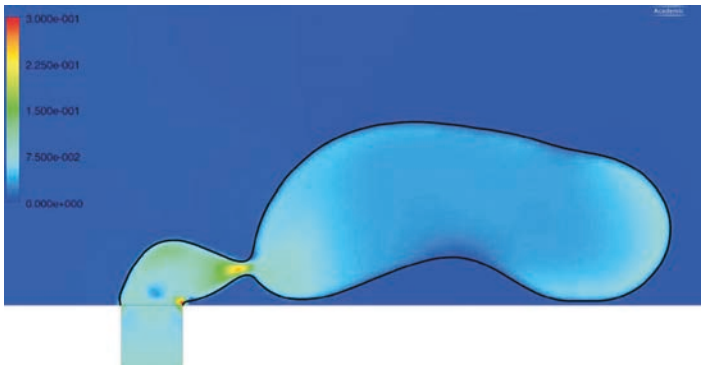

Figure 2: Free interface (black line) dividing the liquid from the gas. Colormap shows the pressure field, indicating a high pressure in the constricting region shortly before the kidney-shaped droplet is released.

Contact:
konrad.boettcher@tu-dortmund.de
daniel4.becker@tu-dortmund.de
peter.ehrhard@tu-dortmund.de

Multiphase Flows in Capillaries

Experimental investigations on rising bubbles in vertical capillaries

Sabrina Grünendahl, Peter Ehrhard

Downsizing devices in industrial production becomes more and more essential, because the process conditions can be controlled more precisely. For single-phase systems, the micro-scale operations are well investigated. In multiphase systems though, the disperse phase interacts with both the walls and the continuous liquid phase. The founded knowledge of the flow and transport processes is mandatory for the design of (micro) devices, so that within this work we investigate the behaviour of rising gas bubbles in capillaries, which clearly differs from the bubble rise in infinitely-extended liquid pools.

Based on the knowledge of rising gas bubbles in an infinitely-extended liquid continuum, the behaviour of individual disperse gas bubbles, rising in vertical capillaries of various diameters, is the focus of our fundamental experimental investigations. Such systematic experiments on the bubble rise in capillaries can hardly be found in literature. For this purpose, a test setup has been constructed and carefully tested within our laboratory. As can be seen in Figure 1, we inject bubbles of a well-defined volume through a hollow needle into the continuous liquid phase. These bubbles eventually rise within the replaceable calibrated capillaries of various inner diameters. The liquid phase may rest or flow through the vertical capillary at a defined volumetric flow rate in either direction in a laminar manner.

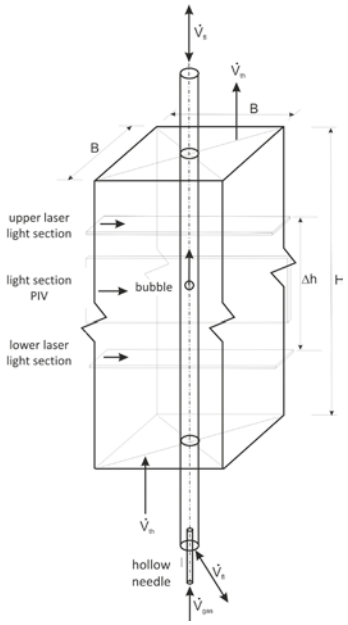

Figure 1: Experimental setup with a coaxial square channel to adjust the refractive index, it includes also three laser light sheets.

The (terminal) rising velocity of the bubble in the vertical capillary is measured by two laser light sheets. Both optical systems are attached to the experimental setup at a defined distance, both span up a parallel light sheet and collect the light on a sensor, after passing through the capillary. A rising bubble first passes the lower, and afterwards the upper laser light sheet, such that at the sensors intensity signals are generated, which are sketched in Figure 2. From the measured time difference Δt between the two peaks, and the defined distance, the rising velocity can be accurately inferred.

The measurement and the generation of the bubble volume appear to be crucial. For this purpose, a calibrated 0.4 mm diameter capillary is installed before the bubble enters the vertical capillary through the hollow needle. As the bubble is strongly elongated within the 0.4 mm capillary, its length can be measured precisely, and moreover a precision syringe pump allows to inject the gas at a T-junction in a controlled manner. As soon as the desired bubble sits in the 0.4 mm capillary, a second syringe pump moves both the liquid and the embedded gas bubble into the vertical capillary at a low volumetric flow rate. The bubble volume can be calculated fairly accurately, by using a cylinder with two hemispheres at each end, whereas all geometrical data are available.

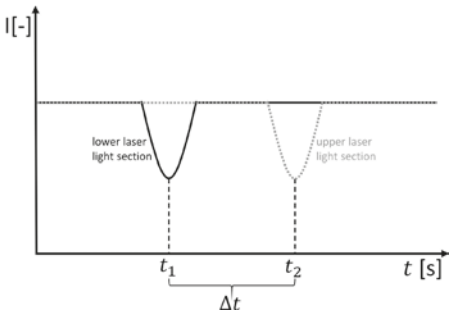

Figure 2: Signals generated by the bubble as it passes the two laser light sheets. The intensities of the laser light at the sensors is recorded as function of time.

While both the bubble volume (and hence, its equivalent diameter) and the terminal bubble velocity can be measured by the above methods, the deformation of the bubble and any velocity fields in the vertical capillary are harder to measure. This is due to the fact that the vertical capillary, though optically transparent, in general strongly distorts any image taken. To produce undistorted images, an adjustment of the refractive indices (liquid, glass) must be arranged. For this purpose, as shown in Figure 1, a coaxial square channel is built around the capillary. As the refractive index of the inner liquid can be adjusted to the refractive index of the glass, we engage a thermostat to circulate the adapted liquid at defined temperature also through the coaxial channel. The temperature control allows for the fine adjustment of the refractive index of this liquid.

Contact:
sabrina.gruenendahl@tu-dortmund.de
peter.ehrhard@tu-dortmund.de

Multiphase Flows in Aerated Tanks

Numerical simulations of the activated-sludge process on a pilot-plant scale

Ann Kathrin Höffmann, Johanna Schmidt, Peter Ehrhard

The energy consumption of municipal waste-water-treatment plants in Germany appears to be substantial. Waste-water-treatment plants working with the activated-sludge process consume up to 80 % of their total energy needs to aerate the respective tanks. To identify saving potentials and to increase the efficiency of the aeration tanks, numerical simulations are conducted to capture the hydrodynamics, the mass transfer, and the biochemical reactions. Numerical simulations allow for the test of system configurations and operating modes without cost-intensive reconstruction work.
The present work concentrates on numerical investigations of the hydrodynamics of rising air bubbles in activated sludge, based on the Euler-Euler method. In a pilot-plant-scale aeration tank, the bubble rise, the oxygen mass-transfer into the activated sludge, and the biochemical reactions are computed and in parallel experimentally examined at our collaboration partner at the Helmholtz Research Centre Dresden-Rossendorf (HZDR).

To compute the hydrodynamics, the oxygen mass-transfer, and the biochemical reactions in a pilot-plant-scale aeration tank, the Euler-Euler method is engaged within *Ansys CFX*. The activated sludge is treated as a continuous phase and air as incompressible monodisperse phase. The biochemical reactions are computed using the ASM model No 1. In an aeration tank of a waste-water-treatment plant, nitrification occurs within the aerated regions, while denitrification occurs within the anoxic regions. In the pilot plant, the entire floor area is equipped with air diffusers. For this reason, only the oxidation of ammonium to nitrate can be observed in both the computations and the experiments.

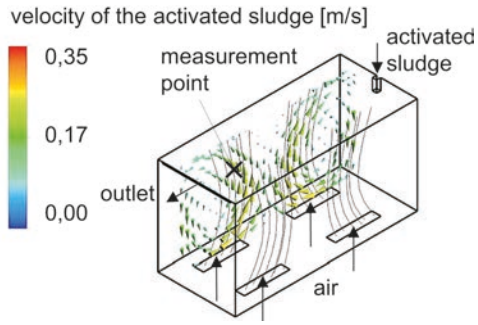

Figure 1: Activated-sludge velocity vectors in a vertical section above the plate diffuser and bubble streamlines.

The figures show some of the results of our computations. The flow topology and the oxygen concentration for a volumetric flow rate of 10 m³/h air can be seen. In Figure 1 the activated-sludge velocity vectors are given in a vertical section above the plate diffuser. Additionally, the bubble streamlines are depicted in grey. It can be concluded, that the rising air bubbles induce two vortices within the activated sludge. Figure 2 shows the oxygen concentration field within two sections, which clearly appears to be affected by the biochemical reactions. It can be seen, that the oxygen concentration in the first vortex after the activated sludge inflow is lower than in the second vortex. This is due to the oxidation of the ammonium within the first vortex, consuming the oxygen in this region. Within the second vortex, the ammonium appears to be already oxidized, though.

Contact:
ann.hoeffmann@tu-dortmund.de
peter.ehrhard@ tu-dortmund.de

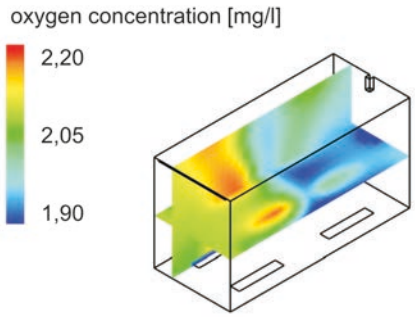

Figure 2: Oxygen concentration in a vertical section above the plate diffuser and in a horizontal section at half tank height.

Finally, Figure 3 shows a comparison of the ammonium concentrations from both simulation and experiments at the measurement point shown in Figure 1. This measurement point is located within the second vortex, the data are collected for different volumetric flow rates of air. The comparison shows a good agreement between numerical and experimental data. In the future, the effect of pulsed aeration, in comparison to continuous aeration, will be the focus of both the experimental and numerical investigations.

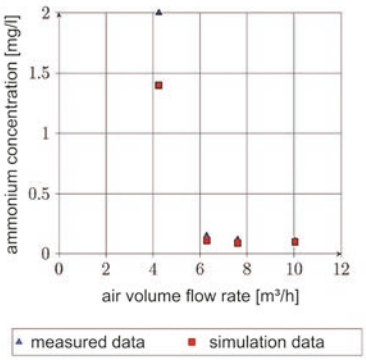

Figure 3: Comparison of the measured and computed data for the ammonium concentration at the measurement point, shown in figure 1.

Publications:
A.K. Höffmann, P. Ehrhard, Proc. Appl. Math. Mech. (PAMM) 2019, in press.

Publications 2018 - 2016

2018

- A. K. Höffmann, P. Lakshmanan, C. Hollmann, T. Ostermann
  An experimental study on oil-dispersion baths generated by the Jungebad apparatus
  Complementary Therapies in Medicine, Vol. 41, pp. 147-153, 2018

- S. F. Reinecke, A. K. Höffmann, M. Stachowske, U. Hampel, P. Ehrhard
  Effizienzsteigerung von Kläranlagen
  GIT Labor-Fachzeitschrift 4/2018, pp. 53-56, 2018

- J. Chaudhuri, A. Baukelmann, K. Boettcher, P. Ehrhard
  Pressure drop in fibrous filters
  European Journal of Mechanics B/Fluids, Vol. 76, pp. 115-121, 2019

- J. Chaudhuri, P. Ehrhard
  Numerical investigation of coalescing filtration process
  Proc. Angewandte Mathematik und Mechanik, Vol. 18, in press, 2018

- L. Gödeke, S. Grünendahl, F. Burzinski, P. Ehrhard
  Experimentelle Untersuchung des Blaseneinschlusses beim Tropfenaufprall auf festen Wänden
  Proc. Fachtagung Experimentelle Strömungsmechanik (GALA), Nr. 10, Rostock, 4.-6. September 2018

2017

- C. Heckmann, S.K. Kurt, P. Ehrhard, N. Kockmann
  Mass Transport in a Liquid-Liquid Plug Flow in a Micro-Capillary Reactor
  Chemie Ingenieur Technik 89 (12), 1642-1649 (2017)

- P. Ehrhard
  in: Prandtl-Führer durch die Strömungslehre (ed. Oertel jun., H.H.)
  14. Auflage, pp. 663-714, Springer Vieweg, Wiesbaden, 2017

- P. Ehrhard, C. Gizewski
  Untersuchung elektrokinetischer Strömungen in Mikrokanälen mit internen Elektroden mithilfe des Mikro-PIV-Verfahrens
  Proc. Fachtagung Experimentelle Strömungsmechanik (GALA), Nr. 6, Karlsruhe, 5.-7. September 2017

- T. Neumann, K. Boettcher, P. Ehrhard
  Modelling the filling process of lithium-ion batteries
  Proc. Angewandte Mathematik und Mechanik, Vol. 17, 659-660, 2017

- A. K. Höffmann, P. Ehrhard
  Numerical investigations of bubbles rising in water
  Proc. Angewandte Mathematik und Mechanik, Vol. 17, 657-658, 2017

- K. Boettcher, M. Bothe
  The liquid droplet on top of a rotating non-isothermal liquid layer
  Proc. Angewandte Mathematik und Mechanik, Vol. 17, 653-654, 2017

2016

- M. Meier
  Modellierung und Simulation von Strömungen und biologischen Reaktionen innerhalb eines Belebtschlammbeckens
  Chemie Ingenieur Technik 88, 1128-1137 (2016)

- P. Lakshmanan, P. Ehrhard
  Enhanced mass transfer in micro-capillary two-phase flow
  Proc. Angewandte Mathematik und Mechanik 16, 603 (2016)

- A.K. Höffmann, P. Lakshmanan, P. Ehrhard, Th. Ostermann
  The Jungebad apparatus for the production of oil-dispersion baths
  Proc. Angewandte Mathematik und Mechanik 16, 599 (2016)

- T. Neumann, K. Boettcher, P. Ehrhard
  Numerical investigation into a liquid displacing a gas in thin porous layers
  Proc. Angewandte Mathematik und Mechanik 16, 605 (2016)

- Ch. Heckmann, P. Ehrhard
  Simulation of mass transfer in liquid/liquid slug flow
  Proc. Angewandte Mathematik und Mechanik 16, 597 (2016)

Technical Biochemistry (TB)

Chemical Fingerprinting of Single Glandular Trichomes of *Cannabis sativa* by Coherent Anti-Stokes Raman Scattering (CARS)

Paul Ebersbach, Felix Stehle, Oliver Kayser, Erik Freier

Cannabis possesses a rich spectrum of phytochemicals i.e. cannabinoids, terpenes and phenolic compounds of industrial and medicinal interests. Most of these high-value plant products are synthesised in the disk cells and stored in the secretory cavity in glandular trichomes. Conventional trichome analysis was so far based on optical microscopy, electron microscopy or extraction based methods that are either limited to spatial or chemical information. Here we combine both information to obtain the spatial distribution of distinct secondary metabolites on a single-trichome level by applying Coherent anti-Stokes Raman scattering (CARS), a microspectroscopic technique, to trichomes derived from sepals of a drug- and a fibre-type.

Hyperspectral CARS imaging in combination with a nonlinear unmixing method allows to identify and localise Δ^9-tetrahydrocannabinolic acid (THCA) in the secretory cavity of drug-type trichomes and cannabidiolic acid (CBDA)/myrcene in the secretory cavity of fibre-type trichomes, thus enabling an easy discrimination between high-THCA and high-CBDA producers. A unique spectral fingerprint is found in the disk cells of drug-type trichomes, which is most similar to cannabigerolic acid (CBGA) and is not found in fibre-type trichomes. Furthermore, we differentiate between different cell types by a combination of CARS with simultaneously acquired two-photon fluorescence (TPF) of chlorophyll a from chloroplasts and organic fluorescence mainly arising from cell walls enabling 3D visualisation of the essential oil distribution and cellular structures.

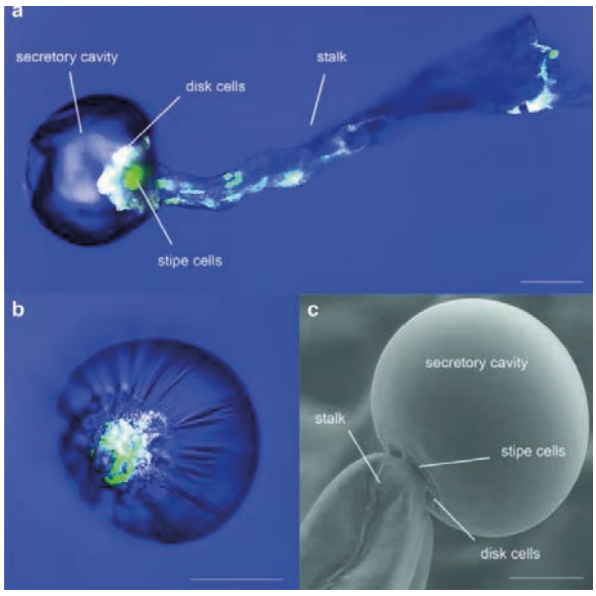

Figure 1: Transmission and single-photon fluorescence images of a glandular trichome (a) and of secretory cavity (b) of *C. sativa* var. Bedrobinol with 561 nm excitation. Anatomy of glandular trichomes captured with SEM (c). Blue: Transmission; White: Fluorescence of organic substances (emission 580–630 nm); Green: Fluorescence of chlorophyll a (em 660–700 nm). Scale bars 50 µm (a and b), 25 µm (c).

Here we demonstrate a label-free and non-destructive method to analyse the distribution of secondary metabolites and distinguish between different cell and chemo-types with high spatial resolution on a single trichome. The record of chemical fingerprints of single trichomes offers the possibility to optimise growth conditions as well as guarantee a direct process control for industrially cultivated medicinal Cannabis plants. Moreover, this method is not limited to Cannabis related issues but can be widely implemented for optimising and monitoring all kinds of natural or biotechnological production processes with simultaneous spatial and chemical information.

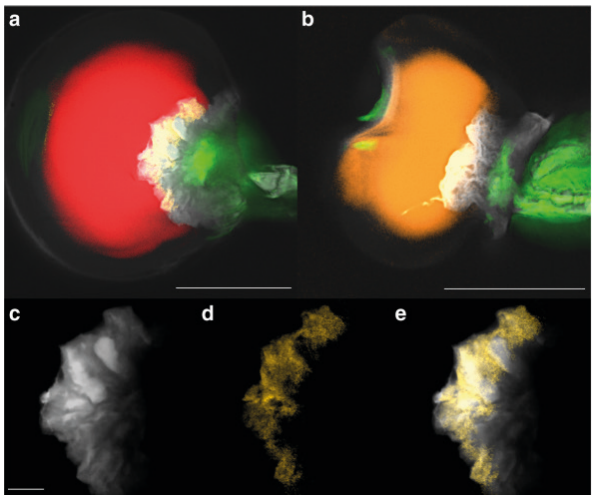

Figure 2: Overlay of F-HCARS relative abundance maps and EPI-HTPF abundance maps of *C. sativa* var. Bedrobinol (a) and *C. sativa* var. Fedora (b). Red: C-H stretching signal similar to THCA; Yellow: C-H stretching signal most similar to CBGA; Orange: C-H stretching similar to CBDA/myrcene, White: TPF of organic substances (em 380–560 nm); Green: TPF of chlorophyll a (em 560–750 nm). Detailed picture of Bedrobinol disk cells (c-e). TPF of organic substances highlight the disk cell morphology (c), F-HCARS signals indicate the presence of CBGA and/or a complex mixture of different aliphatic C-H rich substances (d), F-HCARS signals cover the area of organic fluorescence revealing CBGA and/or a complex mixture of different aliphatic C-H-rich substances is almost exclusively localised inside the disk cells (e). Scale bars 50 µm (a and b); Scale bar 10 µm (c-e).

Contact:
felix.stehle@tu-dortmund.de
oliver.kayser@tu-dortmund.de

Publications:
P. Ebersbach, F. Stehle, O. Kayser, E. Freier, BMC Plant Biology, 18:275 (2018).

Radula Marginata; a Prospective Liverwort as an Alternative Source of Cannabinoid-like Compounds

First report of transcriptomic profiling, annotation and identification of candidate genes for the cannabinoid biosynthetic pathway

Tajammul Hussain, Blue Plunkett, Mahwish Ejaz, Richard V. Espley, Oliver Kayser

Since the recognition of cannabinoids as a clinical significance, it gained interest to investigate the plants, which have similar natural compounds other than Cannabis sativa*. This has led to the identification of liverworts having cannabinoid-like compounds. These liverworts considered as the potential alternative source of cannabinoid like compounds due to a relatively simple architecture and a huge diversity of natural habitats. However, lack of genetic information for such a distinguished liverwort lead us to study* Radula marginata *at transcriptomic level. Therefore, transcriptome was captured, deep sequenced, de novo assembled and annotated leading to the identification and validation of genes for cannabinoids pathway.*

The liverwort *Radula marginata* belongs to the bryophyte division of land plants and is a prospective alternate source of cannabinoid-like compounds. However, mechanistic insights into the molecular pathways directing the synthesis of these cannabinoid-like compounds have been hindered due to the lack of genetic information. This prompted us to do deep sequencing, de novo assembly and annotation of *R. marginata* transcriptome, which resulted in the identification and validation of the genes for cannabinoid biosynthetic pathway. In total, we have identified 11,421 putative genes encoding 1,554 enzymes from 145 biosynthetic pathways. Interestingly, we have identified all the upstream genes of the central precursor of cannabinoid biosynthesis, cannabigerolic acid (CBGA), including its two first intermediates, stilbene acid (SA) and geranyl diphosphate (GPP). Expression of all these genes was validated using quantitative real-time PCR. We have characterized the protein structure of stilbene synthase (STS), which is considered as a homolog of olivetolic acid in *R. marginata*. Moreover, the metabolomics approach enabled us to identify CBGA-analogous compounds using electrospray ionization mass spectrometry (ESI-MS/MS) and gas chromatography mass spectrometry (GC-MS). Transcriptomic analysis revealed 1085 transcription factors (TF) from 39 families. Comparative analysis showed that six TF families have been uniquely predicted in *R. marginata*. In addition, the bioinformatics analysis predicted a large number of simple sequence repeats (SSRs) and non-coding RNAs (ncRNAs). Our results collectively provide mechanistic insights into the putative precursor genes for the biosynthesis of cannabinoid-like compounds and a novel transcriptomic resource for *R. marginata*. The large-scale transcriptomic resource generated in this study would further serve as a reference transcriptome to explore the *Radulaceae* family.

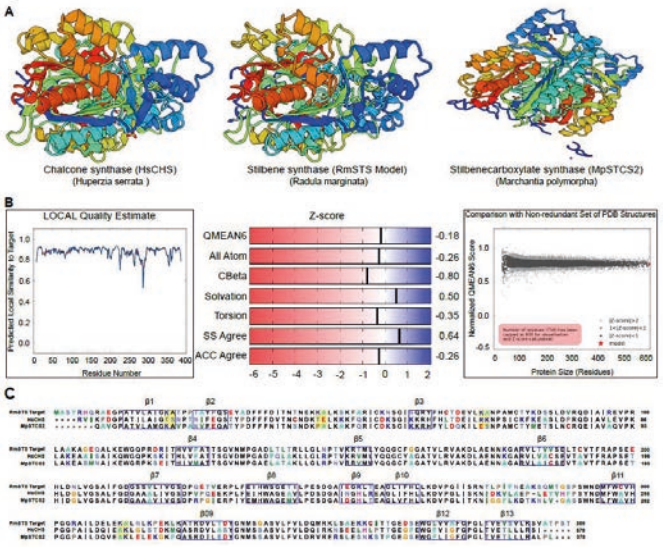

Figure 1a): Crystal structure of stilbene synthase model compared with Chalcone synthase-like polyketide (left, 3awk.1) and Stilbene carboxylate synthase from *Marchantia polymorpha* (right, 2p0u,1A). 1b) Quality estimate of local similarity. Z score of the predicted STS model in *Radula marginata.* 1c) Alignment of the identified stilbene synthase in *Radula marginata* with the respective template model, blue boxes are the beta sheets, yellow boxes in the alignment are the variable sites for both models used as well in olivetolic acid from *Cannabis sativa*.

Publications:
T. Hussain, B. Plunkett, M. Ejaz, R. V. Espley, (2018). Identification of Putative Precursor Genes for the Biosynthesis of Cannabinoid-Like Compound in *Radula marginata*. Front. Plant Sci. 9, 1–17. doi:10.3389/fpls.2018.00537.

Contact:
tajammul.hussain@tu-dortmund.de
oliver.kayser@tu-dortmund.de

Publications 2018 - 2016

2018

Proceedings & Book Chapters

- J. Schachtsiek H. Warzecha, O. Kayser, F. Stehle
  Current Perspectives on Biotechnological Cannabinoid Production in Plants
  Planta Med. 84, 214-220 (2018)

- B. Zirpel, O. Kayser , F. Stehle
  Elucidation of structure-function relationship of THCA and CBDA synthase from *Cannabis sativa* L.
  Journal of Biotechnology 284, 17–26 (2018)

- P. Ebersbach, F. Stehle, O. Kayser, E. Freier
  Chemical fingerprinting of single glandular trichomes of *Cannabis sativa* by Coherent anti-Stokes Raman scattering (CARS) microscopy
  BMC Plant Biology, 18:275 (2018)

- B. Zirpel, F. Degenhardt, C. Zammarelli, D. Wibberg, J. Kalinowski, F. Stehle, O. Kayser
  Optimization of Δ^9-tetrahydrocannabinolic acid synthase production in *Komagataella phaffii* via post-translational bottleneck identification
  Journal of Biotechnology 272–273, 40–47 (2018)

- M. Geissler, J.Volk, F. Stehle, O. Kayser, H. Warzecha
  Subcellular localization defines modification and production of Δ^9-tetrahydrocannabinolic acid synthase in transiently transformed *Nicotiana benthamiana*
  Biotechnology Letters https://doi.org/10.1007/s10529-018-2545-0 (2018)

- H. Aati, A. El-Gamal, O. Kayser, A. Ahmed
  The Phytochemical and Biological Investigation of *Jatropha pelargoniifolia* Root Native to the Kingdom of Saudi Arabia
  Molecules. 23 pii: E1892. doi: 10.3390/molecules23081892 (2018)

- O. Kayser
  Ethnobotany and Medicinal Plant Biotechnology: From Tradition to Modern Aspects of Drug Development
  Planta Med. 84, 834-838 (2018)

- L. Kohnen, S. Sezgin, M. Spiteller, H. Hagels, O. Kayser
  Localization and Organization of Scopolamine Biosynthesis in *Duboisia myoporoides* R. Br.
  Plant Cell Physiol. 59, 107-118 (2018)

- T. Hussain, B. Plunkett, M. Ejaz, R. Espley, O. Kayser
  Identification of Putative Precursor Genes for the Biosynthesis of Cannabinoid-Like Compound in *Radula marginata*
  Front Plant Sci. 9, 537. doi: 10.3389/fpls.2018.00537 (2018)

Presentations & Poster

- T. Hussain O. Kayser
  Transcriptomic analysis of Radula marginata revealed identification of genes for cannabinoid-like compounds
  Emerging Trends in Natural Product Biotechnology, Dortmund, Germany

- T. Pitaktbut, S. Kusari, M. Spiteller, O. Kayser
  Regeneration of Maytenus heterophylla by a stem cutting technique and genome mining for cross-species maytansine biosynthesis
  Emerging Trends in Natural Product Biotechnology, Dortmund, Germany

- J. Schachtsiek, O. Kayser, F. Stehle
  CRISPR-Cas9 mediated reduction of the nicotine content of tetraploid smoking tobacco (*Nicotiana tabacum*)
  Emerging Trends in Natural Product Biotechnology, Dortmund, Germany

- P. Rodziewicz, S. Loroch, L. Marczak, A. Sickmann, O. Kayser
  Catalytic activity of cannabinoid synthases in organic phase
  Emerging Trends in Natural Product Biotechnology, Dortmund, Germany

- T. Hussain, O. Kayser
  ***Radula marginata*: a prospective liverwort an alternate source of cannabinoid-like compounds**
  EMBO Workshop, New shores in land plant evolution, Lisboa, Portugal

Patents

- F. Stehle, O. Kayser
  Biotechnologische Herstellung von Cannabinoiden
  2018071713343200DE (2018)

2017

- B. Zirpel, F. Degenhardt, C. Martin, O. Kayser, F. Stehle
  Engineering yeasts as platform organisms for cannabinoid biosynthesis
  J Biotechnol 259, 204–212 (2017)

- F. Stehle, F. Degenhardt, B. Zirpel, O. Kayser
  Biotechnological synthesis of tetrahydrocannabinolic acid
  PHARMAKON 5, 142–147 (2017)

- Â. Carvalho, E.H. Hansen, O. Kayser, S. Carlsen, F. Stehle
  Designing microorganisms for heterologous biosynthesis of cannabinoids
  FEMS Yeast 17 (4), fox037 (2017)

- K.L. Kohnen, S. Sezgin, M. Spiteller, H. Hagels, O. Kayser
  Localization and Organization of Scopolamine Biosynthesis in Duboisia myoporoides
  Plant Cell Physiol. 59 (1), 107-118 (2017)

- F. Daoud, D. Pelzer, S. Zuehlke, M. Spiteller, O. Kayser
  Ozone pretreatment of process waste water generated in course of fluoroquinolone production
  Chemosphere 185, 953-963 (2017)

- S.F. Ullrich, A. Rothauer, H. Hagels, O. Kayser
  Influence of Light, Temperature, and Macronutrients on Growth and Scopolamine Biosynthesis in Duboisia species
  Planta Med 83, 937-945 (2017)

Publications 2018 - 2016

Proceedings & Book Chapters

- S. Farag, O. Kayser
  The Cannabis Plant: Botanical Aspects
  In: Preedy V (Hrsg.). Handbook of cannabis and related pathologies: biology, pharmacology, diagnosis, and treatment. Elsevier B.V., 3–12 (2017)

- F. Degenhardt, F. Stehle, O. Kayser
  The biosynthesis of cannabinoids
  In: Preedy V (Hrsg.). Handbook of cannabis and related pathologies: biology, pharmacology, diagnosis, and treatment. Elsevier B.V., 13–23 (2017)

2016

- S.F. Ullrich, H. Hagels, O. Kayser
  Scopolamine: a journey from the field to clinics
  Phytochem Rev 2016, DOI: 10.1007/211101-016-9477-x

- J. Sasse, M. Schlegel, L. Borghi, S.F. Ullrich, M. Lee, G.-W. Liu, J.-L. Giner, O. Kayser, L. Bigler, E. Martinoia, Kretzschmar
  T. Petunia hybrida PDR2 is involved in herbivore defense by controlling steroidal contents in trichomes
  Plant, Cell & Environment 2016, DOI: 10.1111/pce. 12828

- S.F. Ullrich, N.J.H. Averesch, L. Castellanos, Y.H. Choi A. Rothauer, O. Kayser
  Discrimination of wild types and hybrids of *Duboisia myoporoides* and *Duboisia leichhardtii* at different growth stages using $_1$H NMR-based metabolite profiling and tropane alkaloidstargeted HPLC-MS analysis
  Phytochemistry 2016, 131: 44-56

- N. Happyana, O. Kayser
  Monitoring metabolite profiles of Cannabis sativa L. trichomes during flowering period using ^{1}H NMR-based metabolomics and Real-Time PCR
  Planta Med 2016, DOI: 10.1055/s-0042-108058

- W.-X. Wang, S. Kusari, H. Laatsch, C. Golz, P. Kusari, C. Strohmann, O. Kayser, M. Spiteller
  Antibacterial azaphilones from an endophytic fungus, *Colletotrichum* sp. BS4
  J Nat Prod 2016, 79: 704-710

Technical Biology (TBL)

Engineering Pseudochelin Production in *Myxococcus xanthus*

A new host for the production of an anti-inflammatory drug

Juliane Korp, Lea Winand, Angela Sester, Markus Nett

Natural products of the myxochelin family are potent inhibitors of the enzyme human 5-lipoxygenase, which is a validated target for the treatment of asthma and other inflammatory diseases. Recently, a novel myxochelin derivative named pseudochelin A was described from the marine bacterium Pseudoalteromonas piscicida*. Unlike other myxochelins, pseudochelin A features a distinctive imidazoline ring. In this project, we elucidated the molecular basis for the biosynthesis of pseudochelin A and we generated a recombinant* Myxococcus xanthus *strain with strongly improved pseudochelin A yields compared to the native producer. For this purpose, a novel plasmid-based expression system was developed.*

The characteristic imidazoline moiety of pseudochelin A was proposed to originate from an intramolecular condensation reaction of the β-aminoethyl amide group in myxochelin B (Figure 1).

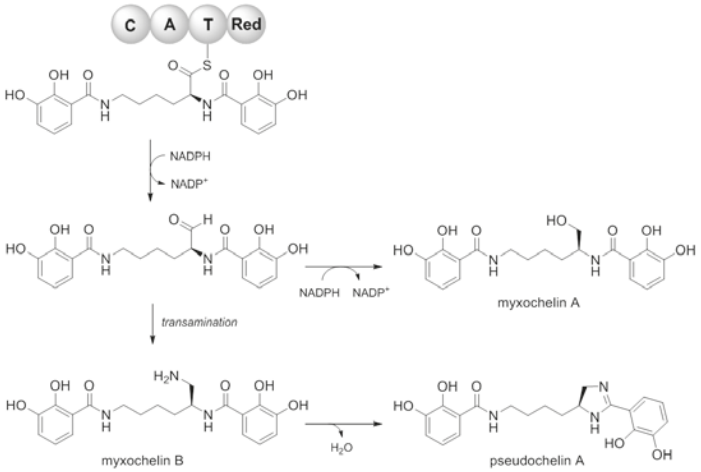

Figure 1: Late steps in the biosynthesis of myxochelins A and B, as well as pseudochelin A.

To identify the enzyme catalyzing this conversion, we compared the myxochelin regulons of two bacteria that produce solely myxochelin A and myxochelin B with that of *P. piscicida*. This approach revealed a gene exclusive to the pseudochelin regulon, coding for an enzyme of the amidohydrolase superfamily. To prove that this enzyme is indeed responsible for the postulated conversion, the reaction was reconstituted *in vitro* using a hexahistidine-tagged recombinant protein made in *Escherichia coli*, with myxochelin B as the substrate (Figure 2).

For the heterologous production of pseudochelin A, the amidohydrolase gene was cloned into a newly developed expression plasmid and placed under the control of a copper-inducible promoter. The resulting vector was subsequently introduced into the myxobacterium *M. xanthus*, a native producer of myxochelin A and B. Following induction with copper, the expression host was found to synthesize small amounts of pseudochelin A. Replacement of the copper-inducible promoter with a constitutive promoter led to significantly increased production levels.

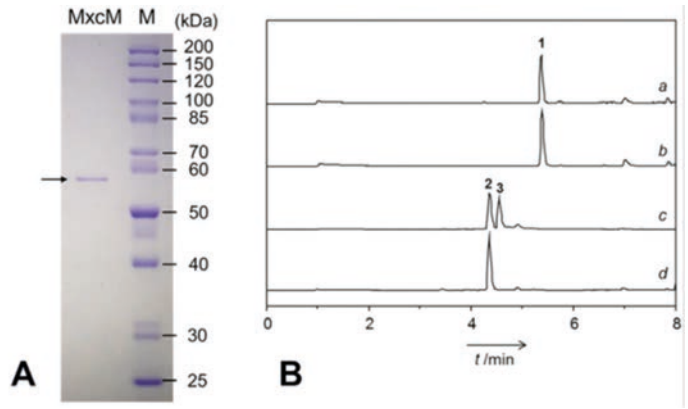

Figure 2: (A) SDS-PAGE of purified 6_His-MxcM. The calculated molecular mass of the recombinant protein is 58.786 kDa. Lane M, protein ladder. (B) Results of the *in vitro* testing of 6_His-MxcM. Total ion chromatograms of myxochelin A (compound 1) with 6_His-MxcM (profile *a*), myxochelin A (compound 1) without 6_His-MxcM (profile *b*), myxochelin B (compound 2) with 6_His-MxcM (profile *c*), and myxochelin B (compound 2) without 6_His-MxcM (profile *d*) are shown. The additional peak in profile *c* corresponds to pseudochelin A (compound 3).

This study described for the first time the heterologous expression of a gene in a myxobacterium without chromosomal integration. Furthermore, it was demonstrated that *M. xanthus* represents a promising alternative to established host systems for the reconstitution and manipulation of biosynthetic pathways.

Contact:
markus.nett@tu-dortmund.de

Publications:
J. Korp, L. Winand, A. Sester, M. Nett, Appl. Environ. Microbiol. 84, e01789-18 (2018).
{selected as Spotlight Article in the respective journal issue}.

Enhancement of Siderophore Production by Algal-Bacterial Cocultivation

Diatoms induce siderophore biosynthesis in *Cupriavidus necator*

Colette Kurth, Markus Nett

Siderophores are low-molecular-weight iron chelators that are produced by diverse microorganisms in order to facilitate the cellular uptake of this biologically important transition metal. Because of their potent complexing properties, siderophores have found numerous applications which range from the medical treatment of iron overload diseases to the recovery of rare earth elements. Previous studies indicated that diatoms are beneficiaries of siderophore production by surrounding bacteria. We could now show that siderophore biosynthesis is actually induced by diatoms irrespective of the iron concentration in the growth medium. This finding has important implications for the biotechnological production of siderophores.

Cupriachelin is a lipopeptide siderophore produced by the freshwater bacterium *Cupriavidus necator* (Figure 1), which is industrially used for the production of biodegradable polyhydroxyalkanoates.

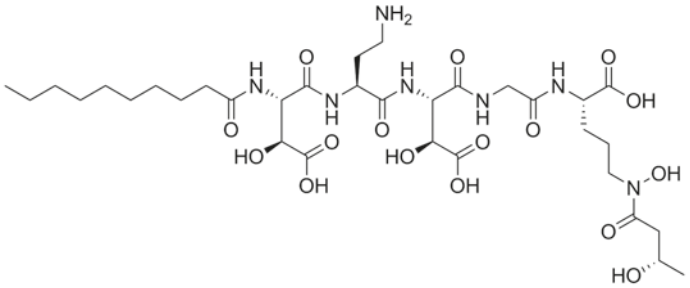

Figure 1: Chemical structure of cupriachelin.

In this study, the cupriachelin-based interaction between *C. necator* and the freshwater diatom *Navicula pelliculosa* was investigated. The two organisms were chosen, because members of the genera *Cupriavidus* and *Navicula* are known to co-occur in the same environments in nature. Furthermore, we had previously observed that the bacterium positively influences the growth of the diatom under iron deficiency. We thus hypothesized that *N. pelliculosa* could trigger the production of cupriachelin and that the concomitant communication could rely on signal molecules secreted by the diatom. To probe this scenario, a *C. necator* reporter harboring the β-galactosidase gene *lacZ* was constructed to study differential expression levels of the cupriachelin biosynthesis gene *cucJ* in response to varying cultivation conditions. The subsequent analyses showed that both iron starvation and culture supernatants of *N. pelliculosa* can induce cupriachelin biosynthesis (Figure 2).

To identify the transcription factors involved in these differential gene expressions, DNA-protein pulldown assays were carried out. For this, a DNA fragment comprising the promoter region of the cucJ gene was generated and incubated with cell lysates of *C. necator*. After several washing steps, bound proteins were eluted from the DNA and analyzed via SDS-PAGE and MALDI-TOF/MS. Besides the iron-dependent ferric uptake regulator (Fur), a NarL-type response regulator was found to influence the expression of cupriachelin biosynthesis genes in the presence of diatom supernatants.

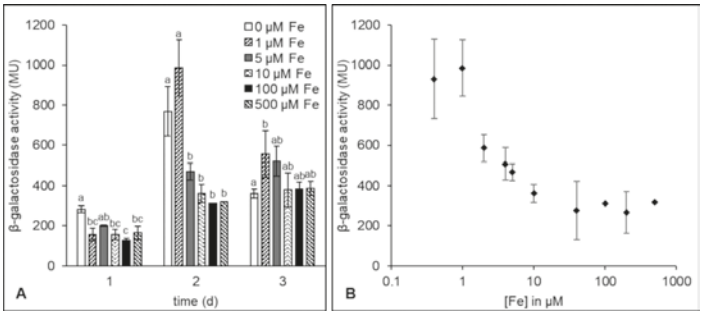

Figure 2: (A) β-Galactosidase activity of the *C. necator* reporter strain on three successive days after inoculation in H-3 mineral medium with different iron concentrations. The values represent the means and standard deviations for samples tested in triplicates. Statistical significance was assessed via one-way ANOVA with Tukey´s post hoc test ($P<0.05$) for every day comparison. Statistical differences are denoted by different letters within each day. (B) β-Galactosidase activity of the *C. necator* reporter strain on the second day after inoculation in H-3 mineral medium plotted against iron concentration in the medium. The values represent the means and standard deviations for samples tested in triplicates. The β-galactosidase activity was significantly (t-test, $P < 0.05$) different at low iron (1 µM) compared to replete conditions (10 µM).

Publications:
C. Kurth, I. Wasmuth, T. Wichard, G. Pohnert, M. Nett, Biometals, doi:10.1007/s10534-018-0159-6 (2018).

Contact:
markus.nett@ tu-dortmund.de

Publications 2018 - 2016

2018

- J. Korp, L. Winand, A. Sester, M. Nett
  Engineering pseudochelin production in *Myxococcus xanthus*
  Applied and Environmental Microbiology 84, e01789-18 (2018)

- C. Kurth, I. Wasmuth, T. Wichard, G. Pohnert, M. Nett
  Algae induce siderophore biosynthesis in the freshwater bacterium *Cupriavidus necator* H16
  Biometals, doi: 10.1007/s10534-018-0159-6 (2018)

- F. Baldeweg, D. Hoffmeister, M. Nett
  A genomics perspective on natural product biosynthesis in plant pathogenic bacteria
  Natural Product Reports, doi: 10.1039/c8np00025e (2018)

- E. Geib, F. Baldeweg, M. Doerfer, M. Nett, M. Brock
  Cross-chemistry leads to product diversity from atromentin synthetases in Aspergilli from section Nigri
  Cell Chemical Biology, doi: 10.1016/j.chembiol.2018.10.021 (2018)

Presentations & Poster

- J. Diettrich, M. Nett
  Massithiazole, a natural product from *Massilia* sp.
  VAAM Workshop Biology of bacteria producing natural products 33 (2018)

- H. Kage
  A genome streamlining-based bacterial chassis generation
  VAAM Workshop Biology of bacteria producing natural products 46 (2018)

- S. Kruth, M. Nett
  Design of vector-based expression systems for myxobacteria
  VAAM Workshop Biology of bacteria producing natural products 38 (2018)

- A. Sester, J. Korp, L. Winand, M. Nett
  Engineering pseudochelin production in *Myxococcus xanthus*
  Emerging Trends in Natural Product Biotechnology 41 (2018)

2017

- F. Baldeweg, H. Kage, S. Schieferdecker, C. Allen, D. Hoffmeister, M. Nett
  Structure of ralsolamycin, the interkingdom morphogen from the crop plant pathogen *Ralstonia solanacearum*
  Organic Letters 19, 4868-4871 (2017)

- P. Brandt, M. García-Altares, M. Nett, C. Hertweck, D. Hoffmeister
  Induced chemical defense of a mushroom by a double-bond-shifting polyene synthase
  Angewandte Chemie International Edition 56, 5937-5941 (2017)

- X. Pan, N. Domin, S. Schieferdecker, H. Kage, M. Roth, M. Nett
  Herpetopanone, a diterpene from *Herpetosiphon aurantiacus* discovered by isotope labeling
  Beilstein Journal of Organic Chemistry 13, 2458-2465 (2017)

- X. Pan, H. Kage, K. Martin, M. Nett
  ***Herpetosiphon gulosus* sp. nov., a filamentous predatory bacterium isolated from sandy soil and *Herpetosiphon giganteus* sp. nov., nom. rev.**
  International Journal of Systematic and Evolutionary Microbiology 67, 2476-2481 (2017)

- S. Schieferdecker, S. König, S. Pace, O. Werz, M. Nett
  Myxochelin-inspired 5-lipoxygenase inhibitors: synthesis and biological evaluation
  ChemMedChem 12, 23-27 (2017)

- V. Valiante, D. J. Mattern, A. Schüffler, F. Horn, G. Walther, K. Scherlach, L. Petzke , J. Dickhaut, R. Guthke, C. Hertweck, M. Nett, E. Thines, A. A. Brakhage
  Discovery of an extended austinoid biosynthetic pathway in *Aspergillus calidoustus*
  ACS Chemical Biology 12, 1227-1234 (2017)

2016

- D. Braga, D. Hoffmeister, M. Nett
  A non-canonical peptide synthetase adenylates 3-methyl-2-oxovaleric acid for auriculamide biosynthesis
  Beilstein Journal of Organic Chemistry 12, 2766-2770 (2016)

- E. Walther, S. Boldt, H. Kage, T. Lauterbach, K. Martin, M. Roth, C. Hertweck, A. Sauerbrei, M. Schmidtke, M. Nett
  Zincophorin – biosynthesis in *Streptomyces griseus* and antibiotic properties
  GMS Infectious Diseases 4, 08.20161128 (2016)

- I. Seccareccia, A. T. Kovacs, R. Gallegos-Monterrosa, M. Nett
  Unraveling the predator-prey relationship of *Cupriavidus necator* and Bacillus subtilis
  Microbiological Research 192, 231-238 (2016)

- C. Kurth, H. Kage, M. Nett
  Siderophores as molecular tools in medical and environmental applications
  Organic & Biomolecular Chemistry 14 (35), 8212-8227 (2016)

- D. Kalb, T. Heinekamp, S. Schieferdecker, M. Nett, A. A. Brakhage, D. Hoffmeister
  An iterative O-methyltransferase catalyzes 1,11-dimethylation of *Aspergillus fumigatus* fumaric acid amides
  ChemBioChem 17 (19), 1813-1817 (2016)

- J. Korp, M. S. Vela-Gurovic, M. Nett
  Antibiotics from predatory bacteria
  Beilstein Journal of Organic Chemistry 12, 594-607 (2016)

- A. M. Schaible, R. Filosa, V. Krauth, V. Temml, S. Pace, U. Garscha, S. Liening, C. Weinigel, S. Rummler, S. Schieferdecker, M. Nett, A. Peduto, S. Collarile, M. Scuotto, F. Roviezzo, G. Spaziano, M. de Rosa, H. Stuppner, D. Schuster, B. D'Agostino, O. Werz
  The 5-lipoxygenase inhibitor RF-22c potently suppresses leukotriene biosynthesis in cellulo and blocks bronchoconstriction and inflammation *in vivo*
  Biochemical Pharmacology 112, 60-71 (2016)

- D. Schwenk, P. Brandt, R. A. Blanchette, M. Nett, D. Hoffmeister
  Unexpected metabolic versatility in a combined fungal fomannoxin/ vibralactone biosynthesis
  Journal of Natural Products 79 (5), 1407-1414 (2016)

- C. Kurth, S. Schieferdecker, K. Athanasopoulou, I. Seccareccia, M. Nett
  Variochelins, lipopeptide siderophores from *Variovorax boronicumulans* discovered by genome mining
  Journal of Natural Products 79 (4), 865-872 (2016)

- S. Schieferdecker, M. Nett
  A fast and efficient method for the preparation of the 5-lipoxygenase inhibitor myxochelin A
  Tetrahedron Letters 57 (12), 1359-1360 (2016)

Industrial Chemistry (TC)

Palladium-catalysed carboxytelomerisation of ß-myrcene to highly branched C_{21}-esters

First Carboxytelomerisation of a branched 1,3-diene

Dennis Vogelsang, Morten Dittmar, Thomas Seidensticker, Andreas J. Vorholt

Herein, the first example of the palladium catalysed linkage of two mole branched 1,3-dienes, one mol carbon monoxide and one mole alcohol to highly branched C_{21}-esters is presented. This homogeneous reaction, called carboxytelomerisation, is a powerful tool to generate esters and amides in a 100% atom economic way with excellent selectivities. Based on a detailed investigation on the influence of different monophosphine ligands, the Tolman angle was determined as a crucial factor for high chemoselectivity towards the desired ester products. Additionally, through the comprehensive design of experiments (DoE), significant reaction parameters were identified leading to optimised reaction conditions for methanol as nucleophile. Finally, the generality of these optimised reaction conditions was proven by applying eight different alcohols yielding in highly branched esters with yields up 99% and excellent chemoselectivities.

In the present work, the first example of a carboxytelomerisation of a 2-alkyl-substituted 1,3-diene with alcohols was shown, with ß-myrcene as representative substrate (Figure 1). Under very mild carbonylative reaction conditions (3 bar carbon monoxide at 80 °C) and a catalyst system comprising of palladium acetate and dicyclohexyl phenyl phosphine, the desired highly-branched C_{21}-esters **3a** were obtained in quantitative yield in the absence of any stabilising solvent (i.e. neat).

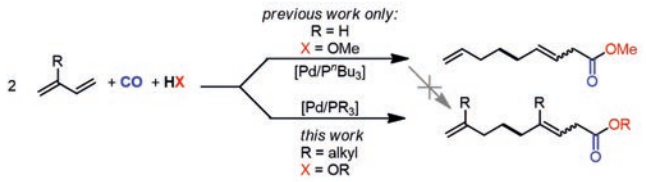

Figure 1: Extension of the carboxytelomerisation of 1,3-butadiene with methanol to ß-myrcene with alcohols.

The Tolman angle of the applied monophosphine ligand was determined to be crucial for ensuring highest chemoselectivity. By applying dicyclohexyl phenyl phosphine with a Tolman angle of 165°, excellent selectivity towards the target products **3a** was achieved. By monitoring the reaction profile, no formation of intermediates in the carboxytelomerisation was detected, supporting a direct reaction pathway with one single catalytic cycle. Additionally, significant trends of crucial reaction parameters were defined and catalytic reaction conditions were optimized by design of experiments (DoE). In the end, the generality of the reaction protocol was proven by converting eight alcohols giving moderate to excellent yields of the corresponding carboxytelomerisation products with excellent selectivities towards the corresponding esters (Figure 2). In ongoing studies, the reason for the limitation to ß-myrcene as 1,3-diene substrate will be studied and subsequently, the reaction protocol widened to apply several classes of 1,3-dienes.

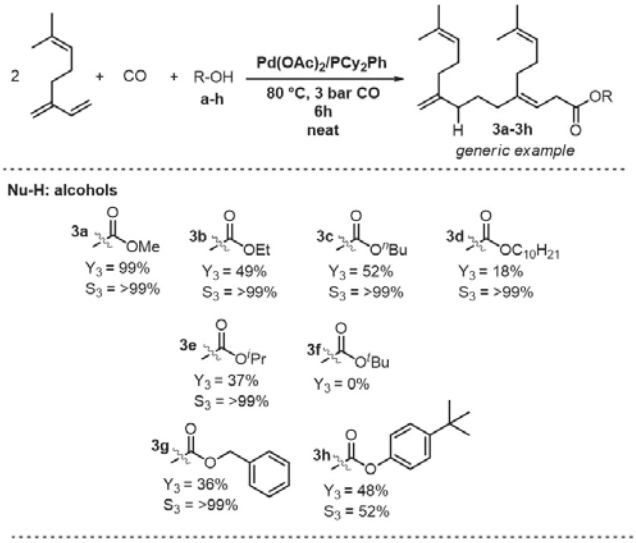

Figure 2: Transfer of optimised reaction conditions to determine the activity of different alcohols in the carboxytelomerisation of ß-myrcene. Reaction conditions: 1.46 mmol alcohol, 7.3 mmol ß-myrcene, 1 mol% $Pd(OAc)_2$, 2 mol% Cy_2Ph as ligand, 80 °C, 3 bar CO, 6 h, 500 rpm; yields (Y) and selectivities (S) reported in %; all results were determined via GC-FID-analysis with dibutyl ether as internal standard; additional data of full characterisation of the products 3a-3h can be found in the ESI.

Contact:
dennis.vogelsang@tu-dortmund.de
thomas.seidensticker@tu-dortmund.de
dieter.vogt@tu-dortmund.de

Publications:
D. Vogelsang, M. Dittmar, T. Seidensticker, A. J. Vorholt, Catal. Sci. Technol. 8, 4332-4337 (2018).

One-Step Palladium-Catalysed Synthetic Route to Unsaturated Pelargonic C_9-Amides Directly From 1,3 Butadiene

Dennis Vogelsang, Johanna Vondran, Andreas J. Vorholt

The first example of the palladium-catalysed amidotelomerisation is presented, in style of the ambitious carboxytelomerisation. A straightforward synthetic tool was generated to produce several industrially relevant pelargonic C_9-amides based on the basic chemical feedstocks: 1,3-butadiene, carbon monoxide and secondary amines. The application of the amidotelomerisation conditions to different classes of amines offered a broad range of the corresponding pelargonic C_9-amides. Understanding this tandem catalysis, significant inhibition factors were uncovered and through a stepwise optimisation, a carbonylation reaction of octadienyl amines (telomer products) was shown for the first time, yielding 99% of the desired linear pelargonic C_9-amides.

Carboxytelomerisation is a 100% atom economic, palladium-catalysed carbonylation reaction, giving access to pelargonic esters and its derivatives. In the present work, we established the amidotelomerisation of 1,3-butadiene, carbon monoxide and amines shown in Figure 1. The target products, pelargonic C_9-amides and its derivatives, are compounds with a versatile application, e.g. as herbicides, rabbit repellents and capsaicin analogues.

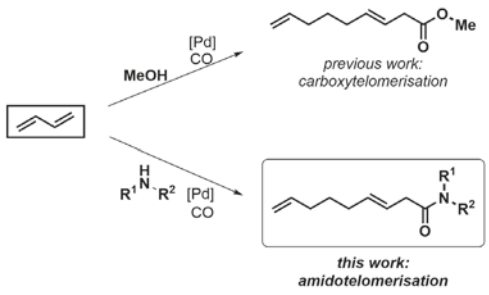

Figure 1: Depiction of the carboxytelomerisation and the here presented novel amidotelomerisation.

Although carboxytelomerisation has been an important tool for ester synthesis, a straightforward transfer to amide synthesis is not possible. In Figure 2, a network of competing reactions comprising hydroamination, telomerisation and carbonylation reactions of the resulting allyl amines is illustrated.

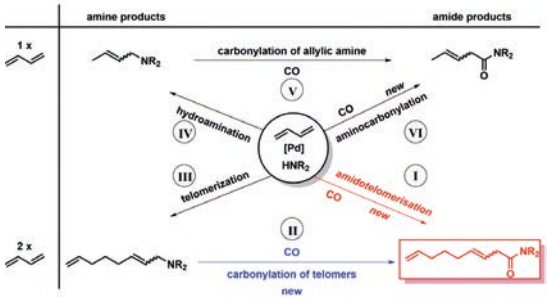

Figure 2: Competing reaction network under amidotelomerisation reaction conditions.

Publications:
D. Vogelsang, J. Vondran, A. J. Vorholt, Journal of Catalysis 365, 24–28 (2018).

Based on a software-supported design of experiments (DoE), significant trends were determined for selected ranges of crucial factors. A sharp increase in the yield of the desired C_9-amide was obtained through a low phosphine to palladium ratio and a high 1,3-butadiene to amine ratio. These trends are in accordance with the reported crucial reaction parameters of the carboxytelomerisation.

After optimisation of the amidotelomerisation in terms of the type of ligand, ligand : palladium-ratio, 1,3-butadiene : diethyl amine-ratio and reaction time, a wide substrate scope of amines with different basicity and sterical demand was investigated. The product spectrum is visualised in Figure 3.

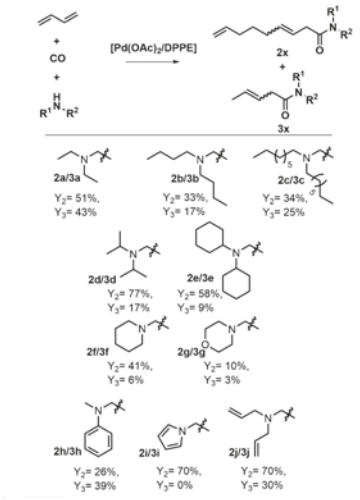

Figure 3: Products spectrum of the amidotelomerisation with different amines.

Interestingly, in case of di-*iso*-propyl amine with a high sterical demand, the highest yields of the corresponding amide with 77% were achieved. Overall, competing hydroamination and carbonylation reactions were observed. In case of pyrrole, the desired C_9-amide was observed with outstanding selectivity.

In conclusion, the network of competing reactions of the amidotelomerisation was uncovered, the influences on the tandem reaction were understood and reaction conditions for each reaction step achieving extremely high reaction rates were developed, resulting in a novel reaction path to unsaturated pelargonic amides.

Contact:
johanna.vondran@tu-dortmund.de
dennis.vogelsang@tu-dortmund.de
dieter.vogt@tu-dortmund.de

Polyhedral Oligomeric Silsesquioxane Modification of Metathesis Catalysts:

Improved Recycling and Lifetime in Membrane Separation

A. Falk, J. M. Dreimann, D. Vogt

Still, the recovery of homogeneous ruthenium catalysts, which are highly efficient in metathesis reactions, is a challenging task. We herein report the synthesis, application and recycling of polyhedral oligomeric silsesquioxane (POSS)-enlarged ruthenium complexes. For the first time, the necessity of modifying two different coordinating moieties in order to achieve catalyst stability and catalyst rejection in a membrane reactor is demonstrated.

Olefin metathesis is a powerful tool to rearrange carbon-carbon double bonds. The synthesis and application of well-defined, highly efficient homogeneous ruthenium catalysts is well known. Available catalysts show excellent functional group-, as well as air and moisture tolerance. However, high costs and tedious recovery and separation from the product disfavor their application in industrial processes.

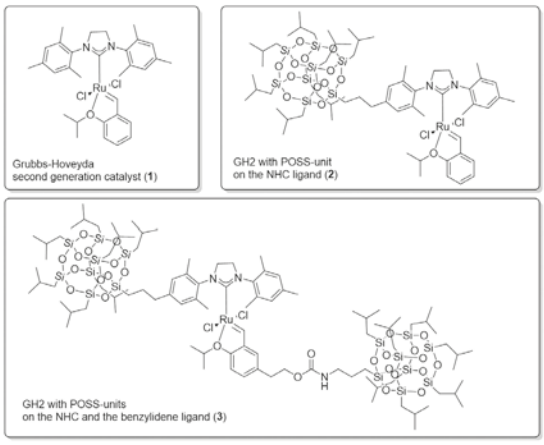

Figure 1: Chemical structure of the metathesis catalysts having different numbers of POSS units on the ligands.

The application of membranes is a very promising approach to separate and reuse the molecular catalyst. Another beneficial aspect in this membrane application approach is the in situ removal of smaller products obtained by the metathesis reaction. In many cases, available membranes suffer from insufficient selectivity, whenever the size of catalyst does not sufficiently differ from the size of the products. Therefore, the molecular weight enlargement of ruthenium complexes having POSS-tags on the coordinating ligands is a promising approach to obtain stable and recyclable metathesis catalysts.

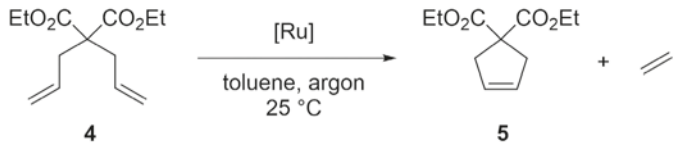

Figure 2: Ring closing metathesis reaction.

Figure 1 shows the initially synthesized metathesis catalyst, which is a Grubbs-Hoveyda catalyst having a POSS-tagged NHC-ligand coordinated. In order to evaluate the performance of the newly synthesized catalyst and to see if the POSS unit on the NHC influences the reaction, ring closing metathesis (Figure 2) was performed. These reactions showed more than 94 % conversion after 2 h having low catalyst loading of 500 µM. Unfortunately separation and recycling of this catalyst complex was not possible since catalyst decomposition was driven forward by the loss of the stabilizing benzylidene ligand through the membrane. As a consequence also the benzylidene moiety of the metathesis catalyst was enlarged with a POSS unit, leading to the synthesis of the new ruthenium complex shown in Figure 1. This catalyst complex allowed four repetitive reaction and filtration cycles as presented in Figure 3. The leaching of the catalyst was lower than 3.5 % in each run.

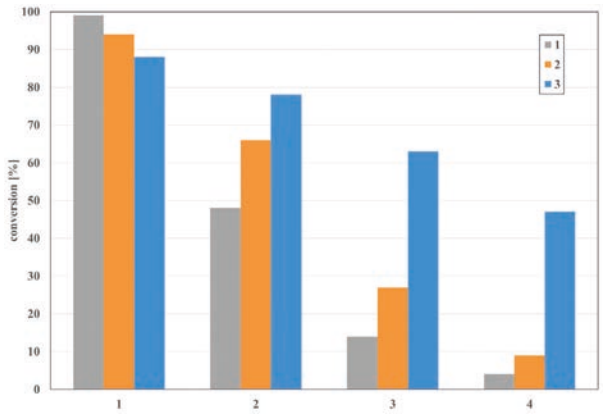

Figure 3: Repetitive batch recycling of catalysts in the ring closing metathesis.

This research demonstrates for the first time the necessity for molecular weight enlargement of both, the NHC and the benzylidene ligand to achieve high catalyst retention. Improving the membrane separation configuration, even better catalyst recovery can be expected. Those experiments are still under investigation.

Contact:
jens.dreimann@tu-dortmund.de
dieter.vogt@tu-dortmund.de

Publications:
A. Falk, J. M. Dreimann, D. Vogt, ACS Sust. Chem. Eng. 6, 7221-7226 (2018).

Amide Versus Amine Ligand Paradigm in the Direct Amination of Alcohols with Ru-PNP Complexes

Dennis Pingen, Jong-Hoo Choi, Henry Allen, George Murray, Prasad Ganji, Piet W. N. M. van Leeuwen, Martin H. G. Prechtl, Dieter Vogt

The catalytic activity of a series of Ru-PNP pincer ligand complexes was studied in the direct amination of alcohols with ammonia. It turned out that all complexes of PNP ligands bearing a secondary amine showed no activity in this hydrogen-shuttling reaction sequence, while all complexes of homologous ligands bearing a tertiary amine gave active catalysts. Further comparative studies on catalysts bearing an acridine-based PNP pincer ligand and a PNP ligand of the Xantphos family provided valuable mechanistic insight that led to the design of a highly active catalyst. It appears that in the group of ligands studied here only ligands that do not form stable Ru-amido complexes are active alcohol amination catalysts.

In view of its synthetic potential, the homogeneously catalysed direct amination of alcohols with ammonia has gained much attention since the first example was described by Milstein in 2008. Since then, several other systems have been developed that are able to convert both primary and secondary alcohols to amines. A number of studies have revealed important information on the mechanism of the reaction, but still there are discrepancies and parts that need further elucidation. One particularly intriguing issue concerns the large differences in activity of the systems known. The usual assumption is that catalysis proceeds via the "Borrowing Hydrogen" or "Hydrogen Shuttling" method; hydrogen is temporarily stored on the catalyst after alcohol dehydrogenation to be re-used later in the hydrogenation of the imine or enamine intermediate (Figure 1).

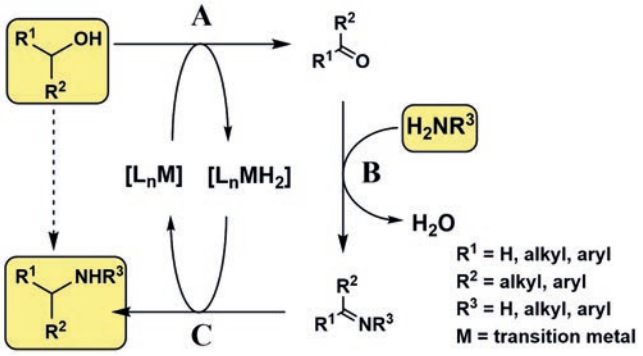

Figure 1: Concept of "Hydrogen Shuttling". A) Alcohol dehydrogenation in which the hydrogen is stored on the catalyst, B) condensation of the carbonyl compound with the amine followed by C) hydrogenation of the imine, using the metal hydride generated in the first step.

Previously it was shown that aromatisation/dearomatisation of the acridine backbone of Milstein´s ligand might not be a prerequisite for the formation of active catalysts. We have now demonstrated that an acridine ligand, in which the dearomatisation is blocked, does not form an active catalyst. In several easily accessible alkyl PNP ligands and their complexes (Figure 2) we have shown that Ru PNP pincer complexes containing a secondary amine in the backbone that are able to form Ru-amide species under reaction conditions are invariably inactive in the direct alcohol amination with ammonia.

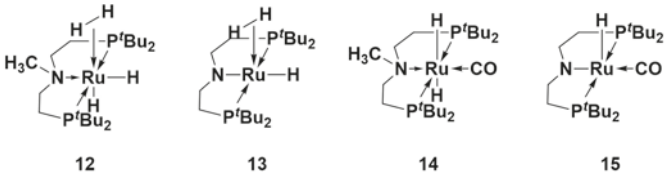

Figure 2: Multi-hydride Ru complexes with aliphatic PNP ligands.

On the contrary, the corresponding PNP ligands with a tertiary amine in the backbone form active catalysts. This leads us to postulate that in order to obtain an active catalyst, no amide bond should be present. Based on these insights a new catalyst system **18** based on the aliphatic PNP ligand bis(di-*tert*-butyl phosphinoethyl)methylamine was prepared with the preferred precursor $RuHCl(CO)(PPh_3)_3$, which on activation with base represents one of the most active catalysts for the direct amination of alcohols with ammonia reported so far (Figure 3).

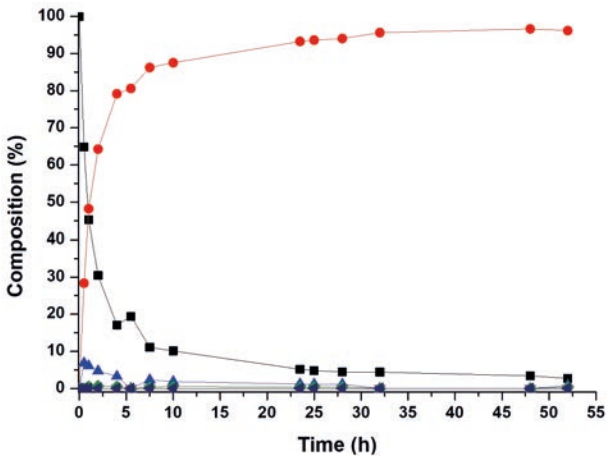

Figure 3: Amination of cyclohexanol employing complex 18 in the presence of KO^{t}Bu. Conditions: 0.04 mmol 18, 5 mmol cyclohexanol, 0.5 mmol KO^{t}Bu, 15 mL *t*-amylalcohol, 2.5 mL NH_3, 150°C. ■ = cyclohexanol, ● = cyclohexylamine, ▲ = cyclohexanone, ▼ = cyclohexylimine, ♦ = dicyclohexylimine, ◀ = dicyclohexylamine.

Publications:
D.L.L. Pingen, J.-H. Choi, H. Allen, G. Murray, O. Diebolt, P.W.N.M. van Leeuwen, P. Ganji, M.H.G. Prechtl, D. Vogt, Catal. Sci. Technol. 8, 3969-3976 (2018).

Contact:
dieter.vogt@tu-dortmund.de

Publications 2018 - 2016

2018

- A. Behr, R. Kuhlmann
  Chemical Conversion of Carbon Dioxide
  Chem. Ing. Tech. 90 (5), 593–601 (2018)

- B. Bibouche, D. Peral, D. Stehl, V. Söderholm, R. Schomäcker, R. von Klitzing, D. Vogt
  Multiphasic Aqueous Hydroformylation of 1-Alkenes with Micelle-like Polymer Particles as Phase Transfer Agents
  RSC Adv. 8 (41), 23332–23338 (2018)

- A. Falk, J. M. Dreimann, D. Vogt
  Polyhedral Oligomeric Silsesquioxane Modification of Metathesis Catalysts: Improved Recycling and Lifetime in Membrane Separation
  ACS Sustain. Chem. Eng. 6 (6), 7221–7226 (2018)

- T. A. Faßbach, S. Püschel, A. Behr, S. Romanski, D. Leinweber, A. J. Vorholt
  Towards a Process for the Telomerization of Butadiene with N-Methylglucamine
  Chem. Eng. Sci. 181, 122–131 (2018)

- T. A. Faßbach, F. O. Sommer, A. J. Vorholt
  Hydroaminomethylation in Aqueous Solvent Systems - An Efficient Pathway to Highly Functionalized Amines
  Adv. Synth. Catal. 360 (7), 1473–1482 (2018)

- S. Fuchs, D. Lichte, T. Jolmes, T. Rösler, G. Meier, H. Strutz, A. Behr, A. J. Vorholt
  Synthesis of Industrial Primary Diamines via Intermediate Diols - Combining Hydroformylation, Hydrogenation and Amination
  ChemCatChem. 10 (18), 4126–4133 (2018)

- S. Fuchs, T. Rösler, B. Grabe, A. Kampwerth, G. Meier, H. Strutz, A. Behr, A. J. Vorholt
  Synthesis of Primary Amines via Linkage of Hydroaminomethylation of Olefins and Splitting of Secondary Amines
  Appl. Catal., A. 550, 198–205 (2018)

- R. Hernandez, J. Dreimann, A. Vorholt, A. Behr, S. Engell
  Iterative Real-Time Optimization Scheme for Optimal Operation of Chemical Processes under Uncertainty: Proof of Concept in a Miniplant
  Ind. Eng. Chem. Res. 57 (26), 8750–8770 (2018)

- R. Hernández, J. Dreimann, S. Engell
  Reliable Iterative RTO of a Continuously Operated Hydroformylation Process
  IFAC-PapersOnLine. 51 (18), 61–66 (2018)

- N. Herrmann, D. Vogelsang, A. Behr, T. Seidensticker
  Homogeneously Catalyzed 1,3-Diene Functionalization – A Success Story from Laboratory to Miniplant Scale
  ChemCatChem. 10 (23), 5342–5365 (2018)

- R. Kuhlmann, M. Nowotny, K. U. Künnemann, A. Behr, A. J. Vorholt
  Identification of key mechanics in the ruthenium catalyzed synthesis of N,N-dimethylformamide from carbon dioxide in biphasic solvent systems
  J. Catal. 361, 45–50 (2018)

- D. Peral, D. Stehl, B. Bibouche, H. Yu, J. Mardoukh, R. Schomäcker, R. von Klitzing, D. Vogt
  Colloidal Polymer Particles as Catalyst Carriers and Phase Transfer Agents in Multiphasic Hydroformylation Reactions
  J. Colloid Interface Sci. 513, 638–646 (2018)

- M. Peters, D. Vogelsang, T. Seidensticker, D. Vogt, J. M. Dreimann
  Prozessintensivierung via organophiler Nanofiltration - Entwicklungen in der Rückgewinnung homogener Übergangsmetallkatalysatoren
  Chem. Ing. Tech. 90 (9), 1177 (2018)

- D. Pingen, J.-H. Choi, H. Allen, G. Murray, P. Ganji, P. W. N. M. van Leeuwen, M. H. G. Prechtl, D. Vogt
  Amide Versus Amine Ligand Paradigm in the Direct Amination of Alcohols with Ru-PNP Complexes
  Catal. Sci. Technol. 8 (15), 3969–3976 (2018)

- D. Pingen, J. B. Schwaderer, J. Walter, J. Wen, G. Murray, D. Vogt, S. Mecking
  Diamines for Polymer Materials via Direct Amination of Lipid- and Lignocellulose-based Alcohols with NH 3
  ChemCatChem. 10 (14), 3027–3033 (2018)

- D. Vogelsang, M. Dittmar, T. Seidensticker, A. J. Vorholt
  Palladium-Catalysed Carboxytelomerisation of B-Myrcene to Highly Branched C 21 -Esters
  Catal. Sci. Technol. 8 (17), 4332–4337 (2018)

- D. Vogelsang, T. A. Faßbach, P. P. Kossmann, A. J. Vorholt
  Terpene-Derived Highly Branched C 30 -Amines via Palladium-Catalysed Telomerisation of β -Farnesene
  Adv. Synth. Catal. 360 (10), 1984–1991 (2018)

- D. Vogelsang, B. A. Raumann, K. Hares, A. J. Vorholt
  From Carboxytelomerization of 1,3-Butadiene to Linear α,ω-C10 -Diester Combinatoric Approaches for an Efficient Synthetic Route
  Chem. Eur. J. 24 (9), 2264–2269 (2018)

- D. Vogelsang, J. Vondran, A. J. Vorholt
  One-Step Palladium Catalysed Synthetic Route to Unsaturated Pelargonic C9-Amides Directly From 1,3-Butadiene
  J. Catal. 365, 24–28 (2018)

Books & Bookarticles

- A. Behr, T. Seidensticker
  Einführung in die Chemie nachwachsender Rohstoffe
  Springer Spektrum

Publications 2018 - 2016

2017

- A. Behr, Z. Bayrak, G. Samli, D. Yildiz, V. Korkmaz, S. Peitz, G. Stochniol
  Recycling and Oligomerization Activity of Ni/Al Catalyst in a Biphasic System with Ionic Liquids
  Chemical Engineering and Technology 40 (1), 196–204 (2017)

- A. Behr, M. Halama, L. Domke
  High throughput screening of homogenously catalyzed hydrogenations in a continuously perfused membrane reactor
  Chem. Eng. Res. Des. 123, 23–34 (2017)

- A. Arno, D. W. Agar, J. Jörissen, A. J. Vorholt
  Einführung in die Technische Chemie
  Berlin, Heidelberg: Springer Berlin Heidelberg

- J. M. Dreimann, T. A. Faßbach, S. Fuchs, M. R. L. Fürst, T. Gaide, R. Kuhlmann et al.
  Vom Laborkuriosum zum kontinuierlichen Prozess
  Chem. Ing. Tech. 89 (3), 252–262 (2017)

- J. M. Dreimann, F. Hoffmann, M. Skiborowski, A. Behr, A. J. Vorholt
  Merging Thermomorphic Solvent Systems and Organic Solvent Nanofiltration for Hybrid Catalyst Recovery in a Hydroformylation Process
  Ind. Eng. Chem. Res. 56 (5), 1354–1359 (2017)

- T. Färber, A. Behr, N. Fink, J. Koop
  A Continuous Process for the Purification of Terpenyl Amines Using a Reversible Acid-Base Reaction
  Chemical Engineering and Technology 40 (10), 1916–1922 (2017)

- T. A. Faßbach, T. Gaide, M. Terhorst, A. Behr, A. J. Vorholt
  Renewable Surfactants through the Hydroaminomethylation of Terpenes
  ChemCatChem 9 (8), 1359–1362 (2017)

- T. A. Faßbach, N. Gösser, F. O. Sommer, A. Behr, X. Guo, S. Romanski et al.
  Palladium-catalyzed hydroamination of farnesene – Long chain amines as building blocks for surfactants based on a renewable feedstock
  Appl. Catal., A 543, 173–179 (2017)

- T. A. Faßbach, R. Kirchmann, A. Behr, A. J. Vorholt
  Recycling of homogeneous catalysts in reactive ionic liquid – solvent-free aminofunctionalizations of alkenes
  Green Chem 19 (21), 5243–5249 (2017)

- T. A. Faßbach, F. O. Sommer, A. Behr, S. Romanski, D. Leinweber, A. J. Vorholt
  Non-ionic surfactants from renewables – amphiphilic ligands in biphasic reactions
  Catal. Sci. Technol. 7 (8), 1650–1653 (2017)

- S. Fuchs, D. Lichte, M. Dittmar, G. Meier, H. Strutz, A. Behr, A. J. Vorholt
  Tertiary Amines as Ligands in a Four-Step Tandem Reaction of Hydroformylation and Hydrogenation
  ChemCatChem 9 (8), 1436–1441 (2017)

- S. Fuchs, M. Steffen, A. Dobrowolski, T. Rösler, L. Johnen, G. Meier et al.
  Secondary diamines as a monomer from bis-hydroaminomethylation of industrial cyclic dienes
  Catal. Sci. Technol. 7 (21), 5120–5127 (2017)

- M. R. L. Furst, V. Korkmaz, T. Gaide, T. Seidensticker, A. Behr, A. J. Vorholt
  Tandem Reductive Hydroformylation of Castor Oil Derived Substrates and Catalyst Recycling by Selective Product Crystallization
  ChemCatChem 9 (23), 4319–4323 (2017)

- T. Gaide, J. Bianga, K. Schlipköter, A. Behr, A. J. Vorholt
  Linear Selective Isomerization/Hydroformylation of Unsaturated Fatty Acid Methyl Esters
  ACS Catal. 7 (6), 4163–4171 (2017)

- T. Gaide, A. Jörke, K. E. Schlipköter, C. Hamel, A. Seidel-Morgenstern, A. Behr, A. J. Vorholt
  Isomerization/hydroformylation tandem reaction of a decene isomeric mixture with subsequent catalyst recycling in thermomorphic solvent systems
  Appl. Catal., A 532, 50–56 (2017)

- A. Jörke, T. Gaide, A. Behr, A. Vorholt, A. Seidel-Morgenstern, C. Hamel
  Hydroformylation and tandem isomerization – hydroformylation of n-decenes using a rhodium-BiPhePhos catalyst
  Chem. Eng. J. 313, 382–397 (2017)

- R. Kuhlmann, A. Prüllage, K. Künnemann, A. Behr, A. J. Vorholt
  Process development of the continuously operated synthesis of N,N- dimethylformamide based on carbon dioxide
  Journal of CO2 Utilization 22, 184–190 (2017)

- R. Kuhlmann, S. Schmitz, K. Haßmann, A. Prüllage, A. Behr
  Synthesis of *N,N*-dimethylformamide from carbon dioxide in aqueous biphasic solvent systems
  Appl. Catal., A 539, 90–96 (2017)

- D. Peral, D. Stehl, B. Bibouche, H. Yu, J. Mardoukh, R. Schomäcker et al.
  Colloidal polymer particles as catalyst carriers and phase transfer agents in multiphasic hydroformylation reactions
  Journal of colloid and interface science 513, 638–646 (2017)

- N. Piens, K. van Hecke, D. Vogt, M. D'hooghe
  Cobalt carbonyl-catalyzed carbonylation of functionalized aziridines to versatile *β*-lactam building blocks
  Organic & biomolecular chemistry 15 (22), 4816–4821 (2017)

- D. Vogelsang, J. M. Dreimann, D. Wenzel, L. Peeva, J. da Silva Burgal, A. G. Livingston et al.
  Continuously Operated Hydroamination – Toward High Catalytic Performance via Organic Solvent Nanofiltration in a Membrane Reactor
  Ind. Eng. Chem. Res. 56 (46), 13634–13641 (2017)

- A. J. Vorholt, S. Immohr, K. A. Ostrowski, S. Fuchs, A. Behr
  Catalyst recycling in the hydroaminomethylation of methyl oleate
  Eur. J. Lipid Sci. Technol. 119 (5), 1600211 (2017)

- H. Warmeling, D. Hafki, T. von Söhnen, A. J. Vorholt
  Kinetic investigation of lean aqueous hydroformylation – An engineer's view on homogeneous catalysis
  Chem. Eng. J. 326, 298–307 (2017)

Publications 2018 - 2016

- H. Warmeling, D. Janz, M. Peters, A. J. Vorholt
  Acceleration of lean aqueous hydroformylation in an innovative jet loop reactor concept
  Chem. Eng. J. 330, 585–595 (2017)

- H. Warmeling, R. Koske, A. J. Vorholt
  Procedural Rate Enhancement of Lean Aqueous Hydroformylation of 1-Octene without Additives
  Chem. Eng. Technol. 40 (1), 186–195 (2017)

Books & Bookarticles

- P. C. J. Kamer, D. Vogt, J. Thybaut (Eds.)
  Contamporary Catalysis; Science, Technology and Applications
  RSC 2017

- A. Behr, A. J. Vorholt (Eds.)
  Homogeneous Catalysis with Renewables
  Springer International Publishing 2017

2016

- A. Kämper, P. Kucmierczyk, T. Seidensticker, A. J. Vorholt, R. Franke, A. Behr
  Ruthenium-Catalyzed Hydroformylation: From Laboratory to Continuous Miniplant Scale
  Catal. Sci. Technol., 2016, 6, 8072-8079, DOI: 10.1039/C6CY01374K

- J. M. Dreimann, M. Skiborowksi, A. Behr, A. J. Vorholt
  Recycling homogeneous catalysts simply via organic solvent nanofiltration: New ways to efficient catalysis
  ChemCatChem, 2016, 8 (21), 3330-3333, DOI: 10.1002/cctc.201601018

- A. J. Vorholt, S. Immohr, K. A. Ostrowski, S. Fuchs, A. Behr
  Catalyst Recycling in the Hydroaminomethylation of Methyl Oleate: A Route to Novel Polyamide Monomers
  Eur. J. Lipid Sci. Technol., 2016, accepted, DOI: 10.1002/ejlt.201600211

- T. Seidensticker, H. Busch, C. Diederichs, J. J. von Dincklage, A. J. Vorholt
  From Oleo Chemicals to Polymer: Bis-Hydroaminomethylation as a Tool for the Preparation of a Synthetic Polymer from Renewables
  Chemcatchem, 2016, 8 (18), 2890-2893, DOI: 10.1002/cctc.201600629

- J. M. Dreimann, H. Warmeling, J. N. Weimann, K. Künnemann, A. Behr, A.J. Vorholt
  Increasing selectivity of the hydroformylation in a miniplant catalyst, solvent and olefin recycle in two loops
  AIChE J., 2016, DOI: 10.1002/aic.15345

- T. Färber, O. Riechert, T. Zeiner, G. Sadowski, A. Behr, A. J. Vorholt
  Homogeneously Catalyzed Hydroamination in a Taylor-Couette Reactor using a Thermormorphic Multicomponent Solvent System
  Chem. Eng. Res. Des., 2016, 112, 263–273; DOI: 10.1016/j.cherd.2016.06.022

- J. Dreimann, A. J. Vorholt, M. Skiborowski, A. Behr
  Removal of homogeneous precious metal catalysts via organic solvent nanofiltration, Chemical Engineering Transactions
  Chem. Eng. Trans., 2016, 47, 343-348; DOI:10.3303/CET1647058

- T. A. Faßbach, R. Kirchmann, A. Behr, S. Romanski, D. Leinweber, A. J. Vorholt
  Telomerization of 1,3-Butadiene with highly substituted Alcohols Using Pd/NHC-Catalysts − Structure-Reactivity-Relationship of the O-Nucleophile
  J. Mol. Catal. A: Chem. 2016, accepted; DOI:10.1016/j.molcata.2016.05.002

- H. Warmeling, A. Behr, A. J. Vorholt
  Jet loop reactors as a versatile reactor set up - Intensifying catalytic reactions: A review
  Chem. Eng. Sci., 2016, 149, 229–248; DOI:10.1016/j.ces.2016.04.032

- P. Neubert, I. Meier, T. Gaide, A. Behr
  Additive-Free Palladium-Catalysed Hydroamination of Piperylene with Morpholine
  Synthesis 48 (2016), A-G

- A. Behr, L. Johnen, A. Wintzer, A. G. Cetin, P. Neubert, L. Domke
  Ruthenium-Catalyzed Cross Metathesis of β-Myrcene and its Derivatives with Methyl Acrylate
  ChemCatChem 8 (2016), 515-522

- A. Kämper, S.J. Warrelmann, K. Reiswich, R. Kuhlmann, R. Franke, A. Behr
  First iridium-catalyzed hydroformylation in a continuously operated miniplant
  Chem. Eng. Sci. 144 (2016), 364-371

Publications 2018 - 2016

- P. Neubert, I. Meier, T. Gaide, R. Kuhlmann, A. Behr
  First telomerisation of piperylene with morpholine using palladium-carbene catalysts
  Catalysis Comm. 77 (2016), 70-74

- J. Haßelberg, A. Behr, C. Weiser, J.B. Bially, I. Sinev
  Process development for the synthesis of saturated branched fatty derivatives: Combination of homogeneous and heterogeneous catalysis in miniplant scale
  Chem. Eng. Sci. 143 (2016), 256-269

- J. Haßelberg, A. Behr
  Saturated branched fatty compounds Proven industrial processes and new alternatives
  Eur. J. Lipid Sci. Technol. 118 (2016) 36-46

- A. Behr, Z. Bayrak, G. Samli, D. Yildiz, S. Peitz, G. Stochniol
  Oligomerization of n-butenes in a two phase reaction system with homogeneous Ni/Al-catalysts
  Chem. Eng. Technol. 39 (2016), 263-270

- M. Zagajewski, J. Dreimann, M. Thönes, A. Behr
  Rhodium catalyzed hydroformylation of 1-dodecene using an advanced solvent system: Towards highly efficient catalyst recycling
  Chem. Eng Process. 99 (2016), 115-123

- K.A. Ostrowski, D. Vogelsang, A. J. Vorholt
  A general and efficient method for the palladium-catalysed conversion of allylic alcohols into their corresponding dienes
  Catal. Sci. Technol., 2016, accepted. DOI: 10.1039/C5CY02096D

- T. Gaide, J. Dreimann, A. Behr, A. J. Vorholt
  Overcoming Phase-Transfer Limitations in the Conversion of Lipophilic Oleo Compounds in Aqueous Media-A Thermomorphic Approach
  Angew. Chem. Int. Ed., 2016, 55, 2924–2928, DOI: 10.1002/anie.201510738

- T. Seidensticker, J. M. Vosberg, K.A. Ostrowski, A. J. Vorholt
  Rhodium-Catalyzed Bis-Hydroaminomethylation of Linear Aliphatic Alkenes with Piperazine
  Adv. Synth. Catal., 2016, 358, 610–621, DOI: 10.1002/adsc.201500896

- K.A. Ostrowski, D. Vogelsang, T. Seidensticker, A. J. Vorholt
  Direct Synthesis of an α,ω-Diester from 2,7-Octadienol as Bulk Feedstock in Three Tandem Catalytic Steps
  Chem. Eur. J. 2016, 22, 1840-1846. DOI: 10.1002/chem.201503785

- T. Seidensticker, D. Möller, A. J. Vorholt
  Merger of Johnson–Claisen rearrangement and alkoxycarbonylation for atom efficient diester synthesis
  Tetrahedron Lett., 2016, 57, 371-374. DOI: 10.1016/j.tetlet.2015.12.032

- K.A. Ostrowski, D. Lichte, M. Stuck, A. J. Vorholt
  A comprehensive investigation and optimisation on the proteinogenic amino acid catalysed homo aldol condensation
  Tetrahedron, 2016, 72, 592-598. DOI: 10.1016/j.tet.2015.11.069

- T. Gaide, A. Behr, M. Terhorst, A. Arns, F. Benski, A.J. Vorholt
  Katalysatorvergleich bei der Hydroesterifizierung von 10-Undecensäuremethylester in thermomorphen Lösungsmittelsystemen
  Chem. Ing. Tech., 2016, 88, 158-167. DOI: 10.1002/cite.201500096

- D.L.L. Pingen, C. Altintas, M. Schaller, D. Vogt
  A Ruthenium Racemisation Catalyst for Synthesis of Primary Amines from Secondary Amines
  Dalton Trans. 2016, 45, 11765-11771. http://dx.doi.org/10.1039/C6DT01525E, first published on the web 10 June, 2016

Thermodynamics (TH)

Triglycerides as Solvents for Pharmaceuticals

Joscha Brinkmann, Christian Luebbert, Gabriele Sadowski

Lipid-based drug delivery systems (LBDDSs) are a promising option to increase the bioavailability of active pharmaceutical ingredients (APIs). In the simplest case, APIs can be dissolved in a triglyceride (TG). However, choosing the best-suited TG, requires a mechanistic understanding of how its properties influence the API solubility and therewith the thermodynamic stability of those formulations. The influences of TG chain length and degree of saturation on API solubility were investigated in this work. Solubility experiments and thermodynamic modeling were combined to allow screening for best-suited LBDDS. This method enables straight-forward formulation development and complements the commonly-used trial and error methods in pharmaceutical industry.

Low water solubility and membrane permeability resulting in low bioavailability impact the majority of newly-developed active pharmaceutical ingredients (APIs) and are thus challenging limitations in pharmaceutical development. It has been shown that bioavailability can be enhanced via formulating the APIs in lipid-based drug delivery systems (LBDDS). LBDDS are usually multicomponent mixtures, which contain a variety of lipids and excipients. In its simplest form, the API is dissolved in only one pure lipid. The most-used lipids are natural oils (e.g. soybean oil), which mostly contain triglycerides (TGs). TGs comprise a glycerol backbone and three fatty-acid ester side groups. Those side groups may differ in chain length and degree of saturation.

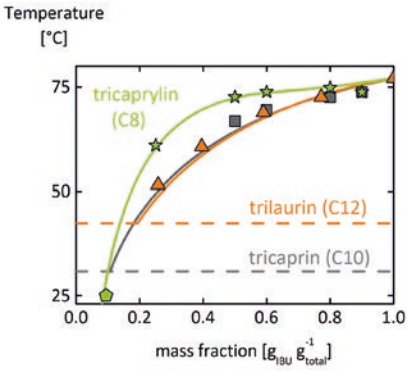

Figure 1: Phase diagrams of IBU in saturated, medium-chained TGs. Symbols are experimental values, solid lines mark the PC-SAFT modeling. Dashed lines are the calculated eutectic temperatures.

Solubility of the APIs in TGs was measured via differential scanning calorimetry at high temperatures. The Perturbed-Chain Statistical Associating Fluid Theory (PC-SAFT) was then applied to extrapolate these solubilities to lower temperatures. Figure 1 shows the influence of fatty-acid chain length on the solubility of the API ibuprofen (IBU) in three fully-saturated TGs, namely tricaprylin ($TG8_08_08_0$), tricaprin ($TG10_010_010_0$) and trilaurin ($TG12_012_012_0$). As to be seen, IBU solubility as well as the eutectic temperature increase only slightly with increasing TG chain length. This means that at high temperatures the solubility of IBU in $TG10_010_010_0$ or $TG12_012_012_0$ is higher than in $TG8_08_08_0$, but IBU will crystallize at room temperature (25 °C).

Contact:
christian.luebbert@tu-dortmund.de
joscha.brinkmann@tu-dortmund.de
gabriele.sadowski@tu-dortmund.de

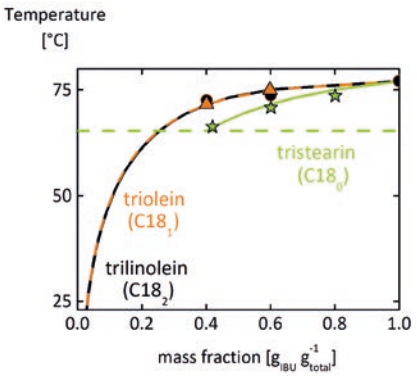

Figure 2: Phase diagrams of IBU in saturated and unsaturated TGs of fatty acids with the same chain length. Symbols are experimental data, lines are PC-SAFT modeling. The dashed green line is the calculated eutectic temperature of $TG18_018_018_0$.

The second structural impact investigated in this work is the influence of the TG degree of saturation on API solubility. Therefore, three TGs with the same side-chain lengths (18 carbon atoms) and different degrees of saturation were compared. Tristearin ($TG18_018_018_0$) is completely saturated, triolein ($TG18_118_118_1$) possesses one double bond in each fatty-acid side chain and trilinolein ($TG18_218_218_2$) two double bonds in each fatty-acid side chain. As depicted in Figure 2, the API solubility strongly decreases by introducing the first double bond in the side-chain, but is not further affected by a higher degree of unsaturation. Moreover, the number of double bonds dramatically decreases the TG melting points, which enables formulating liquid LBDDS at 25 °C. For IBU in $TG18_018_018_0$ the solubility line ends at the eutectic temperature of 65.5 °C, which does not allow formulating liquid LBDDS at ambient temperatures.

It can be summarized that changing fatty-acid chain length revealed to increase the solubility of IBU in TGs only slightly but results in unfavorable, crystalline formulations at 25 °C for $TG10_010_010_0$ or longer side chains. TG unsaturation leads to a distinct decrease of solubility, which makes saturated $TG8_08_08_0$ more favorable for LBDDS formulations with IBU than unsaturated TGs. Thus combining thermodynamic measurements and modeling with PC-SAFT is an appropriate method for screening optimal TG/API combinations for LBDDS and helps finding best-suited TGs for LBDDS.

Publications:
J. Brinkmann, C. Luebbert, D. H. Zaitsau, S. P. Verevkin, G. Sadowski; Thermodynamic Modeling of Triglycerides using PC-SAFT, J. Chem. Eng. Data (2019), DOI: 10.1021/acs.jced.8b01046.

Heterosegmental Modeling of Long-Chain Molecules and Related Mixtures using PC-SAFT

Niklas Haarmann[1], Sabine Enders[2], Gabriele Sadowski[1]
[1]Laboratory of Thermodynamics, TU Dortmund
[2]Institute for Technical Thermodynamics and Refrigeration, Karlsruhe Institute of Technology

Fatty-acid-based, long-chain molecules like fatty-acid methyl esters are progressively used as renewable feedstock for the chemical industry. However, experimental pure-component and mixture data are scarce. Thus, a predictive thermodynamic modeling is desirable. For this purpose, a heterosegmental approach was developed based on the thermodynamic model PC-SAFT, which allows for a predictive description of pure-component and mixture properties of long-chain molecules within a homologous series.

The different species of the homologous series, e.g. long-chain esters, are composed of an identical head domain (e.g., -$COOCH_3$) which is connected to an *n*-alkylic residue that only varies in chain length. In this work, this fact was taken into account for modeling of thermodynamic properties using a new heterosegmental approach of PC-SAFT. Here, a long-chain molecule is modeled as a coarse-grained chain comprising a tail and a head domain representing the *n*-alkylic residue and the functional head moiety, respectively.

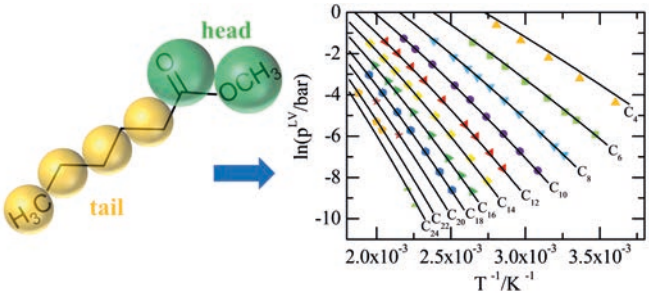

Figure 1: Schematic representation of the heterosegmental approach of PC-SAFT along with the vapor pressures of some methyl alkanoates (methyl butanoate to methyl tetracosanoate). Lines: modeling results with PC-SAFT. Symbols: experimental data taken from literature.

In Figure 1, this modeling concept is illustrated for methyl hexanoate as an example. Due to its similarity, the *n*-alkylic residue is modeled as an *n*-alkane applying the PC-SAFT pure-component parameters of the *n*-alkanes, which were obtained beforehand from independent experimental data of the pure *n*-alkanes. The head domain was modeled as a polar group and its PC-SAFT parameters were determined universally for the entire homologous series. Hence, the proposed approach allows for a predictive description of pure-component properties of long-chain compounds like fatty-acid methyl esters. Applying the new approach, the vapor pressures (Figure 1) and liquid densities of the pure methyl alkanoates could be modeled in remarkable agreement with the available experimental data. Moreover, the excess enthalpies and excess volumes of the binary methyl alkanoate + *n*-alkane mixtures were investigated in this work. Again, the methyl alkanoates were modeled using the heterosegmental approach. It should be emphasized that no experimental data of any binary mixture was used to obtain any model parameter. Hence, the modeling results are full predictions of PC-SAFT. Using this approach, the molar excess enthalpies and molar excess volumes of the binary methyl alkanoate + *n*-alkane mixtures were predicted in very good agreement with the available experimental data as can exemplarily be seen in Figure 2 for the molar excess enthalpies of some binary methyl alkanoate + *n*-tridecane mixtures. Besides the methyl alkanoates, the proposed heterosegmental approach of PC-SAFT was also successfully applied to describe pure-component and mixture properties of long-chain ethyl alkanoates, *n*-aldehydes, *n*-alcohols, *n*-amines, and *n*-alkyl carboxylic acids.

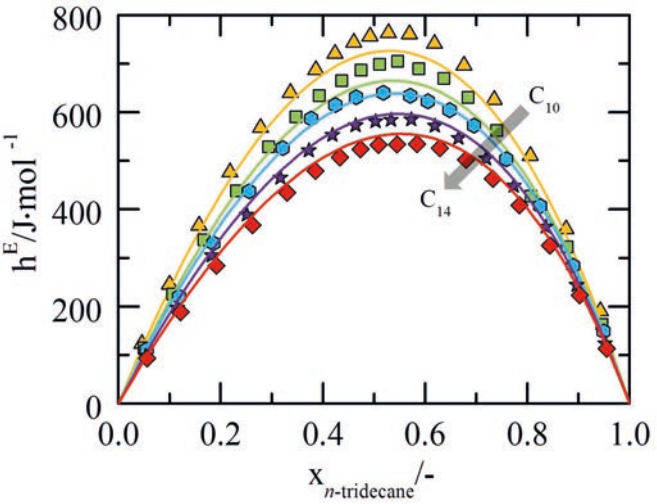

Figure 2: Molar excess enthalpies of the binary methyl alkanoate (methyl decanoate (C_{10}) to methyl tetradecanoate (C_{14})) + *n*-tridecane mixtures. Lines: predictions with PC-SAFT. Symbols: experimental data taken from literature.

Publications:
N. Haarmann, S. Enders, G. Sadowski; Heterosegmental Modeling of Long-Chain Molecules and Related Mixtures using PC-SAFT: 1. Polar Compounds, Ind. Eng. Chem. Res. 2019, 58(7), 2254-2574.

Contact:
gabriele.sadowski@tu-dortmund.de

Influence of High Pressure and of Solvent on a Michael Addition

Michael Knierbein, Thomas Weinbender, Lukas Bittorf, Christoph Held, Oliver Reiser, Gabriele Sadowski

The thermodynamic variable pressure is an important influencing factor for chemical reactions. Even though liquid phases are generally assumed to be incompressible, pressure can have a strong influence on reaction kinetics and could therefore be used to optimize production processes. In this work, the pressure effects on reaction kinetics and reaction equilibrium of a Michael addition were investigated. An activity-based kinetic modeling was used to predict the effect of pressure and of solvent on reaction kinetics and reaction equilibrium using PC-SAFT, which allows predicting molecular interactions as function of pressure and of reaction solvent. Prediction results were in good agreement with experimental data for different reaction solvents for the first time even at pressures in the kilo bar range.

Different properties can be varied (temperature, concentration, pressure, solvent) to optimize a chemical reaction. Even in liquid-phase reactions, pressure influences both, kinetics and equilibrium of a reaction. Pressure effects on kinetics are characterized by the activation volume $\Delta v^{\ddagger}$. A negative activation volume $\Delta v^{\ddagger}$ indicates that the reaction rate will increase with increasing pressure. The class of Michael additions is known to have negative activation volumes of $-40\ cm^3\ mol^{(-1)} < \Delta v^{\ddagger} < -5\ cm^3\ mol^{(-1)}$. Hence, strong dependence of the reaction rate on pressure is expected for reactions of this class.

In this work, the Michael addition of diethyl malonate and nitrostyrene to diethyl nitro-phenylethyl malonate (DENPEM) was investigated.

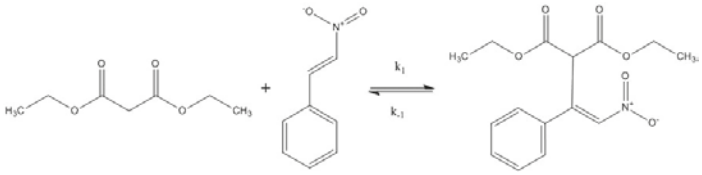

This reaction was analyzed experimentally in toluene, n-hexane and dichloromethane (DCM) at 25 °C at 1 bar and at 4400 bar. Experimental results are shown in Figure 1. It can be seen that an increase in pressure drastically increases the reaction rate. Additionally, the reaction was found to be faster in n-hexane and slower in DCM.

The kinetics of this reaction was described by an activity-based kinetic model. The experimental concentration-over-time plots for the reaction in toluene at 1 bar as well as 4400 bar were used to fit the pressure-dependent kinetic parameters k_1 and $k_{(-1)}$ that are used in the kinetic model. Further, PC-SAFT predicted activities of each reacting agent in the reaction system were required.

PC-SAFT parameters for the reacting agents were fitted to vapor-pressure data and to new experimental density data up to 500 bar. These parameters allowed predicting the pressure and solvent influence on the Michael addition.

The PC-SAFT prediction results are also shown in Figure 1. It can be seen that PC-SAFT correctly predicts an accelerated reaction rate in n-hexane and a slower reaction rate in DCM. These predictions are validated at 1 bar as well as at 4400 bar. The activation volume was calculated to be $\Delta v^{\ddagger} = -24\ cm^3\ mol^{(-1)}$, which is in the expected range for Michael additions.

A solvent screening was performed to predict product yield in different solvents. PC-SAFT predictions suggested highest yield in n-hexane and lowest yield in DCM. These predictions were also validated by the experimental data.

PC-SAFT is a thermodynamic model that accounts for pressure effects. In this work PC-SAFT predictions were for the first time performed in the kilo bar range resulting in an almost quantitative agreement with experimental data.

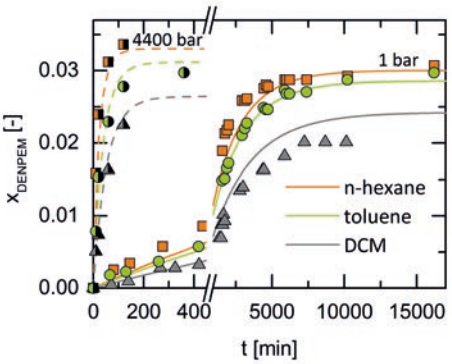

Figure 1: Concentration-over-time plot for the addition of nitrostyrene and diethyl malonate to DENPEM at 25°C. Symbols: experimental data, full lines: PC-SAFT modeling results at 1 bar, dashed lines: PC-SAFT modeling results at 4400 bar.

Contact:
michael.knierbein@tu-dortmund.de
christoph.held@tu-dortmund.de
gabriele.sadowski@tu-dortmund.de

Publications:
M. Knierbein, L. Bittorf, T. Weinbender, O. Reiser, R. Siewert, S.P. Verevkin, C. Held, G. Sadowski; High-Pressure Influence on an Organocatalytic Reaction, Presentation at 30th ESAT 2018, 11 June 2018, Prague.

M. Knierbein, L. Bittorf, T. Weinbender, O. Reiser, C. Held, G. Sadowski; Vorhersage des Hochdruck- und Lösungsmitteleinflusses auf das Reaktionsgleichgewicht einer organokatalytischen Reaktion, Presentation at, Thermodynamik-Kolloquium 2018, 27 September 2018, Kassel.

Simultaneous Prediction of Co-Solvent Influences on Michaelis Constants and Reaction Equilibrium of Ketone Reductions

Experimental and Theoretical Study on Enzyme-Catalyzed Reactions

Anton Wangler, Christoph Held, Gabriele Sadowski

Biotechnologists commonly apply co-solvents in order to improve enzyme-catalyzed reaction systems. The effect of such co-solvents on reaction kinetics and reaction equilibrium of enzyme-catalyzed reactions is mainly studied experimentally. However, this does neither allow explaining nor predicting the observed co-solvent effects on reaction kinetics or equilibrium compositions. In this work, the reaction equilibrium and the Michaelis constants of ketone reductions were predicted with ePC-SAFT. ePC-SAFT showed that adding 17 wt.-% of PEG 6000 is beneficial for reaction kinetics while shifting the reaction equilibrium backwards to the reactant side. Experimental validation showed that these predictions were in a very good agreement to the experimental data. As co-solvent – enzyme interactions were not considered for the predictions co-solvent – reacting agent interactions are decisive for the co-solvent influence on reaction equilibrium and the Michaelis constants for the considered reactions.

New developments in biotechnology have led to new processes in which enzymes pose an alternative to chemical catalysts. However, enzymes are usually stable and active in a small temperature and pH window. Thus, co-solvents have to be added to reaction mixtures to stabilize enzymes and improve reaction kinetics and equilibrium. In this work, the influence of 17 wt.-% of PEG 6000 on the reaction equilibrium and on the Michaelis constants of the reduction of butanone and 2-pentanone was predicted. This approach was based on predicting the influence of co-solvents on the thermodynamic activity coefficients of reacting agents using ePC-SAFT for the following studied reactions:

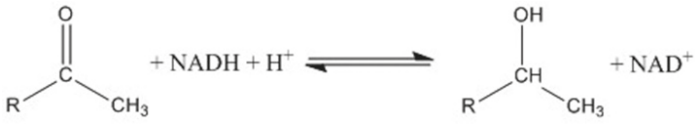

Figure 1: Reaction scheme of the reduction of a ketone to the respective alcohol, catalyzed by ADH270 (25°C, 1 bar, pH 7).

First, reaction equilibrium and kinetics of two reactions (R_1 = C_2H_5 and R_2 = C_3H_7) were measured in water, and activity-based thermodynamic equilibrium constants K_{th} and Michaelis constants K_M^a were determined using these data and ePC-SAFT. This finally allowed predicting the co-solvent influence of 17 wt.-% of PEG 6000 on the reaction equilibrium (expressed as the ratio of reacting agents X^{exp}) and reaction kinetics (characterized by the Michaelis constant K_M). Figure 2 and Figure 3 show results on the simultaneous prediction of the PEG influence on X^{exp} and K_M.

Contact:
anton.wangler@tu-dortmund.de
christoph.held@tu-dortmund.de
gabriele.sadowski@tu-dortmund.de

Publications:
A. Wangler, D. Böttcher, A. Hüser, G. Sadowski, C. Held, Chem. Eur. J. 24, 16418-16425 (2018).
A. Wangler, R. Loll, T. Greinert, G. Sadowski, C. Held, J. Chem. Thermodynamics 128, 275-282 (2019).
A. Wangler, A. Hüser, G. Sadowski, C. Held, ACS Omega 4, 6264-6272 (2019).

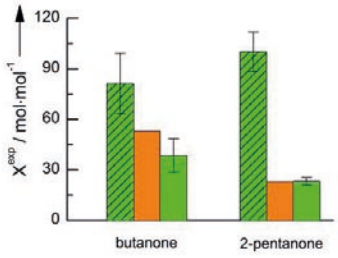

Figure 2: Influence of 17 wt.-% of PEG 6000 on X^{exp} of reduction of butanone or 2-pentanone. Orange: ePC-SAFT, green: experimental data. Striped green bars represent the neat (co-solvent free) values used to determine K_{th}.

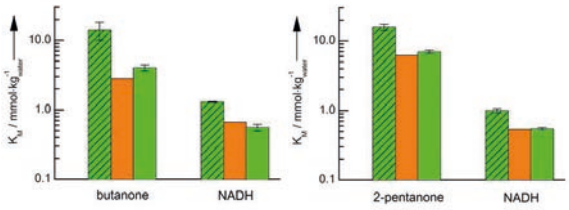

Figure 3: Comparison between the Michaelis constants K_M for neat reaction conditions (striped green bars) and under the influence of 17 wt.-% PEG 6000 (green bars) for the reduction of butanone (left diagram) and 2-pentanone (right diagram). Orange: ePC-SAFT predictions, green: experimental data.

As can be seen from Figure 2, adding PEG decreases the ratio of reacting agents' concentrations, i.e. the reaction equilibrium is shifted to the left-hand side. In Figure 3 it is illustrated that PEG decreases the K_M values, i.e. the kinetics of the reactions is improved upon PEG addition. These influences on the reaction equilibrium and Michaelis constants could be predicted quantitatively correct.

This new approach can serve as screening tool to simultaneously predict co-solvent influences on reaction equilibrium and Michaelis constants of enzyme-catalyzed reactions. As the enzyme was not considered in these predictions it can be concluded that co-solvent – enzyme interactions do not play a major role to understand co-solvent effects on reaction kinetics and equilibrium of the ketone reductions. Rather, co-solvent – reacting agent interactions decisively influence the reaction behavior of the enzyme-catalyzed reactions under investigation.

Publications 2018 - 2016

2018

- Y. Z. Chua, H. T. Do, C. Schick, D. Zaitsau, C. Held
  New experimental melting properties as access for predicting amino-acid solubility
  RSC Advances 8, 6365-6372 (2018)

- N. Haarmann, S. Enders, G. Sadowski
  Heterosegmental Modeling of Long-Chain Molecules and Related Mixtures using PC-SAFT: 1. Polar Compounds
  Industrial & Engineering Chemistry Research 58, 2551-2574 (2018)

- Y. Sun, G. Shen, C. Held, X. Feng, X. Lu, X. Ji
  Modeling Viscosity of Ionic Liquids with Electrolyte Perturbed-Chain Statistical Associating Fluid Theory and Free Volume Theory
  Industrial & Engineering Chemistry Research 57, 8784-8801 (2018)

- A. Wangler, M. J. Bunse, G. Sadowski, C. Held
  Thermodynamic Activity-Based Michaelis Constants
  IntechOpen, DOI: 10.5772/intechopen.80235 (2018)

- A. Wangler, D. Böttcher, A. Hüser, G. Sadowski, C. Held
  Prediction and Experimental Validation of Co-Solvent Influence on Michaelis Constants: A Thermodynamic Activity-Based Approach
  Chemistry – A European Journal 24, 16418-16425 (2018)

- M. A. R. Martins, E. A. Crespo, P. V. A. Pontes, L. P. Silva, M. Bülow, G. J. Maximo, E. A. C. Batista, C. Held, S. P. Pinho, J. A. P. Coutinho
  Tunable Hydrophobic Eutectic Solvents Based on Terpenes and Monocarboxylic Acids
  ACS Sustainable Chemistry & Engineering 6, 8836-8846 (2018)

- N. Haarmann, S. Enders, G. Sadowski
  Modeling binary mixtures of n-alkanes and water using PC-SAFT
  Fluid Phase Equilibria 470, 203-211 (2018)

- V. N. Emel'yanenko, E. Altuntepe, C. Held, A. A. Pimerzin, S. P. Verevkin
  Renewable platform chemicals: Thermochemical study of levulinic acid esters
  Thermochimica Acta 659, 213-221 (2018)

- M. Voges, M. Herhut, C. Held, C. Brandenbusch
  Light-scattering data of protein and polymer solutions: A new approach for model validation and parameter estimation
  Fluid Phase Equilibria 465, 65-72 (2018)

- M. Lemberg, R. Schomäcker, G. Sadowski
  Thermodynamic prediction of the solvent effect on a transesterification reaction
  Chemical Engineering Science 176, 264-269 (2018)

- M. Hübner, C. Lodziak, H. T. Do, C. Held
  Measuring and modeling thermodynamic properties of aqueous lysozyme and BSA solutions
  Fluid Phase Equilibria 472, 62-74 (2018)

- C. Luebbert, M. Wessner, G. Sadowski
  Mutual Impact of Phase Separation/Crystallization and Water Sorption in Amorphous Solid Dispersions
  Molecular Pharmaceutics 15, 669-678 (2018)

- C. Luebbert, G. Sadowski
  In-situ determination of crystallization kinetics in ASDs via water sorption experiments
  European Journal of Pharmaceutics and Biopharmaceutics 127, 183-193 (2018)

- C. Luebbert, D. Real, G. Sadowski
  Choosing Appropriate Solvents for ASD Preparation
  Molecular Pharmaceutics 15, 5397-5409 (2018)

- K. Lehmkemper, S. O. Kyerematen, M. Degenhardt, G. Sadowski
  Influence of Low-Molecular-Weight Excipients on the Phase Behavior of PVPVA64 Amorphous Solid Dispersions
  Pharmaceutical Research 35, 25 (2018)

- K. Lehmkemper, S. O. Kyerematen, M. Bartels, M. Degenhardt, G. Sadowski
  Physical stability of API/polymer-blend amorphous solid dispersions
  European Journal of Pharmaceutics and Biopharmaceutics 124, 147-157 (2018)

- K. Wysoczanska, H. T. Do, C. Held, G. Sadowski, E. A. Macedo
  Effect of different organic salts on amino acids partition behaviour in PEG-salt ATPS
  Fluid Phase Equilibria 456, 84-91 (2018)

- K. Klauke, D. H. Zaitsau, M. Bülow, L. He, M. Klopotowski, T.-O. Knedel, J. Barthel, C. Held, S. P. Verevkin, C. Janiak
  Thermodynamic properties of selenoether-functionalized ionic liquids and their use for the synthesis of zinc selenide nanoparticles
  Dalton Transactions 47, 5083-5097 (2018)

- J. Sauer, H.-D. Kühl
  Analysis of unsteady gas temperature measurements in the appendix gap of a stirling engine
  Journal of Propulsion and Power 34, 1039-1051 (2018)

- S. E. E. Warrag, C. Pototzki, N. R. Rodriguez, M. van Sint Annaland, M. Kroon, C. Held, G. Sadowski, C. J. Peters
  Oil desulfurization using deep eutectic solvents as sustainable and economical extractants via liquid-liquid extraction: Experimental and PC-SAFT predictions
  Fluid Phase Equilibria 467, 33-44 (2018)

- C. Luebbert, C. Klanke, G. Sadowski
  Investigating phase separation in amorphous solid dispersions via Raman mapping
  International Journal of Pharmaceutics 535, 245-252 (2018)

- C. Held, J. Brinkmann, A.-D. Schröder, M. I. Yagofarov, S. P. Verevkin
  Solubility predictions of acetanilide derivatives in water: Combining thermochemistry and thermodynamic modeling
  Fluid Phase Equilibria 455, 43-53 (2018)

- H. B. Rose, T. Greinert, C. Held, G. Sadowski, A. S. Bommarius
  Mutual Influence of Furfural and Furancarboxylic Acids on Their Solubility in Aqueous Solutions: Experiments and Perturbed-Chain Statistical Associating Fluid Theory (PC-SAFT) Predictions
  Journal of Chemical & Engineering Data 63, 1460-1470 (2018)

- A. Wangler, R. Canales, C. Held, T. Q. Luong, R. Winter, D. H. Zaitsau, S. P. Verevkin, G. Sadowski
  Co-solvent effects on reaction rate and reaction equilibrium of an enzymatic peptide hydrolysis
  Physical Chemistry Chemical Physics 20, 11317-11326 (2018)

- A. Wangler, G. Sieder, T. Ingram, M. Heilig, C. Held
  Prediction of CO2 and H2S solubility and enthalpy of absorption in reacting N-methyldiethanolamine /water systems with ePC-SAFT
  Fluid Phase Equilibria, 461, 15-27 (2018)

Publications 2018 - 2016

- H.-D. Kühl
  Auxiliary Heating, Cooloing and Power Generation in Vehicles Based on Sterling Engine Technology
  2. ETA-Tagung-Energie- und Thermomanagement, Klimatisierung, Abwärmenutzunung (2018)

- A. Wangler, C. Schmidt, G. Sadowski, C. Held
  Standard Gibbs Energy of Metabolic Reactions: III The 3-Phosphoglycerate Kinase Reaction
  ACS Omega 3, 1783-1790 (2018)

- E. A. Crespo, L. P. Silva, M. A. R. Martins, M. Bülow, O. Ferreira, G. Sadowski, C. Held, S. Pinho, J. A. P. Coutinho
  The Role of Polyfunctionality in the Formation of [Ch]Cl-Carboxylic Acid-Based Deep Eutectic Solvents
  Industrial & Engineering Chemistry Research 57, 11195-11209 (2018)

2017

- J. Sauer, H.-D. Kuehl
  Numerical model for Stirling cycle machines including a differential simulation of the appendix gap
  Applied Thermal Engineering 111, 819-833 (2017)

- J. Sauer, H.-D. Kuehl
  Analysis of unsteady gas temperature measurements in the appendix gap of a Stirling engine
  Proc. 15th IECEC, AIAA Propulsion and Energy Forum, AIAA 2017-4795 (2017)

- C. Kress, G. Sadowski, C. Brandenbusch
  Solubilization of proteins in aqueous two-phase extraction through combinations of phase-formers and displacement agents
  European Journal of Pharmaceutics and Biopharmaceutics 112, 38-44 (2017)

- J. Gorden, E. Geiser, N. Wierckx, L.M. Blank, T. Zeiner, C. Brandenbusch
  Integrated process development of a reactive extraction concept for itaconic acid and application to a real fermentation broth
  Engineering in Life Science 17, 809-816 (2017)

- Y. Ji, M. Lemberg, A. Prudic, R. Paus, G. Sadowski
  Modeling and analysis of dissolution of paracetamol/Eudragit® formulations
  Chemical Engineering Research and Design 121, 22-31 (2017)

- M. Lemberg, G. Sadowski, M. Gerlach, E. Kohls, M. Stein, C. Hamel, A. Seidel-Morgenstern
  Predicting solvent effects on the 1-dodecene hydroformylation reaction equilibrium
  AIChE Journal 63, 4576-4585 (2017)

- M. Lemberg, G. Sadowski
  Predicting the Solvent Effect on Esterification Kinetics
  ChemPhysChem 18, 1977-1980 (2017)

- K. Lehmkemper, S. O. Kyerematenq, O. Heinzerling, M. Degenhardt, G. Sadowski
  Long-Term Physical Stability of PVP- and PVPVA-Amorphous Solid Dispersions
  Molecular Pharmaceutics 14, 157-171 (2017)

- K. Lehmkemper, S. O. Kyerematenq, O. Heinzerling, M. Degenhardt, G. Sadowski
  Impact of polymer type and relative humidity on the long-term physical stability of amorphous solid dispersions
  Molecular Pharmaceutics 14, 4374-4386 (2017)

- C. Luebbert, G. Sadowski
  Moisture-induced phase separation and recrystallization in amorphous solid dispersions
  International Journal of Pharmaceutics 532, 635-646 (2017)

- C. Luebbert, F. Huxoll, G. Sadowski
  Amorphous-Amorphous Phase Separation in API/Polymer Formulations
  Molecules 22, 296 (2017)

- M. Voges M, I.V. Prikhodko, S. Prill, M. Hübner; G. Sadowski, C. Held
  Influence of pH Value and Ionic Liquids on the Solubility of l-Alanine and l-Glutamic Acid in Aqueous Solutions at 30 °C
  Journal of Chemical & Engineering Data 62, 52-61 (2017)

- F. Meurer, H.T. Do, G. Sadowski, C. Held
  Standard Gibbs energy of metabolic reactions: II. Glucose-6-phosphatase reaction and ATP hydrolysis
  Biophysical Chemistry 223, 30-38 (2017)

- M. Voges, F. Fischer, M. Neuhaus, G. Sadowski, C. Held
  Measuring and Predicting Thermodynamic Limitation of an Alcohol Dehydrogenase Reaction
  Industrial & Engineering Chemistry Research 56, 5535-5546 (2017)

- E. Altuntepe, T. Greinert, F. Hartmann, A. Reinhardt, G. Sadowski, C. Held
  Thermodynamics of enzyme-catalyzed esterifications: I. Succinic acid esterification with ethanol
  Applied Microbiology and Biotechnology 101, 5973-5984 (2017)

- P. Pontes, E.A. Crespo, M.A.R. Martins, L.P. Silva, C.M.M.S. Neves, G.J. Máximo, M.D. Hubinger, E.A.C. Batista, S.P. Pinho, J.A.P. Coutinho, G. Sadowski, C. Held
  Measurement and PC-SAFT Modeling of Solid-Liquid Equilibrium of Deep Eutectic Solvents of Quaternary Ammonium Chlorides and Carboxylic Acids
  Fluid Phase Equilibria 448, 69-80 (2017)

- E. Altuntepe, A. Reinhardt, J. Brinkmann, T. Briesemann, G. Sadowski, C. Held
  Phase behaviour of binary mixtures containing succinic acid or its esters
  Journal of Chemical & Engineering Data 62, 1983-1993 (2017)

- C. H. J. T. Dietz, D. J. G. P van Osch, M. C. Kroon, G. Sadowski, M. van Sint Annaland, F. Gallucci, L. F. Zubeir, C. Held
  PC-SAFT modeling of CO_2 solubilities in hydrophobic deep eutectic solvents
  Fluid Phase Equilibria 448, 94-80 (2017)

- M. Voges, R. Abu, M. T. Gundersen, C. Held, J.M. Woodley, G. Sadowski
  Reaction equilibrium of the ω-transamination of (S)-phenylethylamine: Experiments and ePC-SAFT modeling
  Organic Process Research & Development 21, 976-986 (2017)

- M. Voges, C. Fischer, D. Wolff, C. Held
  Influence of Natural Solutes and Ionic Liquids on Yield of Enzyme-catalyzed Reactions: Measurements and Predictions
  Organic Process Research & Development 21, 1059-1068 (2017)

Publications 2018 - 2016

- M. Gao, C. Held, S. Patra, C. Held, G. Sadowski, R. Winter
  Crowders and Cosolvents–Major Contributors to the Cellular Milieu and Efficient Means to Counteract Environmental Stresses
  ChemPhysChem 18, 2951-2972 (2017)

- E. A. Crespo, L.P. Silva, M.A.R. Martins, L. Fernandez, J. Ortega, O. Ferreira, G. Sadowski, C. Held, S.P. Pinho, J.A.P. Coutinho
  Characterization and Modeling of the Liquid Phase of Deep Eutectic Solvents Based on Fatty Acids/Alcohols and Choline Chloride
  Industrial and Engineering Chemistry Research 56, 12192-12202 (2017)

- E. Altuntepe, V.N. Emel'yanenko, M. Forster-Rotgers, S.P. Verevkin, C. Held
  Thermodynamics of enzyme-catalyzed esterifications: II. Levulinic acid esterification with short-chain alcohols
  Applied Microbiology and Biotechnology 101, 7509-7521 (2017)

- R. I. Canales, C. Held, M. J. Lubben, J. F. Brennecke, G. Sadowski
  Predicting the Solubility of CO_2 in Toluene + Ionic Liquid Mixtures with PC-SAFT
  Industrial and Engineering Chemistry Research 56, 9885-9894 (2017)

2016

- I. Domínguez, B. Gonzalez, B. Orge, C. Held, M. Voges, E.A. Macedo
  Activity coefficients at infinite dilution for different alcohols and ketones in [EMpy][ESO4]: Experimental data and modeling with PC-SAFT
  Fluid Phase Equilibria, 424, 32-40 (2016)

- J. Gorden, T. Zeiner, G. Sadowski, C. Brandenbusch
  Recovery of cis,cis-Muconic Acid from Organic Phase after Reactive Extraction
  Separation and Purification Technology, 169, 1-8 (2016)

- J. Pfeiffer, H.-D. Kühl
  New Analytical Model for Appendix Gap Losses in Stirling Cycle Machines
  Journal of Thermophysics and Heat Transfer, 30, 288-300 (2016)

- J. Pfeiffer, H.-D. Kühl
  Optimization of the Appendix Gap Design in Stirling Engines
  Journal of Thermophysics and Heat Transfer, 30, 831-842 (2016)

- L. Lange, S. Heisel, G. Sadowski
  Predicting the Solubility of Pharmaceutical Cocrystals in Solvent/ Anti-Solvent Mixtures
  Molecules, 21, 593 (2016)

- M. Herhut, C. Brandenbusch, G. Sadowski
  Modeling and prediction of protein solubility using the second osmotic virial coefficient
  Fluid Phase Equilibria, 422, 32-42 (2016)

- M. Voges, F. Schmidt, D. Wolff, G. Sadowski, C. Held
  Thermodynamics of the alanine aminotransferase reaction
  Fluid Phase Equilibria, 422, 87-98 (2016)

- V.N. Emelyanenko, A.V. Yermalayeu, M. Voges, C. Held, G. Sadowski, S.P. Verevkin
  Thermodynamics of a model biological reaction: A comprehensive combined experimental and theoretical study
  Fluid Phase Equilibria, 422, 99-110 (2016)

- S. Glonke, G. Sadowski, C. Brandenbusch
  Applied catastrophic phase inversion: a continuous non-centrifugal phase separation step in biphasic whole-cell biocatalysis
  Journal of Industrial Microbiology & Biotechnology, 43, 1527-1535 (2016)

- S. Mohammad, C. Held, E. Altuntepe, T. Köse, T. Gerlach, I. Smirnova, G. Sadowski
  Salt influence on MIBK/water liquid–liquid equilibrium: Measuring and modeling with ePC-SAFT and COSMO-RS
  Fluid Phase Equilibria, 416, 83-93 (2016)

- S. Mohammad, G. Grundl, R. Müller, W. Kunz, G. Sadowski, C. Held
  Influence of electrolytes on liquid-liquid equilibria of water/1-butanol and on the partitioning of 5-hydroxymethylfurfural in water/1-butanol
  Fluid Phase Equilibria, 428, 102-111 (2016)

- T. Färber, O. Riechert, T. Zeiner, G. Sadowski, A. Behr, A. J. Vorholt
  Homogeneously catalyzed hydroamination in a Taylor–Couette reactor using a thermormorphic multicomponent solvent system
  Chemical Engineering Research and Design, 112, 263-273 (2016)

- T. Reschke, K. V. Zherikova, S. P. Verevkin, C. Held
  Benzoic Acid and Chlorobenzoic Acids: Thermodynamic Study of the Pure Compounds and Binary Mixtures With Water,
  Journal of Pharmaceutical Sciences, 105, 1050-1058 (2016)

- K.V. Zherikova, A. Svetlov, M. Varfolomeev, S.P. Verevkin, C. Held
  Thermochemistry of halogenobenzoic acids as an access to PC-SAFT solubility modeling
  Fluid Phase Equilibria, 409, 399-407 (2016)

- X. Ji, C. Held
  Modeling the density of ionic liquids with ePC-SAFT
  Fluid Phase Equilibria 410, 9-22 (2016)

- Y. Ji, A. K. Lesniak, A. Prudic, R. Paus, G. Sadowski
  Drug Release Kinetics and Mechanism from PLGA Formulations
  AIChE Journal, 62, 4055-4065 (2016)

- C. Held, G. Sadowski
  Thermodynamics of Bioreactions
  Annual Review of Chemical and Biomolecular Engineering, 7, 395-414 (2016)

- C. Kress, G. Sadowski, C. Brandenbusch
  Protein partition coefficients can be estimated efficiently by hybrid shortcut calculations
  Journal of Biotechnology, 233, 151-159 (2016)

- C. Kress, G. Sadowski, C. Brandenbusch
  Novel Displacement Agents for Aqueous 2-Phase Extraction Can Be Estimated Based on Hybrid Shortcut Calculations, J
  Journal of Pharmaceutical Sciences, 105, 3030-3038 (2016)

- C. Held, G. Sadowski: Compatible solutes
  Compatible solutes: Thermodynamic properties relevant for effective protection against osmotic stress
  Fluid Phase Equilibria, 407, 224-235 (2016)

- L.F. Zubeir, C. Held, G. Sadowski, M.C. Kroon
  PC-SAFT Modeling of CO_2 Solubilities in Deep Eutectic Solvents
  The Journal of Physical Chemistry B, 120, 2300-2310 (2016)

- S. Mohammad, C. Held, E. Altuntepe, T. Köse, G. Sadowski
  Influence of Salts on the Partitioning of 5-Hydroxymethylfurfural in Water/MIBK
  The Journal of Physical Chemistry B, 120, 3797-3808 (2016)

Publications 2018 - 2016

- G. Shen, C. Held, X. Lu, X. Ji
  Modelling interfacial properties of ionic liquids with ePC-SAFT combined with density gradient theory
  Molecular Physics, 114, 2492-2499

- L. Lange, K. Lehmkemper, G. Sadowski
  Predicting the Aqueous Solubility of Pharmaceutical Cocrystals As a Function of pH and Temperature
  Crystal Growth & Design, 16, 2726-2740 (2016)

- L. Lange, M. Schleinitz, G. Sadowski
  Predicting the Effect of pH on Stability and Solubility of Polymorphs, Hydrates, and Cocrystals
  Crystal Growth & Design, 16, 4136-4147 (2016)

- N. Gushterov, F. Doghieri, D. Quitmann, E. Niesing, F. Katzenberg, J. C. Tiller, G. Sadowski
  VOC Sorption in Stretched Cross-Linked Natural Rubber
  Industrial & Engineering Chemistry Research, 55, 7191-7200 (2016)

- C. Held, E. N. Tsurko, R. Neueder, G. Sadowski, W. Kunz
  Cation Effect on the Water Activity of Ternary (S)-Aminobutanedioic Acid Magnesium Salt Solutions at 298.15 and 310.15 K
  Journal of Chemical & Engineering Data, 61, 3190-3199 (2016)

- L. Lange, G. Sadowski
  Polymorphs, Hydrates, Cocrystals, and Cocrystal Hydrates: Thermodynamic Modeling of Theophylline Systems
  Crystal Growth & Design, 16, 4439-4449 (2016)

- F. Meurer, M. Bobrownik, G. Sadowski, C. Held
  Standard Gibbs Energy of Metabolic Reactions: I. Hexokinase Reaction
  Biochemistry, 55, 5665-5674 (2016)

- M. Herhut, C. Brandenbusch, G. Sadowski
  Non-monotonic course of protein solubility in aqueous polymer-salt solutions can be modeled using the sol-mxDLVO model
  Biotechnology Journal11, 282-289 (2016)

- M. Herhut, C. Brandenbusch, G. Sadowski
  Inclusion of mPRISM potential for polymer-induced protein interactions enables modeling of second osmotic virial coefficients in aqueous polymer-salt solutions
  Biotechnology Journal, 11, 146-54 (2016)

Impressum

Fakultät Bio- und Chemieingenieurwesen
TU Dortmund
www.bci.tu-dortmund.de

Redaktion: Prof. Joerg C. Tiller
Publication date: June 2019
Printed by: Lensing Druck GmbH & Co. KG